ERCB/AGS Open File Report 2010-03

# Mineralogy, Permeametry, Mercury Porosimetry, Pycnometry and Scanning Electron Microscope Imaging of the Montney Formation in Alberta: Shale Gas Data Release

Energy Resources Conservation Board

Alberta Geological Survey

ERCB/AGS Open File Report 2010-03

# Mineralogy, Permeametry, Mercury Porosimetry, Pycnometry and Scanning Electron Microscope Imaging of the Montney Formation in Alberta: Shale Gas Data Release

S.D.A. Anderson, C.D. Rokosh J.G. Pawlowicz, H. Berhane and A.P. Beaton

Energy Resources Conservation Board
Alberta Geological Survey

May 2010

ISBN 978-0-7758-8627-2



If you use information from this publication in other publications or presentations, please give due acknowledgment to ERCB/AGS. We recommend the following reference format:

Anderson, S.D.A., Rokosh, C.D., Pawlowicz, J.G., Berhane, H. and Beaton, A.P. (2010): Mineralogy, permeametry, mercury porosimetry, pycnometry and scanning electron microscope imaging of the Montney Formation in Alberta: shale gas data release; Energy Resources Conservation Board, ERCB/AGS Open File Report 2010-03, 67 p.

**Published May 2010 by:**
Energy Resources Conservation Board
Alberta Geological Survey
4th Floor, Twin Atria Building
4999 – 98th Avenue
Edmonton, Alberta
T6B 2X3
Canada

Tel: 780-422-1927
Fax: 780-422-1918
E-mail: AGS-Info@ercb.ca
Website: www.ags.gov.ab.ca

# Contents



## Tables



## Figures

## Acknowledgments

The Alberta Energy Innovation Fund, through the Alberta Department of Energy, has provided partial funding for this project. The authors thank S. Rauschning, K. Henderson and L. Enns from the Alberta Department of Energy for their support of this project. Thanks to Obann Resources Ltd. for their excellent work in helping sample and describe Montney Formation core. Thanks also go to the Energy Resources Conservation Board Core Research Centre personnel for sampling assistance, to D-A. Rollings and G. Braybrook for assistance during scanning electron microscope viewing, and to G. Hippolt-Squair of Alberta Geological Survey for her help in putting this report together.

## Abstract

This report constitutes a data release of bulk and clay mineralogy, permeametry and mercury porosimetry analyses, helium pycnometry and scanning electron microscope imaging of selected samples from the Montney Formation generated for the Energy Resources Conservation Board/Alberta Geological Survey project on shale gas resources in Alberta. A few samples were also taken from adjoining formations, such as the Nordegg, Belloy and Doig. This data release complements other manuscripts and data being released from the same project, as listed in Table 1.

# 1 Introduction

The Energy Resources Conservation Board/Alberta Geological Survey (ERCB/AGS) initiated a project in 2007 to evaluate shale gas resources in Alberta, to determine the quantity and spatial extent of these resources. Alberta Geological Survey (AGS) is releasing a series of reports to disseminate data and knowledge from the project. The first formations chosen for evaluation were the Colorado Group (Beaton et al., 2009a; Pawlowicz et al., 2009b), and the Banff and Exshaw formations (Beaton et al., 2009b; Pawlowicz et al., 2009a). These publications are available for download on the AGS website (http://www.ags.gov.ab.ca).

This report disseminates results from bulk and clay mineralogy, permeametry, mercury porosimetry, helium pycnometry and scanning electron microscope (SEM) images from selected samples of the Triassic Montney Formation. Table 1 lists all the analyses and associated reports. The data generated from the project will be combined with additional data to map and estimate shale gas resources in the province.

**Table 1. Analyses performed on core samples, and the organization that performed the analyses as part of the shale gas resource evaluation project.**

| Type of Analysis | Company/ Analyst | Notes |
|---|---|---|
| Adsorption isotherms | Schlumberger/TerraTek | Beaton et al. (2010c, d) |
| Mercury porosimetry, envelope and helium pycnometry. | Department of Physics, University of Alberta (D. Schmitt) | Anderson et al. (2010), this report |
| Permeametry | Department of Earth and Atmospheric Sciences, University of Alberta (M. Gingras) | Anderson et al. (2010), this report |
| Rock Eval™/TOC | Geological Survey of Canada; Schlumberger/TerraTek | Beaton et al. (2010c, d) |
| Organic petrography | Geological Survey of Canada (J. Reyes) | Beaton et al. (2010a, b) |
| Petrographic analysis (thin section) | Alberta Geological Survey | Work in progress |
| Scanning electron microscope (SEM) with energy-dispersive X-ray (EDX) | Department of Earth and Atmospheric Sciences, University of Alberta (D-A. Rollings, G. Braybrook) | Anderson et al. (2010), this report |
| X-ray diffraction (bulk and clay mineral) | SGS Mineral Service Ltd. (H. Zhou) | Anderson et al. (2010), this report |

## 2 Sample Location and Description

Figure 1 displays core sample sites associated with the Montney Formation. Table 2 and Appendix 1 list the locations of the sample sites.

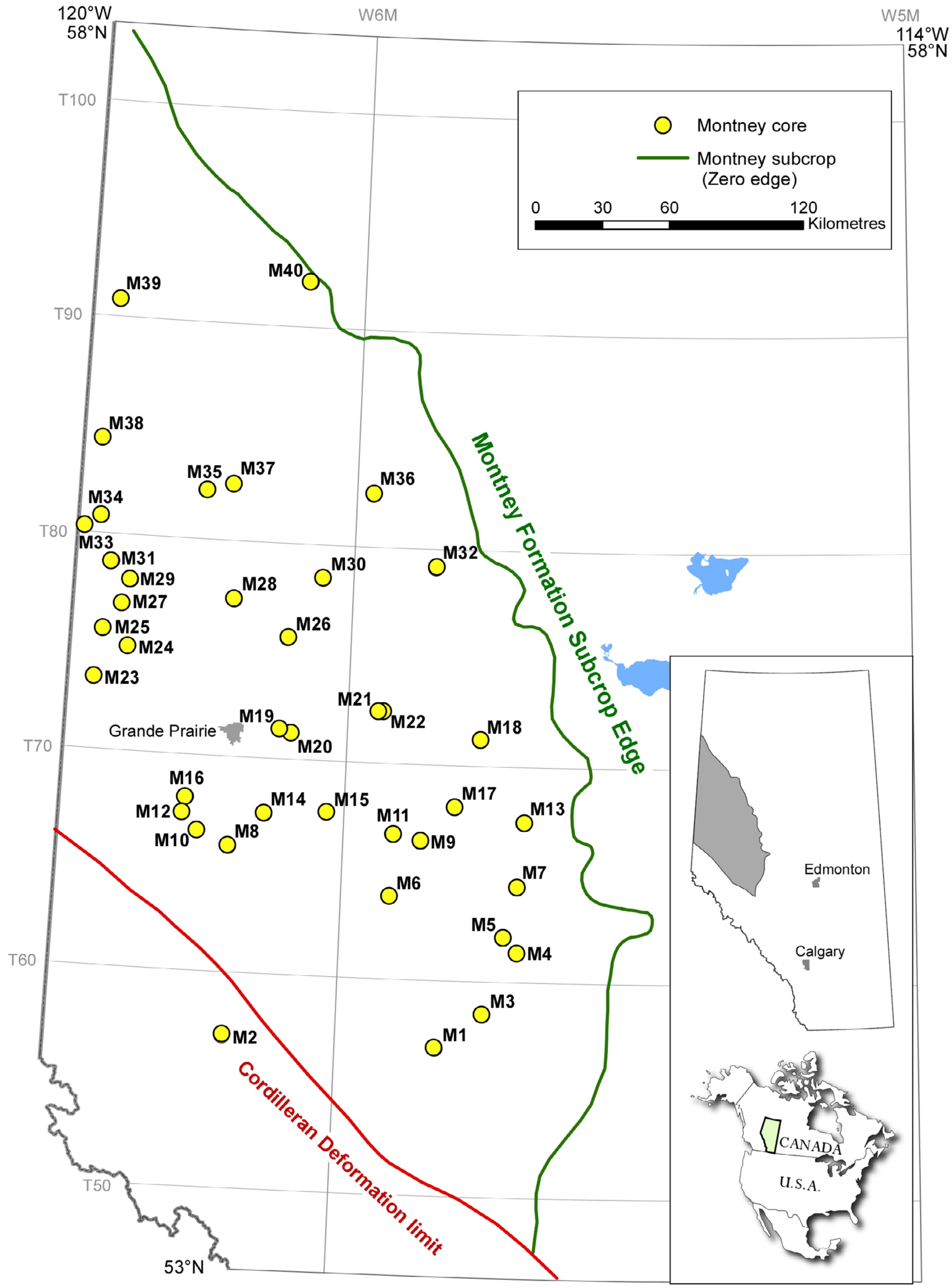


**Figure 1. Core sites sampled from the Montney Formation. See Table 2 and Appendix 1 for a list of all sites and Appendix 2 for the type of analyses run on the samples.**

**Table 2. Core sample sites in the Montney Formation. Figure 1 is a map of the sites.**

| Site No. | Location - UWI | Well Name | Latitude NAD 83 | Longitude NAD 83 | Year Drilled | No. of Samples |
|---|---|---|---|---|---|---|
| M1 | 100/11-14-057-23W5/00 | TALISMAN WILDR 11-14-57-23 | 53.928046 | -117.314072 | 1995 | 6 |
| M2 | 100/16-23-057-06W6/00 | ANDERSON FINDLEY 16-23-57-6 | 53.945460 | -118.771591 | 1976 | 25 |
| M3 | 100/04-06-059-20W5/00 | MOBIL ET AL FIR 4-6-59-20 | 54.068135 | -116.995887 | 1997 | 8 |
| M4 | 102/11-34-061-19W5/00 | BRLINGTON ETAL 102 FOXCK 11-34-61-19 | 54.320254 | -116.767810 | 1996 | 7 |
| M5 | 100/11-24-062-20W5/00 | PENN WEST KAYBOBS 11-24-62-20 | 54.379782 | -116.867662 | 1970 | 8 |
| M6 | 100/07-14-064-25W5/00 | DELPHI SIMONN 7-14-64-25 | 54.535464 | -117.664978 | 1984 | 8 |
| M7 | 103/10-34-064-19W5/00 | TRILOGY ET AL 03 KAYBOB 10-34-64-19 | 54.584938 | -116.780560 | 1996 | 7 |
| M8 | 100/06-14-066-06W6/00 | ANDERSON ET AL BILBO 6-14-66-6 | 54.710226 | -118.798055 | 1979 | 6 |
| M9 | 100/16-31-066-23W5/00 | NCE ENER ANTE 16-31-66-23 | 54.759431 | -117.460327 | 1980 | 7 |
| M10 | 100/07-05-067-07W6/00 | AMOCO ET AL BIG MOUNTAIN 7-5-67-7 | 54.768110 | -119.025448 | 1977 | 7 |
| M11 | 100/12-07-067-24W5/00 | ARC ANTE CREEK 12-7-67-24 | 54.788150 | -117.658255 | 1996 | 9 |
| M12 | 100/14-27-067-08W6/00 | DEVON WAPITI 14-27-67-8 | 54.835461 | -119.131850 | 1998 | 7 |
| M13 | 100/13-31-067-18W5/00 | PARA ET AL GOOSE RIVER 13-31-67-18 | 54.847060 | -116.741498 | 1998 | 5 |
| M14 | 100/13-33-067-04W6/00 | CEQUEL GOLDCK 13-33-67-4 | 54.847494 | -118.556477 | 1995 | 4 |
| M15 | 100/13-05-068-01W6/00 | IMP ECONOMY 13-5-68-1 | 54.863502 | -118.124671 | 1992 | 9 |
| M16 | 100/06-23-068-08W6/00 | NORTHROCK ET AL WAPITI 6-23-68-8 | 54.898674 | -119.111277 | 1980 | 5 |
| M17 | 100/05-24-068-22W5/00 | CHARIOT STURLS 5-24-68-22 | 54.899835 | -117.227282 | 1958 | 8 |
| M18 | 100/02-30-071-20W5/00 | BARR STUMP 2-30-71-20 | 55.174071 | -117.059408 | 1996 | 6 |
| M19 | 100/11-28-071-03W6/00 | BIRCHCLIFF BEZAN 11-28-71-3 | 55.178479 | -118.397982 | 1993 | 15 |
| M20 | 100/06-36-071-04W6/00 | BIRCHCLIFF GRANPR 6-36-71-4 | 55.191378 | -118.475701 | 1993 | 14 |
| M21 | 100/06-33-072-25W5/00 | PCP DEBOLT 6-33-72-25 | 55.278609 | -117.787914 | 1997 | 6 |
| M22 | 100/06-34-072-25W5/00 | PCP DEBOLT 6-34-72-25 | 55.279487 | -117.763567 | 1997 | 6 |
| M23 | 100/05-32-073-12W6/00 | NORTHROCK ET AL SINCLAIR 5-32-73-12 | 55.363395 | -119.815440 | 1999 | 7 |
| M24 | 100/01-14-075-11W6/00 | RIGEL ET AL VALHALLA 1-14-75-11 | 55.493733 | -119.583341 | 1995 | 7 |
| M25 | 100/06-03-076-12W6/00 | DOME SULPETRO GLACIER 6-3-76-12 | 55.554749 | -119.772543 | 1981 | 6 |
| M26 | 100/15-06-076-03W6/00 | PPCL KAKUT 15-6-76-3 | 55.560441 | -118.451191 | 1992 | 8 |
| M27 | 100/14-09-077-11W6/00 | NORCEN POUCE COUPES 14-9-77-11 | 55.661617 | -119.647542 | 1982 | 4 |
| M28 | 100/11-27-077-06W6/00 | CNRL RYCROFT 11-27-77-6 | 55.704273 | -118.845833 | 2001 | 4 |
| M29 | 100/05-14-078-11W6/00 | AECOG (W) PCOUPES 5-14-78-11 | 55.760386 | -119.594242 | 1993 | 7 |
| M30 | 102/11-34-078-02W6/00 | TALISMAN 102 ET AL BELLOY 11-34-78-2 | 55.805873 | -118.221355 | 1997 | 8 |
| M31 | 100/06-12-079-12W6/00 | AECOG (W) GRDONDLE 6-12-79-12 | 55.831641 | -119.737689 | 1993 | 7 |
| M32 | 102/14-20-079-22W5/00 | ANDERSON NORMANDVILLE 14-20-79-22 | 55.867389 | -117.411478 | 1999 | 5 |
| M33 | 100/12-27-080-13W6/00 | STAR POUCE COUPE 12-27-80-13 | 55.966743 | -119.952010 | 1997 | 4 |
| M34 | 100/15-08-081-12W6/00 | TALISMAN POUCE COUPE 15-8-81-12 | 56.011155 | -119.835654 | 1994 | 6 |
| M35 | 100/14-30-082-07W6/00 | STRATAGEM BLUEB 14-30-82-7 | 56.141571 | -119.090112 | 1998 | 9 |
| M36 | 100/11-32-082-25W5/00 | ADAMANT BERWYN 11-32-82-25 | 56.154459 | -117.882771 | 1996 | 7 |
| M37 | 102/13-04-083-06W6/00 | TRICENT ET AL OAK 13-4-83-6 | 56.171475 | -118.895792 | 1984 | 2 |
| M38 | 100/04-32-084-12W6/00 | INVERNESS SCEPTRE BDLKS 4-32-84-12 | 56.322217 | -119.866817 | 1991 | 6 |
| M39 | 102/01-14-091-12W6/00 | JAVELIN CLEAR PR 1-14-91-12 | 56.889041 | -119.804180 | 1999 | 5 |
| M40 | 100/10-21-092-03W6/00 | EXCEL ET AL CUB 10-21-92-3 | 56.998193 | -118.411471 | 1972 | 8 |
| | | | | | Total samples | 293 |

**Legend**

| Column Label | Label Description |
|---|---|
| Site No. | AGS site location number |
| Location - UWI | Well location - unique well identifier |
| Well Name | Name assigned to well when drilling began |
| Latitude (NAD 83) | Well location - degrees latitude, North American Datum 1983 |
| Longitude (NAD 83) | Well location - degrees longitude, North American Datum 1983 |
| Year Drilled | Year the well was drilled |
| No. of Samples | Number of samples taken from the core |

# 3 Analytical Methods and Results

A total of 293 core samples was selected for analysis. The analyses itemized in Table 1 were performed on selected samples, as indicated in Appendix 2.

## 3.1 Bulk and Clay Mineralogy

X-ray powder diffraction (XRD) will identify the mineralogy of a sample. Appendices 3 and 4 provide estimates of the weight percent (wt. %) of each mineral for bulk mineralogy and clay mineralogy, respectively.

X-ray diffraction analysis and interpretation, and X-ray fluorescence spectroscopy (XRF) on core samples were done by SGS Minerals Services Ltd. (http://www.ca.sgs.com/home.htm) using industry-standard techniques.

SGS Minerals uses a Siemens D5000 diffractometer with cobalt radiation and Siemens Search/Match software for peak identification. Mineral proportions are based on relative peak heights and may be strongly influenced by crystallinity, structural group or preferred orientations (H. Zhou, SGS Minerals Services Ltd., pers. comm., 2008; Pecharsky and Zavalij, 2003). The calculation of mineral abundances from both bulk mineral and clay mineral analyses is based on relative peak intensity using the Rietveld reference intensity ratio and is reconciled with a whole-rock chemical analysis by XRF (results provided in Appendix 3b). The detection limit of minerals is approximately 0.5–2.0 wt. % according to SGS, but can be as high as 3–5 wt. % (http://www.xrd.us). Amorphous compounds are not detected by XRD.

Appendix 3 provides bulk mineralogy and X-ray fluorescence spectroscopy data and Appendix 4 gives clay mineralogy. Clay minerals were separated by crushing the sample to 200 mesh and then using a settling column to separate the clay-sized particles. Finally, the sample was centrifuged to remove the liquids before XRD analysis.

## 3.2 Scanning Electron Microscope and EDX Analysis

The purpose of the scanning electron microscope (SEM) analysis is to characterize the microfabric of the samples, and the morphology, size and distribution of the pores. The SEM can also provide a mineralogical analysis using energy dispersive X-rays (EDX), as well as backscattering images on selected samples.

The SEM used is a JEOL 6301F (field emission scanning electron microscope) with magnification ranging from 20× to 250 000×. Semiqualitative elemental analysis (EDX) was available via a PGT X-ray analysis system. The lateral resolution and penetration of EDX mineralogical analysis are both about 1 μm.

Appendix 5 provides the SEM images. A brief description accompanies each image; the descriptions are strictly observational. Interpretation of the images, either separately or collectively, in terms of the relationship of microfabric and sedimentology to depositional environment or permeability and porosity will be published later, either in ERCB/AGS open file reports or as journal articles.

## 3.3 Mercury Porosimetry

Mercury porosimetry is a technique to quantify intrusion pore diameter, size range of diameters, pore volume and pore surface area of the samples (Webb and Orr, 1997). Porosimeter work was done at the University of Alberta. All samples were put under vacuum in a cold oven for degassing prior to analysis. Mercury was introduced into the sample and the volume of mercury forced into pore space in the sample used to calculate pore volume for the sample. The graphs in Appendix 6 show incremental intrusion versus pore diameter, which is meant to portray the concentration of pore throat sizes in the sample, and log differential intrusion versus pore diameter, in which equal peak areas represent equal volume of pore sizes (Webb and Orr, 1997).

The sample size is generally quite small (tens of grams), so the data do not necessarily represent regional pore throat sizes of the formation. A number of other data columns are available for analysis, including cumulative intrusion, incremental intrusion, differential intrusion, log differential intrusion, cumulative pore volume, cumulative pore area and fractal dimensions. The definition and derivation of these values are well explained by Webb and Orr (1997). The lab also calculated a number of other variables using the original measured data, including bulk density, skeletal density, sample porosity, permeability and surface area.

The graphs in Appendix 6 express pore diameter in terms of equivalent spherical diameter (Webb and Orr, 1997). If the pore throat is smaller than the diameter of the pore, then the mercury must first intrude through the smaller pore throat to enter the larger pore; hence, the 'pore diameter' reflected on the graphs is often referred to as the 'pore throat' diameter. All incremental intrusion values that are negative are assigned a value of zero. The graphs include two grain-size scales: the International Union of Pure and Applied Chemistry (IUPAC) pore classification (Rouquerol et al., 1994) used by some authors (e.g., Ross and Bustin, 2008) and the more traditional grain-size scale of Wentworth (1922) with a 3.9 μm clay-silt boundary. The first two sample points at the highest pore diameter generally exhibit a peak that is an artifact of the sample process and is not likely a real pore diameter.

The data in this study were generated using the Washburn equation ($D = -4\gamma\cos\theta/P$), where $\gamma$ is the surface tension, $\theta$ is the assumed contact angle of mercury, $P$ is the applied pressure and $D$ is the equivalent pore diameter. The term 'equivalent' is used because the equation assumes all pores are the equivalent shape of a cylinder; in reality, this is not the case. The surface tension (485 dynes/cm), contact angle (130°) and equilibration time (10 seconds) between successive increases in pressure used in the procedure are all recommended by the manufacturer.

If pores are assumed to be dominated by 'slit-like' openings, as in clay-dominated sediment, then the data may be recalculated using $W = -2\gamma\cos\theta/P$, where $W$ is the width between plates (Webb and Orr 1997). However, the samples in this study are dominantly silt-rich shale/mudstone or shaly siltstone, so we are comfortable using the Washburn equation as a starting point of analysis.

A summary of the procedure can be found in Webb and Orr (1997) and D'Souzae and More (2008).

## 3.4 Permeametry

Spot permeametry analysis (Gingras et al., 2004) was carried out at the University of Alberta on a portable probe permeameter (CoreLabs Model PP-250), with nitrogen and air as the pore fluids. Note that the diameter of a nitrogen molecule is about 0.15 nm (1.5 angstroms), while the diameter of a methane molecule is about 0.4 nm (4.0 angstroms). Each sample is generally tested three or more times in one spot. Horizontal and vertical permeability were tested in some samples. Appendix 7 provides the data for each sample.

## 3.5 Helium Pycnometry

Helium pycnometry measures grain density (often called skeletal density, apparent density, true density or absolute density), which is the density of a substance excluding pores large enough for helium to penetrate (Webb and Orr, 1997). Hence, pores that are not connected are not accounted for in this process. Appendix 8 presents the helium pycnometry data.

# 4 References


Anderson, S.D.A., Rokosh, C.D., Pawlowicz, J.G., Berhane, H. and Beaton, A.P. (2010): Mineralogy, permeametry, mercury porosimetry, pycnometry and scanning electron microscope imaging of the Duvernay and Muskwa Formations in Alberta: shale gas data release; Energy Resources Conservation Board, ERCB/AGS Open File Report 2010-02, 61 p., URL <http://www.ags.gov.ab.ca/publications/abstracts/OFR_2010_02.html> [April 16, 2010].

Beaton, A.P., Pawlowicz, J.G., Anderson, S.D.A. and Rokosh, C.D. (2009a): Rock Eval™, total organic carbon, isotherms and organic petrography of the Colorado Group: shale gas data release; Energy Resources Conservation Board, ERCB/AGS Open File Report 2008-11, 88 p., URL <http://www.ags.gov.ab.ca/publications/abstracts/OFR_2008_11.html> [April 16, 2010].

Beaton, A.P., Pawlowicz, J.G., Anderson, S.D.A. and Rokosh, C.D. (2009b): Rock Eval™, total organic carbon, isotherms and organic petrography of the Banff and Exshaw formations: shale gas data release; Energy Resources Conservation Board, ERCB/AGS Open File Report 2008-12, 65 p., URL <http://www.ags.gov.ab.ca/publications/abstracts/OFR_2008_12.html> [April 16, 2010].

Beaton, A.P., Pawlowicz, J.G., Anderson, S.D.A., Berhane, H. and Rokosh, C.D. (2010a): Organic petrography of the Duvernay and Muskwa formations in Alberta: shale gas data release; Energy Resources Conservation Board, ERCB/AGS Open File Report 2010-06, 20 p., URL <http://www.ags.gov.ab.ca/publications/abstracts/OFR_2010_06.html> [April 16, 2010].

Beaton, A.P., Pawlowicz, J.G., Anderson, S.D.A., Berhane, H. and Rokosh, C.D. (2010b): Organic petrography of the Montney Formation in Alberta: shale gas data release; Energy Resources Conservation Board, ERCB/AGS Open File Report 2010-07, 24 p., URL <http://www.ags.gov.ab.ca/publications/abstracts/OFR_2010_07.html> [April 16, 2010].

Beaton, A.P., Pawlowicz, J.G., Anderson, S.D.A., Berhane, H. and Rokosh, C.D. (2010c): Rock Eval™, total organic carbon, and adsorption isotherms of the Duvernay and Muskwa Formations in Alberta: shale gas data release; Energy Resources Conservation Board, ERCB/AGS Open File Report 2010-04, 32 p., URL <http://www.ags.gov.ab.ca/publications/abstracts/OFR_2010_04.html> [April 2010].

Beaton, A.P., Pawlowicz, J.G., Anderson, S.D.A., Berhane, H. and Rokosh, C.D. (2010d): Rock Eval™, total organic carbon and adsorption isotherms of the Montney Formation in Alberta: shale gas data release; Energy Resources Conservation Board, ERCB/AGS Open File Report 2010-05, 30 p., URL <http://www.ags.gov.ab.ca/publications/abstracts/OFR_2010_05.html> [April 16, 2010].

D'Souzae, J.I. and More, H.N. (2008): Pharmaceutical powder material contains void volume of empty space, distributed within the solid mass in the form of pores, cavities, and cracks of various shapes and sizes; Pharminfo.net, URL <http://www.pharmainfo.net/reviews/mercury-intrusion-porosimetry-tool-pharmaceutical-particle-characterization> [January 13, 2010].

Gingras, M.K., Mendoza, C.A. and Pemberton, S.G. (2004): Fossilized worm burrows influence the resource quality of porous media; AAPG Bulletin, v. 88, no. 7, p. 875–883.

Pawlowicz, J.G., Anderson, S.D.A., Rokosh, C.D. and Beaton, A.P. (2009a): Mineralogy, permeametry, mercury porosimetry and scanning electron microscope imaging of the Banff and Exshaw formations: shale gas data release; Energy Resources Conservation Board, ERCB/AGS Open File Report 2008-13, 59 p., URL <http://www.ags.gov.ab.ca/publications/abstracts/OFR_2008_13.html> [April 16, 2010].

Pawlowicz, J.G., Anderson, S.D.A., Rokosh, C.D. and Beaton, A.P. (2009b): Mineralogy, permeametry, mercury porosimetry and scanning electron microscope imaging of the Colorado Group: shale gas data release; Energy Resources Conservation Board, ERCB/AGS Open File Report 2008-14, 92 p., URL <http://www.ags.gov.ab.ca/publications/abstracts/OFR_2008_14.html> [April 16, 2010].

Pecharsky, V.K. and Zavalij, P.Y. (2003): Fundamentals of powder diffraction and structural characterization of minerals; Kluwer Academic Publishers, New York, 713 p.

Ross, D.J.K. and Bustin, R.M. (2008): The importance of shale composition and pore structure upon gas storage potential of shale gas reservoirs; Marine and Petroleum Geology, v. 26, p. 916–927.

Rouquerol, J., Avnir, D., Fairbridge, C.W., Everett, D.H., Haynes, J.H., Pernicone, N., Ramsay, J.D.F., Sing, K.S.W. and Unger, K. (1994): Recommendations for the characterization of porous solids, International Union of Pure and Applied Chemistry; Pure and Applied Chemistry, v. 68, p. 1739–1758.

Webb, P.A. and Orr, C. (1997): Analytical methods in fine particle technology; Micromeritics Instrument Corporation Publishers, Norcross, Georgia.

Wentworth, C.K. (1922): A scale of grade and class terms for clastic sediments; Journal of Geology, v. 30, p. 377–392.

# Appendices

## Appendix 1 – Montney Formation Core Sample Location, Depth and Lithology

**Legend**

| Column Label | Label Description |
|---|---|
| Sample No. | AGS sample number |
| Site No. | AGS site location number |
| Location - UWI | Well location - unique well identifier |
| Sample Depth (metres) | Depth of core sample in metres (measured from core) |
| Lithology | Brief lithological description of sample |
| Formation/Group | Geological formation or group at depth of sample |

| Sample No. | Site No. | Location - UWI | Sample Depth (Metres) | Lithology | Formation/ Group |
|---|---|---|---|---|---|
| 8113 | M25 | 100/06-03-076-12W6/00 | 2606.4 | siltstone | Montney |
| 8114 | M25 | 100/06-03-076-12W6/00 | 2617.0 | siltstone | Montney |
| 8115 | M25 | 100/06-03-076-12W6/00 | 2618.8 | siltstone | Montney |
| 8116 | M25 | 100/06-03-076-12W6/00 | 2622.5 | siltstone | Montney |
| 8117 | M25 | 100/06-03-076-12W6/00 | 2629.1 | siltstone | Montney |
| 8118 | M25 | 100/06-03-076-12W6/00 | 2639.9 | siltstone | Montney |
| 8119 | M14 | 100/13-33-067-04W6/00 | 2358.2 | siltstone | Montney |
| 8120 | M14 | 100/13-33-067-04W6/00 | 2366.2 | siltstone | Montney |
| 8121 | M14 | 100/13-33-067-04W6/00 | 2372.5 | siltstone | Montney |
| 8122 | M14 | 100/13-33-067-04W6/00 | 2379.4 | siltstone | Montney |
| 8123 | M33 | 100/12-27-080-13W6/00 | 1741.1 | sandstone | Montney |
| 8124 | M33 | 100/12-27-080-13W6/00 | 1743.9 | silty shale | Montney |
| 8125 | M33 | 100/12-27-080-13W6/00 | 1751.0 | sandstone | Montney |
| 8126 | M33 | 100/12-27-080-13W6/00 | 1758.0 | sandstone | Montney |
| 8131 | M37 | 102/13-04-083-06W6/00 | 1080.5 | mudstone | Nordegg |
| 8132 | M37 | 102/13-04-083-06W6/00 | 1088.9 | siltstone | Doig |
| 8701 | M27 | 100/14-09-077-11W6/00 | 2271.6 | siltstone | Montney |
| 8702 | M27 | 100/14-09-077-11W6/00 | 2276.0 | siltstone | Montney |
| 8703 | M27 | 100/14-09-077-11W6/00 | 2279.9 | shaley siltstone | Montney |
| 8704 | M27 | 100/14-09-077-11W6/00 | 2281.5 | siltstone | Montney |
| 8705 | M28 | 100/11-27-077-06W6/00 | 1741.2 | siltstone | Montney |
| 8706 | M28 | 100/11-27-077-06W6/00 | 1746.6 | silty sandstone | Montney |
| 8707 | M28 | 100/11-27-077-06W6/00 | 1750.2 | siltstone | Montney |
| 8708 | M28 | 100/11-27-077-06W6/00 | 1751.1 | siltstone | Montney |
| 8709 | M29 | 100/05-14-078-11W6/00 | 2189.9 | siltstone | Montney |
| 8710 | M29 | 100/05-14-078-11W6/00 | 2193.5 | siltstone | Montney |
| 8711 | M29 | 100/05-14-078-11W6/00 | 2200.9 | siltstone | Montney |
| 8712 | M29 | 100/05-14-078-11W6/00 | 2206.2 | siltstone | Montney |
| 8713 | M29 | 100/05-14-078-11W6/00 | 2214.4 | siltstone | Montney |
| 8714 | M29 | 100/05-14-078-11W6/00 | 2220.9 | siltstone | Montney |
| 8715 | M29 | 100/05-14-078-11W6/00 | 2225.5 | siltstone | Montney |
| 8716 | M20 | 100/06-36-071-04W6/00 | 1889.2 | siltstone and sandstone | Montney |
| 8717 | M20 | 100/06-36-071-04W6/00 | 1894.6 | siltstone | Montney |
| 8718 | M20 | 100/06-36-071-04W6/00 | 1899.4 | siltstone | Montney |
| 8719 | M20 | 100/06-36-071-04W6/00 | 1903.6 | sandy siltstone | Montney |
| 8720 | M20 | 100/06-36-071-04W6/00 | 1907.5 | siltstone | Montney |
| 8721 | M20 | 100/06-36-071-04W6/00 | 1911.1 | siltstone | Montney |
| 8722 | M20 | 100/06-36-071-04W6/00 | 1916.6 | sandstone | Montney |
| 8723 | M20 | 100/06-36-071-04W6/00 | 1919.2 | siltstone | Montney |
| 8724 | M20 | 100/06-36-071-04W6/00 | 1922.6 | siltstone | Montney |
| 8725 | M20 | 100/06-36-071-04W6/00 | 1931.2 | siltstone and sandstone | Montney |
| 8726 | M20 | 100/06-36-071-04W6/00 | 1933.1 | siltstone and sandstone | Montney |
| 8727 | M20 | 100/06-36-071-04W6/00 | 1938.7 | siltstone and sandstone | Montney |
| 8728 | M20 | 100/06-36-071-04W6/00 | 1940.1 | siltstone | Montney |
| 8729 | M20 | 100/06-36-071-04W6/00 | 1943.0 | siltstone | Montney |
| 8730 | M23 | 100/05-32-073-12W6/00 | 2815.1 | siltstone | Montney |
| 8731 | M23 | 100/05-32-073-12W6/00 | 2816.4 | siltstone | Montney |
| 8732 | M23 | 100/05-32-073-12W6/00 | 2817.9 | siltstone | Montney |
| 8733 | M23 | 100/05-32-073-12W6/00 | 2819.4 | siltstone | Montney |
| 8734 | M23 | 100/05-32-073-12W6/00 | 2823.3 | siltstone | Montney |
| 8735 | M23 | 100/05-32-073-12W6/00 | 2825.9 | siltstone | Montney |
| 8736 | M23 | 100/05-32-073-12W6/00 | 2832.2 | sandstone | Montney |
| 8737 | M7 | 103/10-34-064-19W5/00 | 1768.5 | siltstone and sandstone | Montney |

| Sample No. | Site No. | Location - UWI | Sample Depth (Metres) | Lithology | Formation/ Group |
|---|---|---|---|---|---|
| 8738 | M7 | 103/10-34-064-19W5/00 | 1770.7 | siltstone and sandstone | Montney |
| 8739 | M7 | 103/10-34-064-19W5/00 | 1776.2 | sandstone | Montney |
| 8740 | M7 | 103/10-34-064-19W5/00 | 1778.5 | muddy siltstone | Montney |
| 8741 | M7 | 103/10-34-064-19W5/00 | 1778.7 | coquina | Montney |
| 8742 | M7 | 103/10-34-064-19W5/00 | 1781.2 | muddy siltstone and sandstone | Montney |
| 8743 | M7 | 103/10-34-064-19W5/00 | 1785.9 | sandy siltstone | Montney |
| 8744 | M4 | 102/11-34-061-19W5/00 | 2163.5 | sandy siltstone | Montney |
| 8745 | M4 | 102/11-34-061-19W5/00 | 2166.3 | sandy siltstone | Montney |
| 8746 | M4 | 102/11-34-061-19W5/00 | 2169.7 | silty sandstone | Montney |
| 8747 | M4 | 102/11-34-061-19W5/00 | 2171.4 | sandy siltstone | Montney |
| 8748 | M4 | 102/11-34-061-19W5/00 | 2172.0 | coquina | Montney |
| 8749 | M4 | 102/11-34-061-19W5/00 | 2176.6 | siltstone | Montney |
| 8750 | M4 | 102/11-34-061-19W5/00 | 2180.4 | sandstone | Montney |
| 8751 | M10 | 100/07-05-067-07W6/00 | 3076.3 | sandy siltstone | Montney |
| 8752 | M10 | 100/07-05-067-07W6/00 | 3078.8 | sandy siltstone | Montney |
| 8753 | M10 | 100/07-05-067-07W6/00 | 3080.3 | siltstone | Montney |
| 8754 | M10 | 100/07-05-067-07W6/00 | 3081.4 | siltstone | Montney |
| 8755 | M10 | 100/07-05-067-07W6/00 | 3084.5 | siltstone | Montney |
| 8756 | M10 | 100/07-05-067-07W6/00 | 3088.4 | sandy siltstone | Montney |
| 8757 | M10 | 100/07-05-067-07W6/00 | 3093.7 | sandy siltstone | Montney |
| 8758 | M19 | 100/11-28-071-03W6/00 | 1820.5 | siltstone and sandstone | Montney |
| 8759 | M19 | 100/11-28-071-03W6/00 | 1823.6 | siltstone and sandstone | Montney |
| 8760 | M19 | 100/11-28-071-03W6/00 | 1826.4 | siltstone | Montney |
| 8761 | M19 | 100/11-28-071-03W6/00 | 1829.9 | siltstone and sandstone | Montney |
| 8762 | M19 | 100/11-28-071-03W6/00 | 1836.1 | siltstone and sandstone | Montney |
| 8763 | M19 | 100/11-28-071-03W6/00 | 1839.1 | sandy siltstone | Montney |
| 8764 | M19 | 100/11-28-071-03W6/00 | 1840.7 | silty sandstone | Montney |
| 8765 | M19 | 100/11-28-071-03W6/00 | 1845.8 | siltstone | Montney |
| 8766 | M19 | 100/11-28-071-03W6/00 | 1849.6 | sandstone | Montney |
| 8767 | M19 | 100/11-28-071-03W6/00 | 1852.1 | sandy siltstone | Montney |
| 8768 | M19 | 100/11-28-071-03W6/00 | 1857.6 | siltstone and sandstone | Montney |
| 8769 | M19 | 100/11-28-071-03W6/00 | 1858.3 | siltstone | Montney |
| 8770 | M19 | 100/11-28-071-03W6/00 | 1862.8 | siltstone | Montney |
| 8771 | M19 | 100/11-28-071-03W6/00 | 1864.9 | sandstone | Montney |
| 8772 | M19 | 100/11-28-071-03W6/00 | 1869.8 | sandy siltstone | Montney |
| 8773 | M40 | 100/10-21-092-03W6/00 | 778.5 | muddy siltstone | Montney |
| 8774 | M40 | 100/10-21-092-03W6/00 | 781.1 | muddy siltstone | Montney |
| 8775 | M40 | 100/10-21-092-03W6/00 | 783.3 | siltstone | Montney |
| 8776 | M40 | 100/10-21-092-03W6/00 | 784.6 | sandy siltstone | Montney |
| 8777 | M40 | 100/10-21-092-03W6/00 | 787.3 | siltstone | Montney |
| 8778 | M40 | 100/10-21-092-03W6/00 | 791.6 | muddy siltstone with sandstone | Montney |
| 8779 | M40 | 100/10-21-092-03W6/00 | 795.7 | mudstone | Montney |
| 8780 | M40 | 100/10-21-092-03W6/00 | 798.3 | sandstone | Montney |
| 8781 | M15 | 100/13-05-068-01W6/00 | 2044.4 | siltstone | Montney |
| 8782 | M15 | 100/13-05-068-01W6/00 | 2047.7 | coquina | Montney |
| 8783 | M15 | 100/13-05-068-01W6/00 | 2048.8 | sandstone | Montney |
| 8784 | M15 | 100/13-05-068-01W6/00 | 2055.4 | silty sandstone | Montney |
| 8785 | M15 | 100/13-05-068-01W6/00 | 2057.4 | siltstone | Montney |
| 8786 | M15 | 100/13-05-068-01W6/00 | 2235.3 | sandy siltstone | Montney |
| 8787 | M15 | 100/13-05-068-01W6/00 | 2238.5 | siltstone | Montney |
| 8788 | M15 | 100/13-05-068-01W6/00 | 2240.9 | siltstone | Montney |
| 8789 | M15 | 100/13-05-068-01W6/00 | 2245.8 | grainstone | Belloy |
| 8790 | M13 | 100/13-31-067-18W5/00 | 1628.1 | shale | Nordegg |
| 8791 | M13 | 100/13-31-067-18W5/00 | 1658.7 | sandy mudstone and siltstone | Montney |
| 8792 | M13 | 100/13-31-067-18W5/00 | 1662.1 | sandy siltstone | Montney |
| 8793 | M13 | 100/13-31-067-18W5/00 | 1665.9 | sandy siltstone | Montney |
| 8794 | M13 | 100/13-31-067-18W5/00 | 1672.9 | silty sandstone | Montney |
| 8795 | M32 | 102/14-20-079-22W5/00 | 864.7 | sandy siltstone | Montney |
| 8796 | M32 | 102/14-20-079-22W5/00 | 866.6 | siltstone and sandstone | Montney |
| 8797 | M32 | 102/14-20-079-22W5/00 | 872.0 | silty sandstone | Montney |
| 8798 | M32 | 102/14-20-079-22W5/00 | 876.7 | siltstone and sandstone | Montney |
| 8799 | M32 | 102/14-20-079-22W5/00 | 879.2 | sandy siltstone | Montney |

| Sample No. | Site No. | Location - UWI | Sample Depth (Metres) | Lithology | Formation/ Group |
|---|---|---|---|---|---|
| 8800 | M5 | 100/11-24-062-20W5/00 | 2080.9 | shale | Nordegg |
| 8801 | M5 | 100/11-24-062-20W5/00 | 2087.6 | coquina | Montney |
| 8802 | M5 | 100/11-24-062-20W5/00 | 2090.3 | coquina | Montney |
| 8803 | M5 | 100/11-24-062-20W5/00 | 2094.9 | coquina | Montney |
| 8804 | M5 | 100/11-24-062-20W5/00 | 2097.3 | sandy siltstone | Montney |
| 8805 | M5 | 100/11-24-062-20W5/00 | 2102.2 | sandy siltstone | Montney |
| 8806 | M5 | 100/11-24-062-20W5/00 | 2105.1 | sandy siltstone | Montney |
| 8807 | M5 | 100/11-24-062-20W5/00 | 2107.8 | sandy siltstone | Montney |
| 8808 | M3 | 100/04-06-059-20W5/00 | 2643.9 | shale | Nordegg |
| 8809 | M3 | 100/04-06-059-20W5/00 | 2644.3 | shale | Nordegg |
| 8810 | M3 | 100/04-06-059-20W5/00 | 2645.9 | sandstone | Montney |
| 8811 | M3 | 100/04-06-059-20W5/00 | 2648.2 | silty sandstone | Montney |
| 8812 | M3 | 100/04-06-059-20W5/00 | 2651.1 | sandy siltstone | Montney |
| 8813 | M3 | 100/04-06-059-20W5/00 | 2656.4 | sandy siltstone | Montney |
| 8814 | M3 | 100/04-06-059-20W5/00 | 2658.8 | sandy siltstone | Montney |
| 8815 | M3 | 100/04-06-059-20W5/00 | 2660.9 | sandy siltstone | Montney |
| 8816 | M1 | 100/11-14-057-23W5/00 | 3007.1 | siltstone | Montney |
| 8817 | M1 | 100/11-14-057-23W5/00 | 3008.7 | sandy siltstone | Montney |
| 8818 | M1 | 100/11-14-057-23W5/00 | 3010.8 | siltstone | Montney |
| 8819 | M1 | 100/11-14-057-23W5/00 | 3013.3 | siltstone | Montney |
| 8820 | M1 | 100/11-14-057-23W5/00 | 3013.9 | coquina | Montney |
| 8821 | M1 | 100/11-14-057-23W5/00 | 3019.4 | sandstone | Montney |
| 8822 | M21 | 100/06-33-072-25W5/00 | 1590.1 | siltstone | Montney |
| 8823 | M21 | 100/06-33-072-25W5/00 | 1592.2 | siltstone | Montney |
| 8824 | M21 | 100/06-33-072-25W5/00 | 1595.5 | sandy siltstone | Montney |
| 8825 | M21 | 100/06-33-072-25W5/00 | 1597.5 | sandy siltstone | Montney |
| 8826 | M21 | 100/06-33-072-25W5/00 | 1602.0 | siltstone | Montney |
| 8827 | M21 | 100/06-33-072-25W5/00 | 1607.4 | sandy siltstone | Montney |
| 8828 | M22 | 100/06-34-072-25W5/00 | 1535.4 | shale | Nordegg |
| 8829 | M22 | 100/06-34-072-25W5/00 | 1536.1 | shale | Nordegg |
| 8830 | M22 | 100/06-34-072-25W5/00 | 1538.3 | siltstone | Montney |
| 8831 | M22 | 100/06-34-072-25W5/00 | 1542.5 | sandy siltstone | Montney |
| 8832 | M22 | 100/06-34-072-25W5/00 | 1545.4 | siltstone | Montney |
| 8833 | M22 | 100/06-34-072-25W5/00 | 1550.0 | sandy siltstone | Montney |
| 8834 | M2 | 100/16-23-057-06W6/00 | 2479.9 | silty shale | Doig |
| 8835 | M2 | 100/16-23-057-06W6/00 | 2480.8 | siltstone | Doig |
| 8836 | M2 | 100/16-23-057-06W6/00 | 2481.1 | shaley siltstone | Doig |
| 8837 | M2 | 100/16-23-057-06W6/00 | 2482.4 | lag | Doig |
| 8838 | M2 | 100/16-23-057-06W6/00 | 2485.3 | siltstone | Montney |
| 8839 | M2 | 100/16-23-057-06W6/00 | 2487.2 | siltstone | Montney |
| 8840 | M2 | 100/16-23-057-06W6/00 | 2489.3 | siltstone | Montney |
| 8841 | M2 | 100/16-23-057-06W6/00 | 2491.1 | siltstone | Montney |
| 8842 | M2 | 100/16-23-057-06W6/00 | 2515.2 | siltstone | Montney |
| 8843 | M2 | 100/16-23-057-06W6/00 | 2516.4 | siltstone | Montney |
| 8844 | M2 | 100/16-23-057-06W6/00 | 2519.2 | siltstone | Montney |
| 8845 | M2 | 100/16-23-057-06W6/00 | 2521.0 | silty sandstone | Montney |
| 8846 | M2 | 100/16-23-057-06W6/00 | 2522.8 | siltstone | Montney |
| 8847 | M2 | 100/16-23-057-06W6/00 | 2646.6 | siltstone | Montney |
| 8848 | M2 | 100/16-23-057-06W6/00 | 2649.0 | siltstone | Montney |
| 8849 | M2 | 100/16-23-057-06W6/00 | 2650.2 | siltstone | Montney |
| 8850 | M2 | 100/16-23-057-06W6/00 | 2652.1 | siltstone | Montney |
| 8851 | M2 | 100/16-23-057-06W6/00 | 2687.4 | siltstone | Montney |
| 8852 | M2 | 100/16-23-057-06W6/00 | 2688.0 | sandstone | Montney |
| 8853 | M2 | 100/16-23-057-06W6/00 | 2689.6 | siltstone | Montney |
| 8854 | M2 | 100/16-23-057-06W6/00 | 2691.7 | siltstone | Montney |
| 8855 | M2 | 100/16-23-057-06W6/00 | 2694.4 | sandy siltstone | Montney |
| 8856 | M2 | 100/16-23-057-06W6/00 | 2696.3 | sandy siltstone | Montney |
| 8857 | M2 | 100/16-23-057-06W6/00 | 2699.9 | sandy siltstone | Montney |
| 8858 | M2 | 100/16-23-057-06W6/00 | 2703.6 | siltstone | Montney |
| 8859 | M30 | 102/11-34-078-02W6/00 | 1770.3 | shaley siltstone | Montney |
| 8860 | M30 | 102/11-34-078-02W6/00 | 1774.8 | siltstone | Montney |
| 8861 | M30 | 102/11-34-078-02W6/00 | 1778.0 | sandy siltstone | Montney |

| Sample No. | Site No. | Location - UWI | Sample Depth (Metres) | Lithology | Formation/ Group |
|---|---|---|---|---|---|
| 8862 | M30 | 102/11-34-078-02W6/00 | 1779.9 | sandy siltstone | Montney |
| 8863 | M30 | 102/11-34-078-02W6/00 | 1780.7 | silty sandstone | Montney |
| 8864 | M30 | 102/11-34-078-02W6/00 | 1782.2 | sandy siltstone | Montney |
| 8865 | M30 | 102/11-34-078-02W6/00 | 1785.3 | siltstone and sandstone | Montney |
| 8866 | M30 | 102/11-34-078-02W6/00 | 1787.3 | sandy siltstone | Montney |
| 8867 | M26 | 100/15-06-076-03W6/00 | 1444.9 | sandy siltstone | Doig |
| 8868 | M26 | 100/15-06-076-03W6/00 | 1446.0 | siltstone | Doig |
| 8869 | M26 | 100/15-06-076-03W6/00 | 1449.6 | siltstone | Doig |
| 8870 | M26 | 100/15-06-076-03W6/00 | 1452.0 | siltstone | Doig |
| 8871 | M26 | 100/15-06-076-03W6/00 | 1453.7 | siltstone | Doig |
| 8872 | M26 | 100/15-06-076-03W6/00 | 1457.6 | siltstone | Montney |
| 8873 | M26 | 100/15-06-076-03W6/00 | 1458.6 | sandy siltstone | Montney |
| 8874 | M26 | 100/15-06-076-03W6/00 | 1458.9 | siltstone | Montney |
| 8875 | M9 | 100/16-31-066-23W5/00 | 1708.6 | sandy siltstone | Montney |
| 8876 | M9 | 100/16-31-066-23W5/00 | 1711.5 | sandy siltstone | Montney |
| 8877 | M9 | 100/16-31-066-23W5/00 | 1713.7 | silty sandstone | Montney |
| 8878 | M9 | 100/16-31-066-23W5/00 | 1718.1 | siltstone | Montney |
| 8879 | M9 | 100/16-31-066-23W5/00 | 1720.0 | sandy siltstone | Montney |
| 8880 | M9 | 100/16-31-066-23W5/00 | 1721.9 | siltstone | Montney |
| 8881 | M9 | 100/16-31-066-23W5/00 | 1725.5 | siltstone | Montney |
| 8882 | M11 | 100/12-07-067-24W5/00 | 1904.4 | shale or calcilutite | Nordegg |
| 8883 | M11 | 100/12-07-067-24W5/00 | 1905.9 | shale | Nordegg |
| 8884 | M11 | 100/12-07-067-24W5/00 | 1908.3 | shale | Nordegg |
| 8885 | M11 | 100/12-07-067-24W5/00 | 1908.8 | sandy siltstone | Montney |
| 8886 | M11 | 100/12-07-067-24W5/00 | 1910.1 | siltstone | Montney |
| 8887 | M11 | 100/12-07-067-24W5/00 | 1914.4 | sandy siltstone | Montney |
| 8888 | M11 | 100/12-07-067-24W5/00 | 1917.6 | siltstone | Montney |
| 8889 | M11 | 100/12-07-067-24W5/00 | 1920.5 | sandy siltstone | Montney |
| 8890 | M11 | 100/12-07-067-24W5/00 | 1922.6 | siltstone | Montney |
| 8891 | M6 | 100/07-14-064-25W5/00 | 2289.0 | shale or calcilutite. | Nordegg |
| 8892 | M6 | 100/07-14-064-25W5/00 | 2289.6 | shale | Nordegg |
| 8893 | M6 | 100/07-14-064-25W5/00 | 2291.5 | sandy siltstone | Montney |
| 8894 | M6 | 100/07-14-064-25W5/00 | 2295.2 | sandy siltstone | Montney |
| 8895 | M6 | 100/07-14-064-25W5/00 | 2297.3 | siltstone | Montney |
| 8896 | M6 | 100/07-14-064-25W5/00 | 2300.2 | siltstone | Montney |
| 8897 | M6 | 100/07-14-064-25W5/00 | 2304.0 | shaley siltstone | Montney |
| 8898 | M6 | 100/07-14-064-25W5/00 | 2306.9 | shaley siltstone | Montney |
| 8899 | M8 | 100/06-14-066-06W6/00 | 3026.4 | siltstone | Montney |
| 8900 | M8 | 100/06-14-066-06W6/00 | 3030.6 | siltstone | Montney |
| 8901 | M8 | 100/06-14-066-06W6/00 | 3034.3 | siltstone | Montney |
| 8902 | M8 | 100/06-14-066-06W6/00 | 3037.8 | siltstone | Montney |
| 8903 | M8 | 100/06-14-066-06W6/00 | 3040.6 | siltstone | Montney |
| 8904 | M8 | 100/06-14-066-06W6/00 | 3044.1 | siltstone | Montney |
| 8905 | M39 | 102/01-14-091-12W6/00 | 1110.8 | shaley siltstone | Montney |
| 8906 | M39 | 102/01-14-091-12W6/00 | 1111.9 | silty sandstone | Montney |
| 8907 | M39 | 102/01-14-091-12W6/00 | 1113.4 | silty sandstone | Montney |
| 8908 | M39 | 102/01-14-091-12W6/00 | 1116.9 | silty sandstone | Montney |
| 8909 | M39 | 102/01-14-091-12W6/00 | 1118.2 | sandy siltstone | Montney |
| 8910 | M38 | 100/04-32-084-12W6/00 | 1581.3 | siltstone | Montney |
| 8911 | M38 | 100/04-32-084-12W6/00 | 1582.3 | sandy siltstone | Montney |
| 8912 | M38 | 100/04-32-084-12W6/00 | 1584.1 | siltstone | Montney |
| 8913 | M38 | 100/04-32-084-12W6/00 | 1586.0 | silty sandstone | Montney |
| 8914 | M38 | 100/04-32-084-12W6/00 | 1587.0 | sandy siltstone | Montney |
| 8915 | M38 | 100/04-32-084-12W6/00 | 1592.5 | siltstone | Montney |
| 8916 | M35 | 100/14-30-082-07W6/00 | 1231.2 | siltstone | Montney |
| 8917 | M35 | 100/14-30-082-07W6/00 | 1233.9 | siltstone | Montney |
| 8918 | M35 | 100/14-30-082-07W6/00 | 1235.6 | siltstone | Montney |
| 8919 | M35 | 100/14-30-082-07W6/00 | 1238.7 | sandy siltstone | Montney |
| 8920 | M35 | 100/14-30-082-07W6/00 | 1240.6 | siltstone | Montney |
| 8921 | M35 | 100/14-30-082-07W6/00 | 1241.6 | silty sandstone | Montney |
| 8922 | M35 | 100/14-30-082-07W6/00 | 1243.9 | siltstone | Montney |
| 8923 | M35 | 100/14-30-082-07W6/00 | 1245.7 | siltstone | Montney |

| Sample No. | Site No. | Location - UWI | Sample Depth (Metres) | Lithology | Formation/ Group |
|---|---|---|---|---|---|
| 8924 | M35 | 100/14-30-082-07W6/00 | 1248.3 | sandy siltstone | Montney |
| 8925 | M34 | 100/15-08-081-12W6/00 | 1824.9 | siltstone | Montney |
| 8926 | M34 | 100/15-08-081-12W6/00 | 1827.7 | siltstone | Montney |
| 8927 | M34 | 100/15-08-081-12W6/00 | 1830.1 | siltstone | Montney |
| 8928 | M34 | 100/15-08-081-12W6/00 | 1833.1 | siltstone | Montney |
| 8929 | M34 | 100/15-08-081-12W6/00 | 1836.0 | siltstone | Montney |
| 8930 | M34 | 100/15-08-081-12W6/00 | 1839.1 | siltstone | Montney |
| 8931 | M36 | 100/11-32-082-25W5/00 | 924.8 | shale | Nordegg |
| 8932 | M36 | 100/11-32-082-25W5/00 | 926.4 | shale | Nordegg |
| 8933 | M36 | 100/11-32-082-25W5/00 | 927.4 | sandy siltstone | Montney |
| 8934 | M36 | 100/11-32-082-25W5/00 | 929.0 | sandy siltstone | Montney |
| 8935 | M36 | 100/11-32-082-25W5/00 | 933.9 | siltstone | Montney |
| 8936 | M36 | 100/11-32-082-25W5/00 | 936.7 | siltstone | Montney |
| 8937 | M36 | 100/11-32-082-25W5/00 | 940.4 | sandstone | Montney |
| 8938 | M18 | 100/02-30-071-20W5/00 | 1316.1 | shale | Nordegg |
| 8939 | M18 | 100/02-30-071-20W5/00 | 1318.1 | shale | Nordegg |
| 8940 | M18 | 100/02-30-071-20W5/00 | 1319.6 | sandstone | Montney |
| 8941 | M18 | 100/02-30-071-20W5/00 | 1322.2 | sandstone | Montney |
| 8942 | M18 | 100/02-30-071-20W5/00 | 1324.3 | sandy siltstone | Montney |
| 8943 | M18 | 100/02-30-071-20W5/00 | 1327.4 | siltstone | Montney |
| 8944 | M12 | 100/14-27-067-08W6/00 | 3013.6 | sandy siltstone | Montney |
| 8945 | M12 | 100/14-27-067-08W6/00 | 3017.1 | silty sandstone | Montney |
| 8946 | M12 | 100/14-27-067-08W6/00 | 3019.3 | silty sandstone | Montney |
| 8947 | M12 | 100/14-27-067-08W6/00 | 3021.5 | siltstone | Montney |
| 8948 | M12 | 100/14-27-067-08W6/00 | 3026.9 | siltstone | Montney |
| 8949 | M12 | 100/14-27-067-08W6/00 | 3029.7 | sandy siltstone | Montney |
| 8950 | M12 | 100/14-27-067-08W6/00 | 3032.0 | sandy siltstone | Montney |
| 8951 | M16 | 100/06-23-068-08W6/00 | 2972.8 | sandstone | Montney |
| 8952 | M16 | 100/06-23-068-08W6/00 | 2975.0 | sandstone | Belloy |
| 8953 | M16 | 100/06-23-068-08W6/00 | 2975.7 | conglomerate | Belloy |
| 8954 | M16 | 100/06-23-068-08W6/00 | 2980.7 | sandstone | Belloy |
| 8955 | M16 | 100/06-23-068-08W6/00 | 2982.4 | sandstone | Belloy |
| 8956 | M31 | 100/06-12-079-12W6/00 | 2013.6 | sandy siltstone | Montney |
| 8957 | M31 | 100/06-12-079-12W6/00 | 2016.1 | sandy siltstone | Montney |
| 8958 | M31 | 100/06-12-079-12W6/00 | 2020.1 | sandy siltstone | Montney |
| 8959 | M31 | 100/06-12-079-12W6/00 | 2024.0 | sandy siltstone | Montney |
| 8960 | M31 | 100/06-12-079-12W6/00 | 2024.7 | sandy siltstone | Montney |
| 8961 | M31 | 100/06-12-079-12W6/00 | 2028.5 | sandy siltstone | Montney |
| 8962 | M31 | 100/06-12-079-12W6/00 | 2030.9 | sandy siltstone | Montney |
| 8963 | M24 | 100/01-14-075-11W6/00 | 2477.5 | sandy siltstone | Montney |
| 8964 | M24 | 100/01-14-075-11W6/00 | 2480.3 | siltstone | Montney |
| 8965 | M24 | 100/01-14-075-11W6/00 | 2483.0 | shaley siltstone | Montney |
| 8966 | M24 | 100/01-14-075-11W6/00 | 2486.5 | sandy siltstone | Montney |
| 8967 | M24 | 100/01-14-075-11W6/00 | 2489.2 | siltstone | Montney |
| 8968 | M24 | 100/01-14-075-11W6/00 | 2491.8 | shaley siltstone | Montney |
| 8969 | M24 | 100/01-14-075-11W6/00 | 2495.1 | silty sandstone | Montney |
| 8970 | M17 | 100/05-24-068-22W5/00 | 1552.9 | shale | Nordegg |
| 8971 | M17 | 100/05-24-068-22W5/00 | 1553.5 | shale | Nordegg |
| 8972 | M17 | 100/05-24-068-22W5/00 | 1556.3 | coquina | Montney |
| 8973 | M17 | 100/05-24-068-22W5/00 | 1559.2 | silty sandstone | Montney |
| 8974 | M17 | 100/05-24-068-22W5/00 | 1560.2 | silty sandstone | Montney |
| 8975 | M17 | 100/05-24-068-22W5/00 | 1562.5 | silty sandstone | Montney |
| 8976 | M17 | 100/05-24-068-22W5/00 | 1564.7 | sandy siltstone | Montney |
| 8977 | M17 | 100/05-24-068-22W5/00 | 1568.3 | sandy siltstone | Montney |
| 9247 | M15 | 100/13-05-068-01W6/00 | 2240.9 | duplicate of sample 8788 | Montney |
| 9248 | M13 | 100/13-31-067-18W5/00 | 1662.1 | duplicate of sample 8792 | Montney |
| 9249 | M5 | 100/11-24-062-20W5/00 | 2105.1 | duplicate of sample 8806 | Montney |
| 9250 | | standard | | standard Green River shale USGS (SRG-1b) | standard |
| 9251 | M18 | 100/02-30-071-20W5/00 | 1324.3 | duplicate of sample 8942 | Montney |
| 9252 | M17 | 100/05-24-068-22W5/00 | 1568.3 | duplicate of sample 8977 | Montney |
| 9253 | M31 | 100/06-12-079-12W6/00 | 2013.5 | duplicate of sample 8956 | Montney |
| 9254 | M21 | 100/06-33-072-25W5/00 | 1590.1 - 1592.2 | combined samples 8822 and 8823 | Montney |

| Sample No. | Site No. | Location - UWI | Sample Depth (Metres) | Lithology | Formation/ Group |
|---|---|---|---|---|---|
| 9255 | M23 | 100/05-32-073-12W6/00 | 2816.4 - 2823.3 | combined samples 8731, 8732, 8733, 8734 | Montney |
| 9256 | M10 | 100/07-05-067-07W6/00 | 3088.4 - 3093.7 | combined samples 8756, 8757 | Montney |
| 9257 | M2 | 100/16-23-057-06W6/00 | 2646.6 - 2650.2 | combined samples 8847, 8848, 8849 | Montney |
| 9258 | M6 | 100/07-14-064-25W5/00 | 2297.3 - 2306.9 | combined samples 8895, 8896, 8897, 8898 | Montney |
| 9259 | M8 | 100/06-14-066-06W6/00 | 3030.6 - 3044.1 | combined samples 8900, 8901, 8902, 8903, 8904 | Montney |
| 9260 | M34 | 100/15-08-081-12W6/00 | 1827.7 - 1839.1 | combined samples 8926, 8927, 8928, 8929, 8930 | Montney |

## Appendix 2 – Montney Formation Core Samples Analyzed

**Legend**

Y = Sample data presented in this report
x = Sample data presented in other Alberta Geological Survey reports (see Table 1 for details)
z = Data are being analyzed and will be distributed in a future report
Analyses presented in this report

| Column Label | Label Description |
|---|---|
| Sample No. | AGS sample number |
| Site No. | Site location number |
| Rock Eval™ TOC | Rock Eval™ pyrolysis is used to identify the type and maturity of organic matter and to detect petroleum potential in sediments. Total Organic Carbon is a measure of the amount of organic carbon in the sediment (in weight per cent). |
| XRD-Bulk | X-Ray diffraction analysis of whole rock mineralogy |
| XRD-Clay | X-Ray diffraction analysis of clay mineralogy |
| Organic Pet. | Petrographic imaging and description of organic macerals |
| Thin Section | Thin section of sample |
| Adsorption Isotherm | Gas adsorption analysis to determine gas-holding capacity of sample |
| SEM | Scanning electron microscope |
| Mini-perm | Analysis to determine permeability |
| Porosimetry | Analysis to determine pore-throat size |
| Pycnometry | Analysis to determine grain density |
| Texture with Clay Mineralogy | Determination of sand, silt and clay size distribution in weight per cent with clay mineralogy on clay separates. |

| Sample No. | Site No. | RockEval TOC | XRD-Bulk | XRD-Clay | Organic Pet. | Thin Section | Adsorption Isotherm | SEM | Mini-perm | Porosimetry | Pycnometry | Texture with Clay Mineralogy |
|---|---|---|---|---|---|---|---|---|---|---|---|---|
| 8113 | M25 | x | | | | | | | | | | |
| 8114 | M25 | x | | | | | | | | | | |
| 8115 | M25 | x | | | | z | | | Y | | | |
| 8116 | M25 | x | | | | | | | | | | |
| 8117 | M25 | x | | | x | | | | | | | |
| 8118 | M25 | x | | | | | | | | | | |
| 8119 | M14 | x | | | | | | | Y | | | z |
| 8120 | M14 | x | | | | | | | | | | |
| 8121 | M14 | x | | | | | | | | | | |
| 8122 | M14 | x | | | x | | | | | | | |
| 8123 | M33 | x | | | | | | | | | | |
| 8124 | M33 | x | | | x | | | | | | | z |
| 8125 | M33 | x | | | | z | | | | | | |
| 8126 | M33 | x | Y | | | | | | | | | |
| 8131 | M37 | x | | | x | | | | | | | |
| 8132 | M37 | x | | | | | | | | | | |
| 8701 | M27 | x | | | | | | | | | | |
| 8702 | M27 | x | | | x | | | | | Y | Y | |
| 8703 | M27 | x | | | | | | | | | | |
| 8704 | M27 | x | | | | | | | | | | |
| 8705 | M28 | x | | | x | | | Y | | | | |
| 8706 | M28 | x | | | | | | | | | | z |
| 8707 | M28 | x | | | | z | | | Y | | | |
| 8708 | M28 | x | | | | | | | | | | |
| 8709 | M29 | x | | | x | | | Y | | | | |
| 8710 | M29 | x | | | | | | | | | | |
| 8711 | M29 | x | | | | | | | | | | |
| 8712 | M29 | x | | | | | | | | | | |
| 8713 | M29 | x | | | | | | | | | | |
| 8714 | M29 | x | | | x | | | | | | | |
| 8715 | M29 | x | | | | | | | | | | |
| 8716 | M20 | x | | | | | | | | | | |
| 8717 | M20 | | | | | | | | | | | |
| 8718 | M20 | x | | | | z | | | Y | | | |
| 8719 | M20 | x | | | | | | | | | | |
| 8720 | M20 | x | | | | | | | | | | |
| 8721 | M20 | x | | | | | | | | | | |
| 8722 | M20 | x | | | | | | | | | | |
| 8723 | M20 | x | | | | | | | | | | |
| 8724 | M20 | x | | | x | | | | | | | |
| 8725 | M20 | x | | | | | | | | | | |
| 8726 | M20 | | | | | | | | | | | |
| 8727 | M20 | x | | | | | | | | | | |
| 8728 | M20 | | | | | | | | | | | |
| 8729 | M20 | x | | | x | | | | | | | |
| 8730 | M23 | x | Y | Y | | | | | | | | |
| 8731 | M23 | | | | | | | Y | | | | |
| 8732 | M23 | x | | | x | | | | | | | |
| 8733 | M23 | | | | | | | | | | | |
| 8734 | M23 | x | | | | | | | | | | |
| 8735 | M23 | | | | | | | | | | | |
| 8736 | M23 | x | | | | | | | | | | |
| 8737 | M7 | x | | | | | | | | | | |
| 8738 | M7 | | | | | | | | | | | |
| 8739 | M7 | x | | | x | | | Y | | | | |
| 8740 | M7 | | | | | | | | | | | |
| 8741 | M7 | | | | | | | | | | | |
| 8742 | M7 | | | | | | | | | | | |
| 8743 | M7 | x | | | | | | | | | | |
| 8744 | M4 | | | | | | | Y | | | | |
| 8745 | M4 | x | | | x | | | | | | | |
| 8746 | M4 | | | | | | | | | | | |
| 8747 | M4 | x | | | | | | | | | | |
| 8748 | M4 | | | | | | | | | | | |
| 8749 | M4 | | | | | | | | | | | |
| 8750 | M4 | x | | | | | | | | | | |
| 8751 | M10 | x | | | x | | | | | | | |
| 8752 | M10 | | | | | | | | | | | |
| 8753 | M10 | x | Y | Y | | | | | | | | |
| 8754 | M10 | x | | | | | | | | | | |
| 8755 | M10 | x | | | x | | | | | | | |

| Sample No. | Site No. | RockEval TOC | XRD-Bulk | XRD-Clay | Organic Pet. | Thin Section | Adsorption Isotherm | SEM | Mini-perm | Porosimetry | Pycnometry | Texture with Clay Mineralogy |
|---|---|---|---|---|---|---|---|---|---|---|---|---|
| 8756 | M10 | x | | | | | | | | | | |
| 8757 | M10 | x | | | x | | | | | | | |
| 8758 | M19 | x | | | | | | | | | | |
| 8759 | M19 | | | | | | | | | | | |
| 8760 | M19 | x | | | | | | | | | | |
| 8761 | M19 | x | Y | Y | | | | | | | | |
| 8762 | M19 | x | | | | | | | | | | |
| 8763 | M19 | | | | | | | | | | | |
| 8764 | M19 | x | | | | | | | | z | Y | |
| 8765 | M19 | x | | | x | | | | | | | |
| 8766 | M19 | | | | | | | | | | | |
| 8767 | M19 | x | | | | | | | | | | |
| 8768 | M19 | x | | | | | | | | | | |
| 8769 | M19 | | | | | | | | | | | |
| 8770 | M19 | x | | | x | | | | | | | |
| 8771 | M19 | | | | | | | | | | | |
| 8772 | M19 | x | | | | | | | | | | |
| 8773 | M40 | | | | | | | | | | | |
| 8774 | M40 | x | | | x | | | | | | | |
| 8775 | M40 | | | | | | | | | | | |
| 8776 | M40 | | | | | | | | | | | |
| 8777 | M40 | | | | | | | | | | | |
| 8778 | M40 | | | | | | | | | | | |
| 8779 | M40 | | | | | | | | | | | |
| 8780 | M40 | x | | | | | | | | | | |
| 8781 | M15 | x | | | | | | | | | | |
| 8782 | M15 | x | | | | | | | | | | |
| 8783 | M15 | | | | | | | | | | | |
| 8784 | M15 | x | | | | | | | | | | |
| 8785 | M15 | x | | | x | | | | | | | |
| 8786 | M15 | x | | | | z | | | Y | | | z |
| 8787 | M15 | | | | | | | | | | | |
| 8788 | M15 | x | | | x | | | | | | | |
| 8789 | M15 | x | | | x | | | | | | | |
| 8790 | M13 | x | | | x | | | | | | | |
| 8791 | M13 | | | | | | | | | | | |
| 8792 | M13 | x | | | | | | | | | | |
| 8793 | M13 | x | | | x | | | | | | | |
| 8794 | M13 | x | | | | | | | | | | |
| 8795 | M32 | | | | | | | | | | | |
| 8796 | M32 | x | | | x | | | | | | | |
| 8797 | M32 | | | | | | | | | | | |
| 8798 | M32 | | | | | | | | | | | |
| 8799 | M32 | x | | | | | | | | | | |
| 8800 | M5 | x | | | | | | | | | | |
| 8801 | M5 | | | | | | | | | | | |
| 8802 | M5 | | | | | | | | | | | |
| 8803 | M5 | | | | | | | | | | | |
| 8804 | M5 | | | | | | | | | | | |
| 8805 | M5 | | | | | | | | | | | |
| 8806 | M5 | x | | | x | | | | | | | |
| 8807 | M5 | | | | | | | | | | | |
| 8808 | M3 | x | | | | | | | | | | |
| 8809 | M3 | | | | | | | | | | | |
| 8810 | M3 | | | | | | | | | | | |
| 8811 | M3 | | | | | | | | | | | |
| 8812 | M3 | | | | | | | | | | | |
| 8813 | M3 | x | | | x | | | | | | | |
| 8814 | M3 | | | | | | | | | | | |
| 8815 | M3 | | | | | | | | | | | |
| 8816 | M1 | | | | | | | | | | | |
| 8817 | M1 | | | | | | | | | | | |
| 8818 | M1 | | | | | | | | | | | |
| 8819 | M1 | x | Y | Y | x | | | | | | | |
| 8820 | M1 | | | | | | | | | | | |
| 8821 | M1 | | | | | | | | | | | |
| 8822 | M21 | x | | | | | | | | | | |
| 8823 | M21 | x | | | | | | | | | | |
| 8824 | M21 | x | | | x | | | | | | | |
| 8825 | M21 | | | | | | | | | | | |
| 8826 | M21 | x | | | | | | | | | | |
| 8827 | M21 | x | | | | | | | | | | |
| 8828 | M22 | x | | | | | | | | | | |
| 8829 | M22 | | | | | | | | | | | |
| 8830 | M22 | | | | | | | | | | | |
| 8831 | M22 | x | | | x | | | | | | | |
| 8832 | M22 | | | | | | | | | | | |
| 8833 | M22 | | | | | | | | | | | |
| 8834 | M2 | x | | | | | | | | | | |
| 8835 | M2 | | | | | | | | | | | |
| 8836 | M2 | | | | | | | | | | | |
| 8837 | M2 | x | | | | | | | | | | |
| 8838 | M2 | x | | | | | | | | | | |
| 8839 | M2 | x | | | | | | | | | | |
| 8840 | M2 | x | | | | z | | | Y | | | |
| 8841 | M2 | x | | | | | | | | | | |
| 8842 | M2 | x | | | | | | | | | | |
| 8843 | M2 | x | | | | | | | | | | |
| 8844 | M2 | x | | | | | | | | | | |
| 8845 | M2 | | | | | | | | | | | |
| 8846 | M2 | | | | | | | | | | | |
| 8847 | M2 | x | | | x | | | | | | | |
| 8848 | M2 | x | | | | | | | | | | |
| 8849 | M2 | x | | | | | | | | | | |

| Sample No. | Site No. | RockEval TOC | XRD-Bulk | XRD-Clay | Organic Pet. | Thin Section | Adsorption Isotherm | SEM | Mini-perm | Porosimetry | Pycnometry | Texture with Clay Mineralogy |
|---|---|---|---|---|---|---|---|---|---|---|---|---|
| 8850 | M2 | x | | | | | | | | | | z |
| 8851 | M2 | x | | | | | | | | | | |
| 8852 | M2 | | | | | | | | | | | |
| 8853 | M2 | x | | | x | | | | | | | |
| 8854 | M2 | x | Y | Y | | | | | | | | |
| 8855 | M2 | x | | | | | | | | | | |
| 8856 | M2 | x | | | | | | | Y | | | z |
| 8857 | M2 | x | | | | | | | | | | |
| 8858 | M2 | x | | | | | | Y | | z | Y | |
| 8859 | M30 | x | | | | | | | | | | |
| 8860 | M30 | | | | | | | | | | | |
| 8861 | M30 | | | | | | | | | | | |
| 8862 | M30 | x | | | x | | | | | | | |
| 8863 | M30 | | | | | | | | | | | |
| 8864 | M30 | | | | | | | | | | | |
| 8865 | M30 | | | | | | | | | | | |
| 8866 | M30 | x | | | | | | | | | | |
| 8867 | M26 | x | | | | | | | | | | |
| 8868 | M26 | | | | | | | | | | | |
| 8869 | M26 | x | | | | | | | | | | |
| 8870 | M26 | | | | | | | | | | | |
| 8871 | M26 | | | | | | | | | | | |
| 8872 | M26 | | | | | | | | | | | |
| 8873 | M26 | | | | | | | | | | | |
| 8874 | M26 | x | | | x | | | | | | | |
| 8875 | M9 | x | | | x | | | | | | | |
| 8876 | M9 | x | | | | | | | | | | |
| 8877 | M9 | | | | | | | | | | | |
| 8878 | M9 | x | | | | z | | Y | Y | z | Y | |
| 8879 | M9 | x | | | | | | | | | | |
| 8880 | M9 | | | | | | | | | | | |
| 8881 | M9 | x | | | | | | | | | | |
| 8882 | M11 | x | | | | | | | | | | |
| 8883 | M11 | x | | | | | | | | | | |
| 8884 | M11 | x | | | | | | | | | | |
| 8885 | M11 | | | | | | | | | | | |
| 8886 | M11 | x | | | | | | | | | | |
| 8887 | M11 | x | | | | | | | | | | |
| 8888 | M11 | x | | | x | | | | | | | |
| 8889 | M11 | x | | | | | | | | | | |
| 8890 | M11 | | | | | | | | | | | |
| 8891 | M6 | x | | | | | | | | | | |
| 8892 | M6 | | | | | | | | | | | |
| 8893 | M6 | x | | | | | | | | | | |
| 8894 | M6 | x | | | | | | | | | | |
| 8895 | M6 | x | | | | z | | | | | | |
| 8896 | M6 | | | | | | | | | | | |
| 8897 | M6 | x | Y | | x | | | | | | | |
| 8898 | M6 | x | | | | | | | | | | |
| 8899 | M8 | x | Y | Y | | | | | | | | |
| 8900 | M8 | x | | | | | | | | | | |
| 8901 | M8 | x | | | | | | Y | | | | |
| 8902 | M8 | x | | | x | z | | | Y | | | |
| 8903 | M8 | x | | | | | | | | | | |
| 8904 | M8 | x | | | | | | | | z | Y | |
| 8905 | M39 | x | Y | | | | | | | | | |
| 8906 | M39 | | | | | | | | | | | |
| 8907 | M39 | | | | | | | | | | | |
| 8908 | M39 | x | | | | z | | | Y | z | Y | |
| 8909 | M39 | x | | | x | | | | | | | |
| 8910 | M38 | x | | | x | | | | | | | |
| 8911 | M38 | | | | | | | | | | | |
| 8912 | M38 | x | | | | | | | | | | |
| 8913 | M38 | | | | | | | | | | | |
| 8914 | M38 | x | | | | | | | | | | |
| 8915 | M38 | x | | | | | | | | | | |
| 8916 | M35 | x | | | | | | | | | | |
| 8917 | M35 | | | | | | | | | | | |
| 8918 | M35 | x | | | | | | | Y | | | |
| 8919 | M35 | x | Y | Y | | | | | | | | |
| 8920 | M35 | | | | | | | | | | | |
| 8921 | M35 | x | | | | | | | | | | |
| 8922 | M35 | | | | | | | | | | | |
| 8923 | M35 | x | | | x | | | | | | | |
| 8924 | M35 | x | | | | z | | | | | | |
| 8925 | M34 | | | | | | | | | | | |
| 8926 | M34 | x | | | | | | Y | | | | |
| 8927 | M34 | | | | | | | | | | | |
| 8928 | M34 | x | | | x | | | | | | | |
| 8929 | M34 | | | | | | | | | | | |
| 8930 | M34 | x | | | | | | | | | | |
| 8931 | M36 | x | | | | | | | | | | |
| 8932 | M36 | | | | | | | | | | | |
| 8933 | M36 | x | | | | | | | | | | |
| 8934 | M36 | x | | | x | | | | | | | |
| 8935 | M36 | x | | | | | | | | | | |
| 8936 | M36 | x | | | | | | | | | | |
| 8937 | M36 | x | | | | | | | | | | |
| 8938 | M18 | x | | | | | | | | | | |
| 8939 | M18 | | | | | | | | | | | |
| 8940 | M18 | x | | | | | | | | | | |
| 8941 | M18 | | | | | | | | | | | |
| 8942 | M18 | x | | | x | | | | | | | |
| 8943 | M18 | | | | | | | | | | | |

| Sample No. | Site No. | RockEval TOC | XRD-Bulk | XRD-Clay | Organic Pet. | Thin Section | Adsorption Isotherm | SEM | Mini-perm | Porosimetry | Pycnometry | Texture with Clay Mineralogy |
|---|---|---|---|---|---|---|---|---|---|---|---|---|
| 8944 | M12 | | | | | | | | | | | |
| 8945 | M12 | x | | | | | | | | | | |
| 8946 | M12 | | | | | | | | | | | |
| 8947 | M12 | x | | | | | | | | | | |
| 8948 | M12 | x | | | | z | | | | | | z |
| 8949 | M12 | | | | | | | | | | | |
| 8950 | M12 | x | | | x | | | | | | | |
| 8951 | M16 | x | | | | | | | | | | |
| 8952 | M16 | x | | | | | | | | | | |
| 8953 | M16 | x | | | | | | | | | | |
| 8954 | M16 | | | | | | | | | | | |
| 8955 | M16 | x | | | | | | | | | | |
| 8956 | M31 | x | | | | z | | | | | | |
| 8957 | M31 | x | | | | | | | | | | |
| 8958 | M31 | x | | | | | | | | | | |
| 8959 | M31 | x | | | | | | | | | | |
| 8960 | M31 | | | | | | | | | | | |
| 8961 | M31 | x | | | x | | | | | | | |
| 8962 | M31 | | | | | | | | | | | |
| 8963 | M24 | x | | | | | | | | | | |
| 8964 | M24 | x | | | x | | | | | | | |
| 8965 | M24 | | | | | | | | | | | |
| 8966 | M24 | x | | | | | | | | | | |
| 8967 | M24 | x | | | | | | | | | | |
| 8968 | M24 | | | | | | | | | | | |
| 8969 | M24 | x | | | | | | | | | | |
| 8970 | M17 | | | | | | | | | | | |
| 8971 | M17 | x | | | | | | | | | | |
| 8972 | M17 | x | | | | | | | | | | |
| 8973 | M17 | x | | | x | | | | | | | |
| 8974 | M17 | | | | | | | | | | | |
| 8975 | M17 | x | | | | | | | | | | |
| 8976 | M17 | | | | | | | | | | | |
| 8977 | M17 | x | | | | | | | | | | |
| 9247 | M15 | x | | | | | | | | | | |
| 9248 | M13 | x | | | | | | | | | | |
| 9249 | M5 | x | | | | | | | | | | |
| 9250 | Standard | | | | | | | | | | | |
| 9251 | M18 | x | | | | | | | | | | |
| 9252 | M17 | x | | | | | | | | | | |
| 9253 | M31 | x | | | x | | | | | | | |
| 9254 | M21 | | Y | Y | | | | | | | | |
| 9255 | M23 | | | | | | x | | | | | |
| 9256 | M10 | | | | | | x | | | | | |
| 9257 | M2 | | | | | | x | | | | | |
| 9258 | M6 | | | | | | x | | | | | |
| 9259 | M8 | | | | | | x | | | | | |
| 9260 | M34 | | | | | | x | | | | | |

## Appendix 3 – Montney Formation Bulk Sample Mineralogy (XRD)

### *Appendix 3a – Bulk X-Ray Diffraction*

| Sample No. | Site No. | Quartz | Feldspars | | | Pyrite | Hem. | Clay Minerals | | | | | | | Carbonates | | | | Sulphate | FlAp. | Brkt. | Total |
|---|---|---|---|---|---|---|---|---|---|---|---|---|---|---|---|---|---|---|---|---|---|---|
| | | | Albite | Micro. | Ortho. | | | Musc. | Bio. | Paly. | Kaol. | Illite | Mont. | ClCh. | Calcite | Dolo. | Ank. | Rhod. | Gyp. | | | |
| 8126 | M23 | 44.7 | 9.5 | 15.1 | | 0.2 | | 3.2 | | | 1.7 | | | 1.1 | 1.7 | 12.9 | 8.5 | | | 0.9 | 0.5 | 100.0 |
| 8730 | M23 | 38.5 | 7.6 | | 14.6 | 1.7 | | 10.3 | 2.8 | | | 1.4 | | | 0.7 | 9.8 | 10.5 | 0.4 | | 0.9 | 0.6 | 99.8 |
| 8753 | M10 | 40.6 | 9.2 | | 9.2 | 4.7 | | 16.8 | 1.8 | | 1.0 | 0.6 | | 1.3 | 0.1 | 13.5 | | | | 0.4 | 0.7 | 99.9 |
| 8761 | M19 | 42.5 | 6.9 | | 7.6 | 3.0 | | 9.8 | 1.1 | | | 1.7 | | | | 26.0 | | | | 1.0 | 0.5 | 100.1 |
| 8819 | M1 | 38.5 | 2.6 | | 22.2 | 2.7 | | 8.5 | 3.6 | | | 3.3 | | | | 17.4 | | | | 0.5 | 0.7 | 100.0 |
| 8854 | M2 | 41.2 | 7.3 | | 13.9 | 2.3 | 0.6 | 9.1 | 2.4 | | | 0.9 | | 1.4 | 0.4 | 19.3 | | | | 0.5 | 0.6 | 99.9 |
| 8897 | M6 | 20.7 | 7.9 | | 13.7 | 8.9 | | 31.4 | 4.3 | 2.0 | 3.8 | | | | | 4.5 | | | | 1.6 | 1.3 | 100.1 |
| 8899 | M8 | 38.2 | 5.5 | | 8.2 | 4.4 | 0.6 | 20.4 | 3.2 | | | 4.1 | | | | 13.1 | | | 0.1 | 1.5 | 0.7 | 100.0 |
| 8905 | M39 | 27.4 | 3.3 | | 8.4 | 5.3 | | 20.0 | 2.1 | | | | | | 5.6 | 9.5 | 10.4 | | | 7.5 | 0.6 | 100.1 |
| 8919 | M35 | 40.1 | 10.6 | | 11.8 | 0.2 | | 9.6 | | | | 2.0 | | | 7.3 | 8.6 | 8.6 | 0.1 | | 0.4 | 0.7 | 100.0 |
| 9254 | M21 | 23.4 | 7.6 | | 17.7 | 8.3 | | 22.5 | 3.2 | 0.2 | 3.0 | 1.6 | | | | 9.9 | | | | 1.5 | 1 | 99.9 |

**Legend**

| Column Label | Description | Column Label | Description |
|---|---|---|---|
| Sample No. | AGS sample number | Hem. | Hematite |
| Site No. | AGS site location number | Kaol. | Kaolinite |
| Ank. | Ankerite | Micro. | Microcline |
| Bio. | Biotite | Mont. | Montmorillonite |
| Brkt. | Brookite | Musc. | Muscovite |
| ClCh. | Clinochlore | Ortho. | Orthoclase |
| Dolo. | Dolomite | Paly. | Palygorskite |
| FlAp. | Fluorapatite | Rhod. | Rhodochrosite |
| Gyp. | Gypsum | | |

All values are in weight per cent (wt.%)

Analysis performed by SGS Minerals Ltd.

Software: Bruker AXS Diffrac Plus EVA

The semiquantitative analysis of EVA is performed on the basis of relative peak heights and I/Icor values of those detected crystalline phases with PDF files. Amorphous or crystalline mineral species present in trace amounts may go undetected.

## *Appendix 3b – X-Ray Fluorescence*

| Sample No. | Site No. | $SiO_2$ | $Al_2O_3$ | $Fe_2O_3$ | MgO | CaO | $Na_2O$ | $K_2O$ | $TiO_2$ | $P_2O_5$ | MnO | $Cr_2O_3$ | $V_2O_5$ | LOI | Total |
|---|---|---|---|---|---|---|---|---|---|---|---|---|---|---|---|
| | | wt. % | wt. % | wt. % | wt. % | wt. % | wt. % | wt. % | wt. % | wt. % | wt. % | wt. % | wt. % | wt. % | wt. % |
| 8126 | M33 | 63.40 | 6.66 | 1.86 | 3.94 | 7.61 | 1.09 | 2.87 | 0.46 | 0.35 | 0.20 | 0.01 | <0.01 | 10.70 | 99.2 |
| 8730 | M23 | 56.30 | 8.93 | 3.40 | 3.81 | 6.72 | 0.90 | 3.80 | 0.59 | 0.31 | 0.22 | 0.02 | <0.01 | 11.60 | 96.6 |
| 8753 | M10 | 61.40 | 10.20 | 3.50 | 3.60 | 4.28 | 1.09 | 3.84 | 0.70 | 0.15 | 0.07 | 0.02 | 0.00 | 8.51 | 97.4 |
| 8761 | M19 | 57.10 | 6.41 | 2.19 | 5.43 | 8.46 | 0.08 | 2.76 | 0.46 | 0.44 | 0.18 | 0.03 | <0.01 | 12.60 | 96.1 |
| 8819 | M1 | 55.90 | 15.70 | 5.92 | 1.99 | 2.35 | 1.15 | 5.18 | 1.44 | 0.46 | 0.09 | 0.03 | <0.01 | 7.92 | 98.1 |
| 8854 | M2 | 59.50 | 8.56 | 3.26 | 4.30 | 5.86 | 0.79 | 3.48 | 0.58 | 0.18 | 0.12 | 0.02 | <0.01 | 9.06 | 95.7 |
| 8897 | M6 | 52.40 | 17.10 | 6.33 | 2.07 | 2.13 | 0.86 | 5.94 | 1.04 | 0.54 | 0.04 | 0.02 | 0.02 | 9.03 | 97.5 |
| 8899 | M8 | 59.00 | 11.00 | 4.09 | 3.36 | 4.19 | 0.72 | 4.35 | 0.72 | 0.21 | 0.06 | 0.02 | 0.02 | 9.40 | 97.1 |
| 8905 | M39 | 44.20 | 8.96 | 6.34 | 2.43 | 10.10 | 0.28 | 3.87 | 0.46 | 3.08 | 0.03 | 0.04 | 0.13 | 16.90 | 96.8 |
| 8919 | M35 | 59.90 | 8.42 | 2.51 | 2.24 | 8.85 | 1.16 | 3.20 | 0.65 | 0.18 | 0.07 | 0.02 | 0.04 | 9.36 | 96.6 |
| 9254 | M21 | 51.20 | 15.20 | 6.82 | 2.82 | 3.22 | 0.63 | 5.17 | 0.80 | 0.58 | 0.06 | 0.02 | 0.02 | 10.80 | 97.3 |
| 8854DUP | M2 | 59.60 | 8.49 | 3.24 | 4.29 | 5.84 | 0.81 | 3.48 | 0.59 | 0.18 | 0.11 | 0.01 | <0.01 | 8.89 | 95.5 |

**Legend**

| Column Label | Description | Column Label | Label Description |
|---|---|---|---|
| Sample No. | AGS sample number | $TiO_2$ | Titanium oxide |
| Site No. | AGS site location number | $P_2O_5$ | Phosphorus oxide |
| $SiO_2$ | Silicon oxide | MnO | Manganese oxide |
| $Al_2O_3$ | Aluminum oxide | $Cr_2O_3$ | Chromium oxide |
| $Fe_2O_3$ | Iron oxide | $V_2O_5$ | Vanadium oxide |
| MgO | Magnesium oxide | LOI | Loss-on-ignition - amount of material lost due to heating |
| CaO | Calcium oxide | Total | Total weight per cent |
| $Na_2O$ | Sodium oxide | wt. % | Weight per cent |
| $K_2O$ | Potassium oxide | DUP | Duplicate |

## Appendix 4 – Montney Formation Clay Mineralogy (Qualitative XRD)

| Sample No. | Site No. | Sample Type | Crystalline Mineral Assemblage (Relative Proportions Based on Peak Height) | | | |
|---|---|---|---|---|---|---|
| | | | Major (> 30 wt. %) | Moderate (10-30 wt. %) | Minor ( <10 wt. %) | Trace (< 1 wt. %) |
| 8730 | M23 | Core | (quartz) | (ankerite) | illite, (*plagioclase), (*potassium-feldspar) | (*pyrite), (*calcite) |
| 8753 | M10 | Core | (quartz) | (dolomite) | illite, chlorite, (plagioclase), (potassium-feldspar) | (*pyrite), (*apatite) |
| 8761 | M19 | Core | (quartz) | (dolomite) | illite, (*plagioclase), (*potassium-feldspar) | (*pyrite) |
| 8819 | M1 | Core | (quartz) | illite | (mica), (dolomite), (plagioclase), (potassium-feldspar), (pyrite) | (*brookite) |
| 8854 | M2 | Core | (quartz) | (dolomite) | illite, (plagioclase), (potassium-feldspar) | *chlorite, (*calcite), (*pyrite), (*brookite) |
| 8899 | M8 | Core | (quartz) | | illite, (plagioclase), (potassium-feldspar), (dolomite) | (*gypsum), (*pyrite), (*brookite) |
| 8919 | M35 | Core | (quartz) | (calcite) | illite, (dolomite), (ankerite), (plagioclase), (potassium-feldspar), (pyrite) | (*rhodochrosite) |
| 9254 | M21 | Core | (quartz) | | illite, (dolomite) | *kaolinite, (*potassium-feldspar), (*apatite), (*pyrite) |

**Legend:**

| Column Label | Label Description |
|---|---|
| Sample No. | AGS sample number |
| Site No. | AGS site location number |
| Sample Type | Core, outcrop or cuttings |
| wt. % | Weight per cent (relative proportion of clay sized minerals only) |

* Tentative identification due to low concentrations, diffraction line overlap or poor crystallinity

( ) Not a clay mineral, according to SGS Minerals Ltd.

## Appendix 5 – Montney Formation Scanning Electron Microscope (SEM) Images and Descriptions

The SEM images in this appendix are thumbnails. Full-size JPGs are in the ZIP file that accompanied this report, available at http://www.ags.gov.ab.ca/publications/abstracts/OFR_2010_03.html.

## Montney Formation Scanning Electron Microscope (SEM) Images and Descriptions

The SEM descriptions include an interpretation of energy dispersive X-ray (EDX) analysis. Please note that not all the graphs of the EDX analyses were saved for later interpretation; we have therefore made the comment ‘not saved’ within the body of this document where appropriate.

### *Lower Montney Formation, Sample 8705, UWI 100/11-27-077-06W6/00, 1741.2 m Core Depth*

The sample is dark grey siltstone interbedded with light grey calcareous siltstone to very fine sandstone. Beds are 0.5–1.0 cm thick. The sample was taken above an ~4.0 m thick sandstone.


| Image | Magnification |
|---|---|
| 8705_7 | 25x |
| 8705_2 | 50x |
| 8705_1 | 100x |
| 8705_3 | 250x |
| 8705_4 | 500x |
| 8705_5 | 2000x |
| 8705_6 | 850x |
| 8705_8 | 250x |
| 8705_9 | 500x |
| 8705_10 | 2500x |
| 8705_11 | 1500x |

Image **8705_7** is a low-magnification (25×) view that was taken in the upper dark silty portion of the sample. Along the northwest edge is a thin shaly layer that is approximately 400 µm thick. This is the only ‘shale’ lamina that we found in all of the Montney samples. The remainder of the sample is silty or sandy silt. The bedding trend is northeast in all images.

Image **8705_2** (50× magnification) shows the homogeneity of the dark silty layer. The next image is taken near the white arrow. The red arrow in this image points to the location of image 8705_8, which is described later in this section.

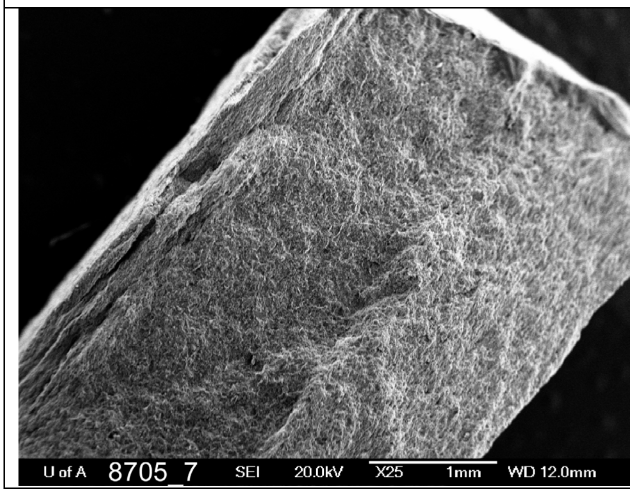


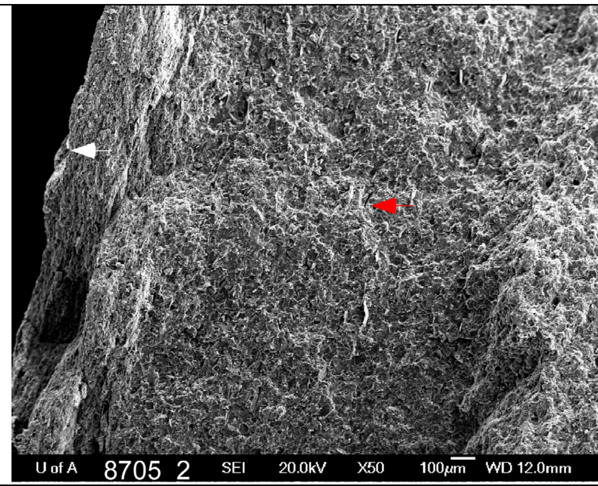


Image **8705_1** (100× magnification) is a slightly higher magnification of the shaly layer. Notice the abundance of darker minerals, likely dolomite crystals that will be examined in more detail in later images. An EDX overview of the sample shows dominance of quartz, perhaps potassium feldspar and, to a lesser degree, dolomite. There are a few scattered pores in the size range 20-40 µm, but otherwise little porosity is visible at this level of magnification.

Image **8705_3** (250× magnification) shows a distinct north-south fabric in the shaly layer. An EDX overview of the sample is similar to the first analysis but with somewhat stronger indication of the presence of potassium feldspar and/or illite. Porosity is now discernible, some of which appears as lineations, up to 50 µm in length, parallel to bedding. A few large grains, up to 50 µm in diameter, are scattered throughout the sample. The next image is taken to the left of the white arrow.

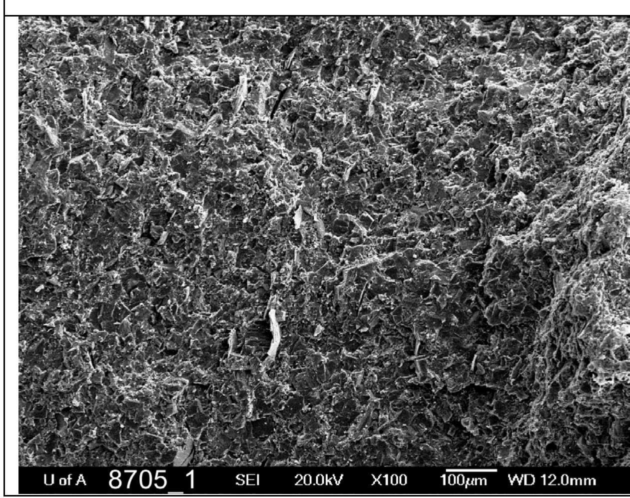


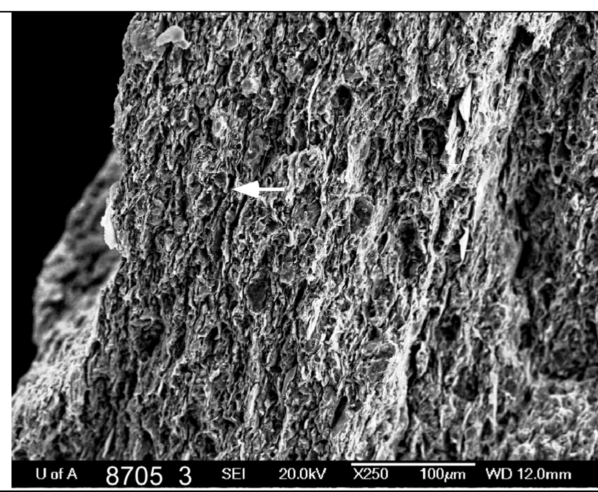

In image **8705_4** (500× magnification), the fabric trends parallel to bedding, with silt-sized particles up to 20 µm in diameter. Mineralogical analysis on the sample yielded the following results, beginning at the bottom of the image: potassium feldspar at site 1, dolomite at site 2, mica at site 3, dolomite at site 4, a possible kaolinite and illite mix at site 5, pyrite at site 6 and quartz at site 7. The next image is taken near the pyrite framboid in the upper left corner.

Microporosity, to use the term loosely, is visible within the framboid of image **8705_5** (2000× magnification). Surrounding the pyrite are grains up to 10 µm in diameter, although most are less than 5 µm. The linear pores mentioned earlier are visible between clay domains. Core expansion during recovery may enhance or create these features along lines of weakness in the sample, often grain or clay domain contacts. An example of the enhancement or creation of porosity is at the tip of the yellow arrow, where the curvature of the clay domain matches the curvature of the particle. This pore may have been closed at depth. The wavy character of the clay suggests that the clay domains are compacting around the particles, thus reducing porosity. Otherwise, it is difficult in this sample to estimate primary porosity.

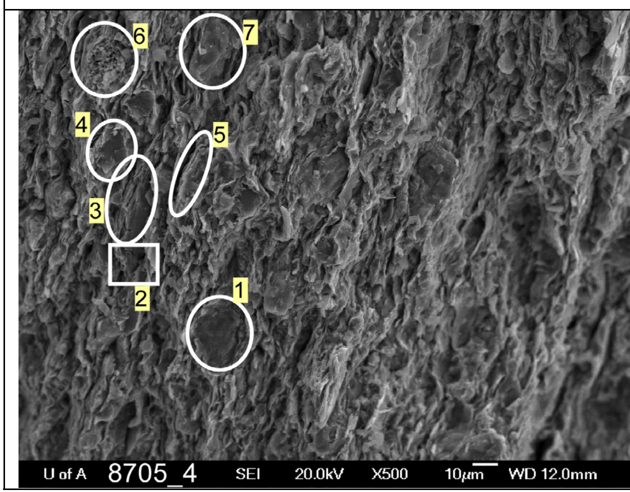


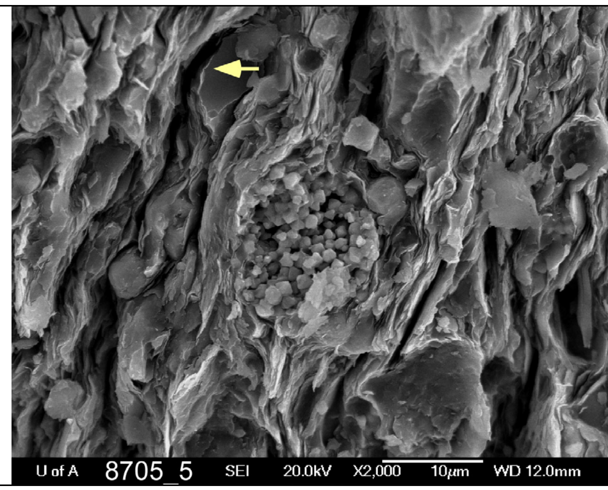

Image **8705_6** (850× magnification) is a lower magnification view of the previous image. Note the pyrite framboid in the upper left corner for reference. If we assume that the linear pores are open due to core expansion, then there is little porosity in this view. Clay sheets are well compacted around diagenetic or primary grains. In summary, there is more clay minerals in the ~400 µm thick shaly layer than we have seen in any other SEM image of the Montney Formation.

Image **8705_8** (250× magnification) is full of subrounded to angular grains that appear to have poor sphericity; some of the grains are more than 50 µm in diameter. Porosity is evident between the crystals, but the pore size is dominantly quite small (<10–20 µm) at this level of magnification. Nonetheless, the porosity is quite well distributed. An EDX overview of the sample yielded an elemental content very high in silicon and low in aluminum, perhaps indicating low clay content and high quartz and feldspar content. The yellow, red and white arrows point to the locations of images 8705_9, 8705_10 and 8705_11, respectively.

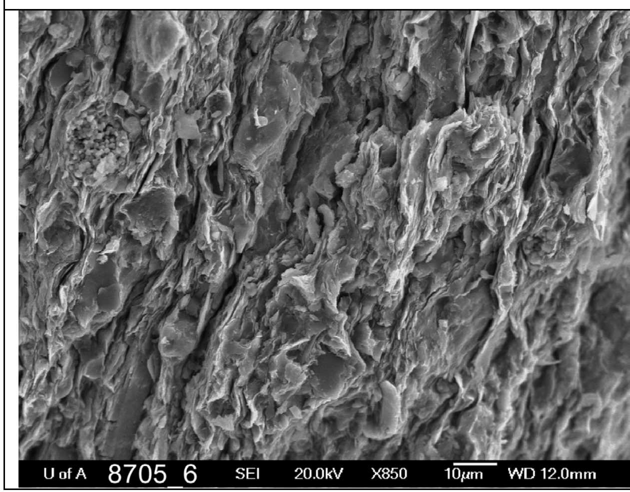


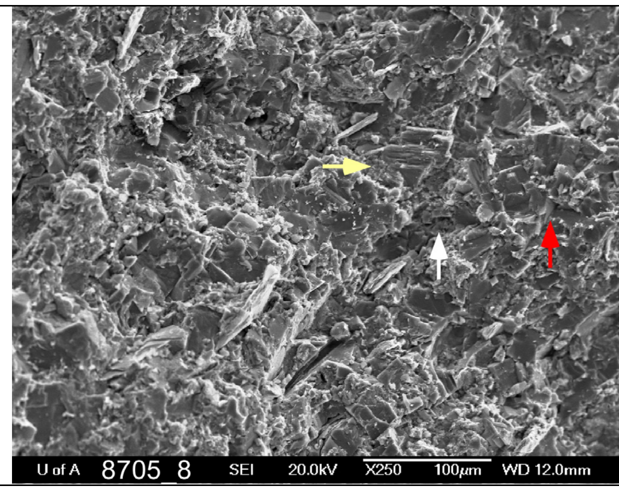

| |
|---|
| An EDX analysis on individual grains in image **8705_9** (500× magnification) yielded the following mineralogy: quartz at site 8, feldspar at site 9, possibly chert at site 10, mica at site 11, dolomite at site 12 (EDX_008), and calcium-rich, sodium, magnesium feldspar at site 13 (EDX_009). Intercrystalline porosity is more evident in this view. There are a few pores greater than 10 µm, the majority being less than 5 µm.<br><br>Image **8705_10** (2500× magnification) is a high-magnification view of mineralogy and porosity between the larger grains. The calcium-rich feldspar from the previous image is in the lower right corner. The arrows point to what is probably illite (no EDX analysis) that abuts the feldspar. However, the calcium-rich sodium feldspar is not likely the source material for the illite, since illite is potassium-rich. Illite appears to form a late-diagenetic pore-filling mineral. Pore sizes in the image vary from less than about 1 µm to perhaps 5 µm. |

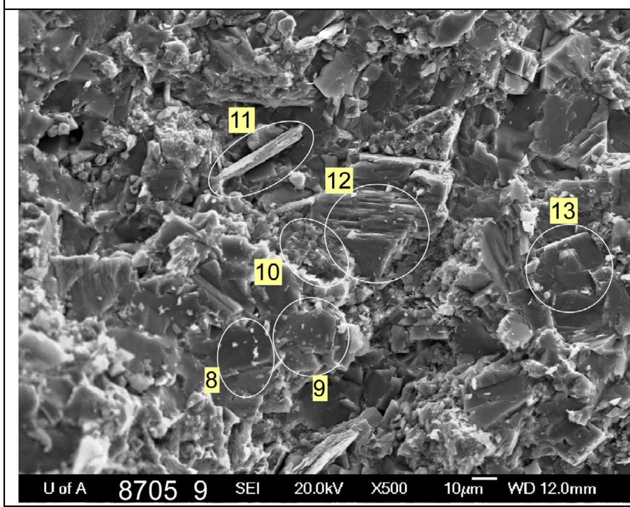


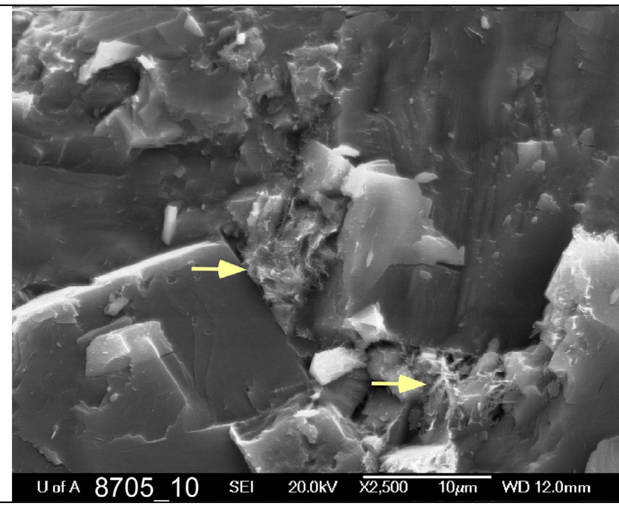


| |
|---|
| Image **8705_11** (1500× magnification) is a very busy looking image with a variety of crystal morphologies. Intercrystalline porosity is clearly evident, and there is a small amount of intracrystalline porosity (yellow arrow). The fractured grain (red arrow) likely occurred during sample handling and preparation. |

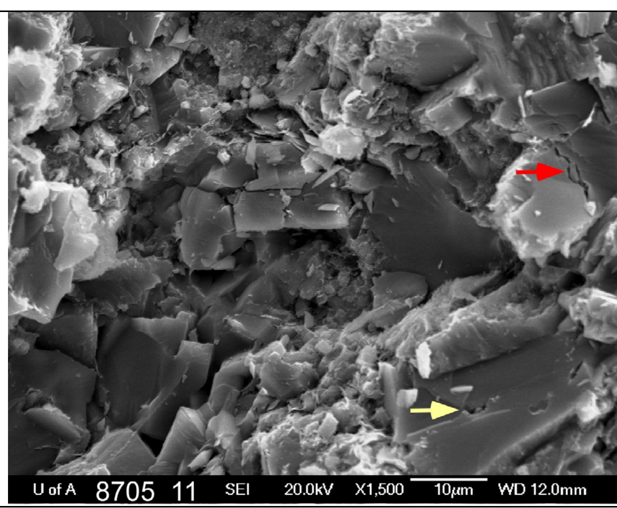

EDX results for sample 8705:

| Composition | Image | ID on Image |
|---|---|---|
| Potassium feldspar, (EDX_8705_003) | 8705_4 | 1 |
| Dolomite (8705_005) | 8705_4 | 2 |
| Mica (EDX not saved) | 8705_4 | 3 |
| Dolomite (EDX not saved) | 8705_4 | 4 |
| Possible kaolinite and illite mix (8705_006) | 8705_4 | 5 |
| Pyrite (EDX_8705_004) | 8705_4 | 6 |
| Quartz (EDX not saved) | 8705_4 | 7 |
| Quartz (EDX not saved) | 8705_8 | 8 |
| Feldspar (EDX not saved) | 8705_8 | 9 |
| Chert (?; EDX not saved) | 8705_8 | 10 |
| Mica (EDX not saved) | 8705_8 | 11 |
| Dolomite (EDX_8705_008) | 8705_8 | 12 |
| Calcium-rich feldspar (EDX_8705_009) | 8705_8 | 13 |

Note: The depth of the EDX analysis is ~1–2 µm, so the chemistry below the surface may dominate the surface mineral.

### *Montney Formation, Sample 8709, UWI 100/05-14-78-11W6/00, 2189.9 m Core Depth*

The sample is dark grey, slightly sandy, noncalcareous siltstone.


| Image | Magnification |
|---|---|
| 8709_1 | 100x |
| 8709_2 | 200x |
| 8709_3 | 900x |
| 8709_4 | 4500x |
| 8709_5 | 5500x |
| 8709_6 | 1300x |
| 8709_7 Backscatter | 1000x |
| 8709_8 | 370x |
| 8709_9 | 750x |
| 8709_10 | 650x |

Image **8709_1** is a low-magnification (100×) image showing fairly good porosity over a range of scales. No bedding trend is evident in this view. An EDX overview suggests the sample is dominated by quartz, feldspar and clay, with a lesser amount of dolomite. There are dark-coloured, sand-sized particles in this view that vary in sphericity and roundness. The white arrow points to the location of the next image.

Image **8709_2** is higher magnification (200×) view of porosity in the sample. A considerable number of pores are greater than 30 µm, but we cannot judge the effectiveness of the porosity. An EDX analysis of the area within the circle yielded muscovite, which we believe to represent both the light-coloured plates (white arrow) and the projecting grain (yellow arrow). The red arrow points to the location of image 8709_6.

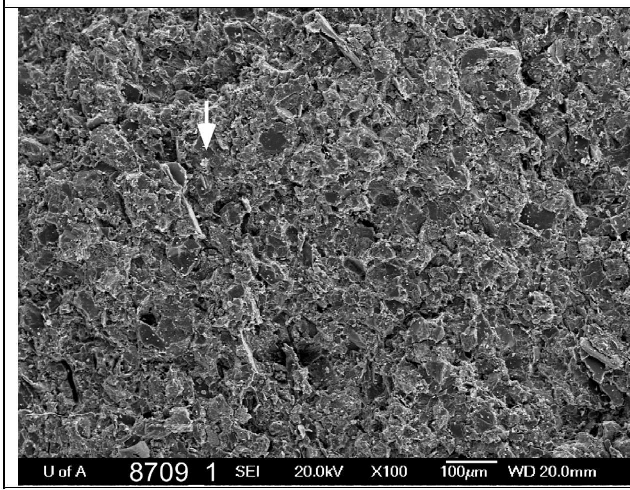


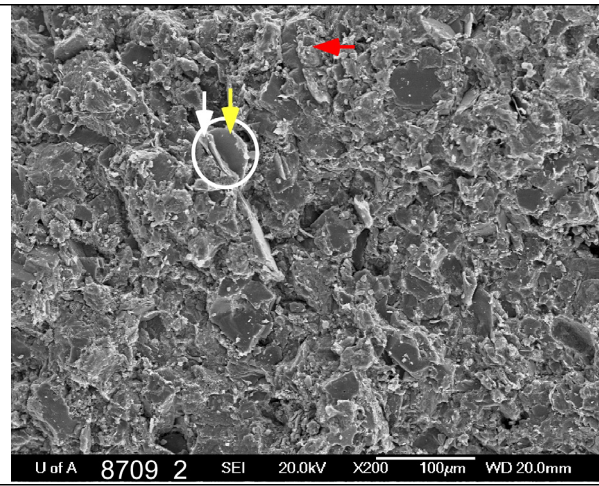


Image **8709_3** (900× magnification) is a close-up view of muscovite and the surrounding material in the previous image. Surrounding the muscovite is a relative abundance of intercrystalline pores less than about 1–2 µm. There is a wide range of particle sizes and shapes, including coated grains, suggesting a complex diagenetic history.

Image **8709_4** (4500× magnification) is an interesting view of a cluster of illite-coated grains of unknown mineralogy. Multiple clay sheets completely surround the grains. The dark areas within the grains suggest the presence of intragranular porosity. Illite is also apparent west and north of the cluster (white arrows), as a coating on other grains. The yellow arrows indicate what is likely mica. A dolomite rhomb is visible at the red arrow. There is a considerable amount of porosity in this view.

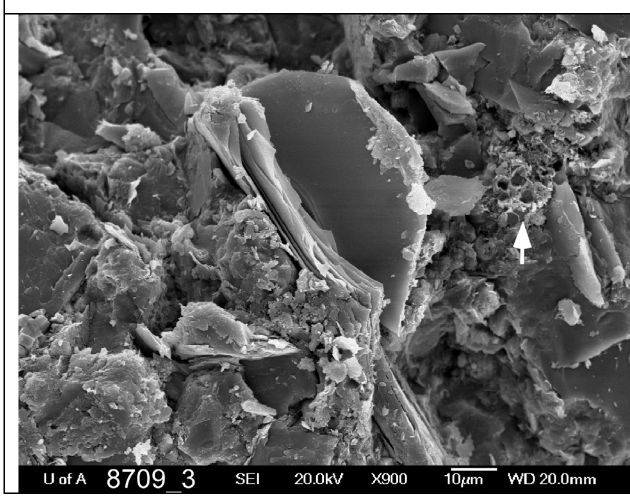


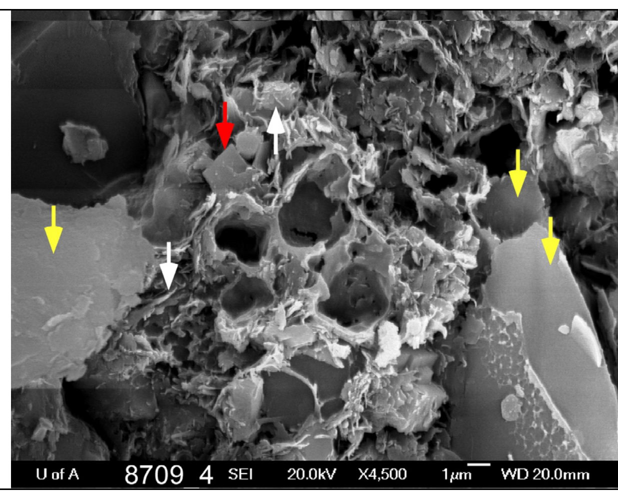

Image **8709_5** (5500× magnification) of the pyrite framboid (EDX_8709_003) was taken just north of the previous image. The framboid and surrounding grains are covered in authigenic illite, which is occluding porosity. There is a smaller framboid just beneath the larger pyrite.

Image **8709_6** (1300× magnification) contains a large grain of potassium feldspar at site 1 (EDX_8709_004), a dolomite crystal at site 2 (EDX_8709_005) and a cube of pyrite at site 3 (EDX not saved). The yellow arrows point to what appears to be a late stage of illite growth that occludes porosity. Both grains and overgrowth are well packed in this view.

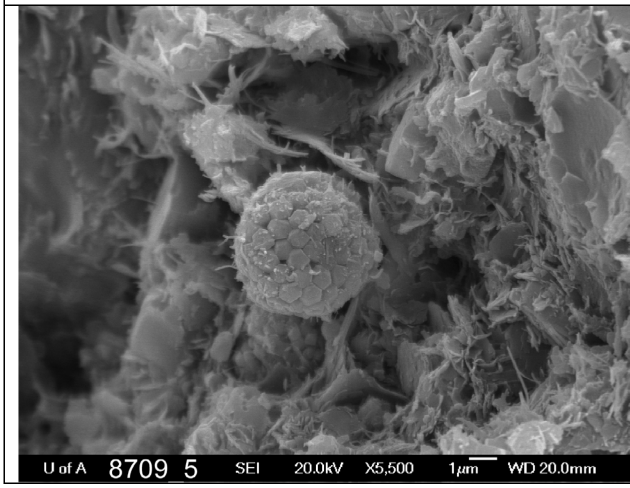


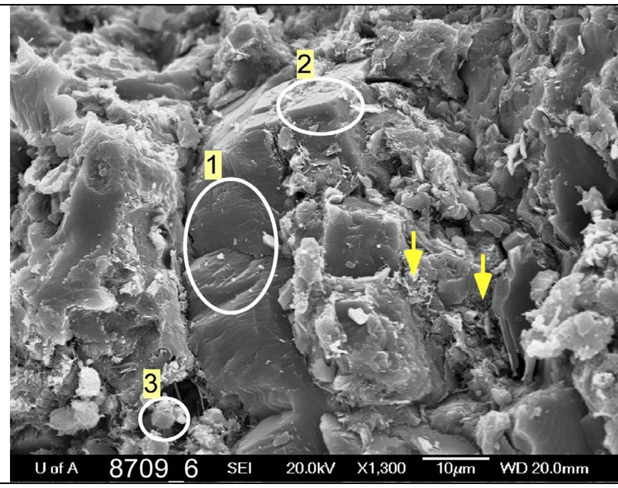


Image **8709_7** (1000× magnification) is a back scattering image taken at a slightly lower magnification. Pyrite framboids and the earlier mentioned pyrite cube are seen at the white arrows. There may be more heavy minerals in this image than we have indicated.

Image **8709_8** (370× magnification) was taken at a new spot on the sample. Fracturing along grain contacts can be seen at the green arrows. The fractures likely occurred during core retrieval and pressure unloading. A few pores that are ~10 µm in diameter are visible in the left centre of the image. The white arrow points to what is likely a quartz grain, and the yellow arrow identifies a possible dolomite crystal. The red arrow points to a crenulated mica, the crenulation likely due to the mica being forced out of alignment during adjacent crystal growth. The light blue arrow indicates the location of the next image, and the lower green arrow points to the location of image 8709_10.

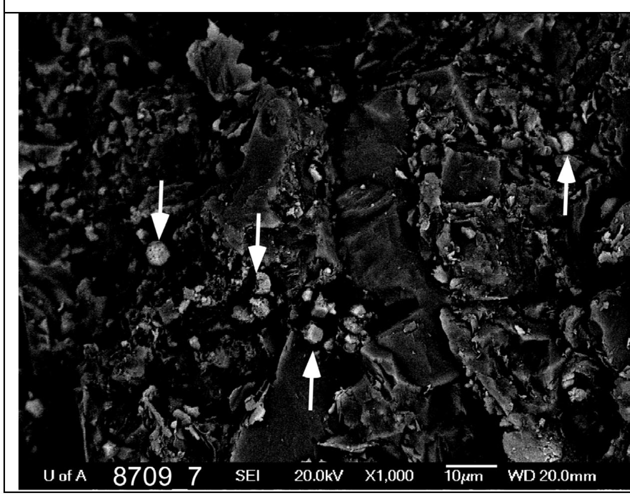


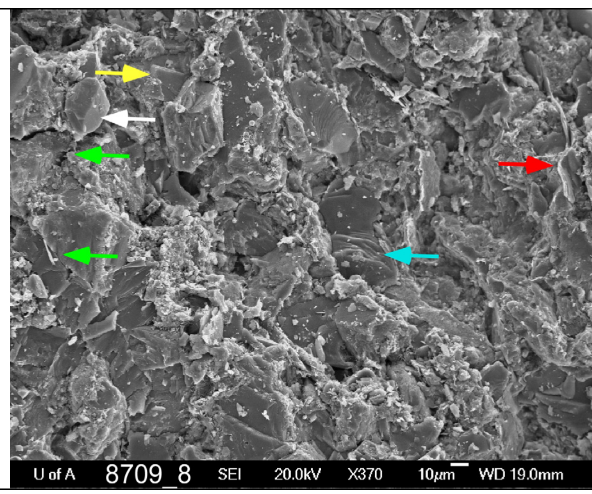

An EDX analysis (EDX_8709_006) on the circled grain in image **8709_9** (750× magnification) identified quartz. An additional grain of quartz is indicated by the white arrow. Oddly enough, quartz grains are not easily located in some Montney samples due the large degree of overgrowth or coating on the grains. The yellow arrow points to the position where a dolomite crystal was located and fell off the sample. There appears to be illite located at the pore opening identified by the red arrows, although you may need to zoom in to see it. The green arrow identifies fractures along grain contacts. Although this type of fracture is usually the result of pressure release upon core unloading, the configuration of the fracture and grain contacts suggests that some porosity was likely present at depth.

Image **8709_10** (650× magnification) is an interesting view of a fracture (identified by the red arrow). It appears that the fracture is partially filled; the grains identified by the white arrow protrude into the fracture. The fracture is about 8–10 µm wide near the red arrow. The width and length of the fracture-fill is difficult to determine, but the thin white dashed line outlines our interpretation of the trend. We have placed the lines just above the fracture trend so you can see the fractures.

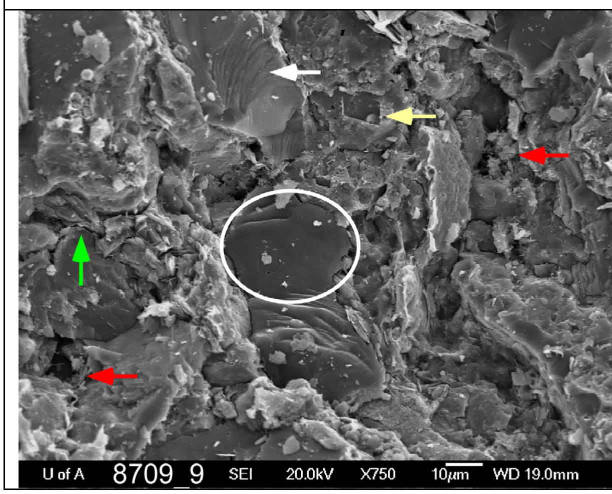


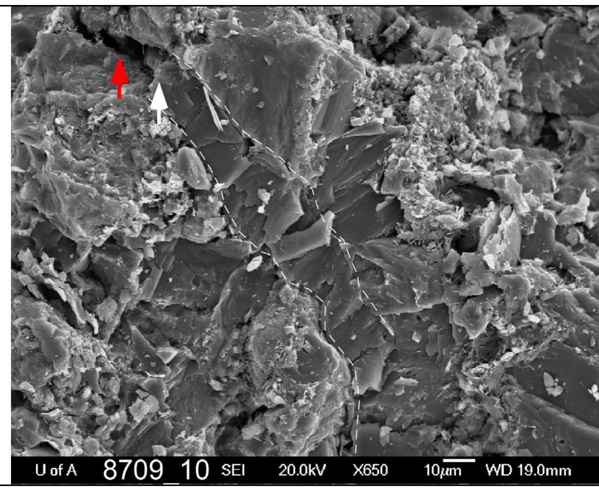


EDX results for sample 8709:

| Composition | Image | ID on Image |
|---|---|---|
| Muscovite (EDX 8709_002) | 8709_2 | Circle |
| Pyrite (EDX_8790_003) | 8709_5 | None |
| Potassium feldspar (EDX_8709_004) | 8709_6 | 1 |
| Dolomite (EDX_8709_005) | 8709_6 | 2 |
| Pyrite cube (EDX not saved) | 8709_6 | 3 |
| Quartz (EDX_8709_006) | 8709_9 | Circle |

Note: The depth of the EDX analysis is ~1–2 µm, so the chemistry below the surface may dominate the surface mineral.

### *Lower Montney Formation, Sample 8731, UWI 100/05-32-073-12W6/00, 2816.4 m Core Depth*

The sample is black siltstone with occasional light-coloured siltstone laminae. It was taken in a sand-dominated interval.


| Image | Magnification |
|---|---|
| 8731_1 | 100x |
| 8731_2 | 800x |
| 8731_3 | 11000x |
| 8731_4 | 1500x |
| 8731_5 | 8500x |
| 8731_6 | 600x |
| 8731_7 | 1900x |

Image **8731_1** (100× magnification) appears to be relatively homogeneous. There are a few sand-sized grains (dark coloured) at this level of magnification. It is difficult at this scale to distinguish porosity from the dark-coloured grains. An EDX overview of the sample suggests that mineralogy is dominated by quartz, feldspar and perhaps calcite. The arrow points to the location of the next image.

Image **8731_2** (800× magnification) displays closely packed particles with little porosity. Most grains are difficult to view given the amount of cement and perhaps quartz overgrowth that is present. An EDX analysis revealed the presence of muscovite at site 1 (EDX_8731_002), dolomite at site 2 (EDX_8731_003), calcite at site 3 (EDX_8731_004) and pyrite at site 4 (EDX_8731_005). The next image is taken near site 4.

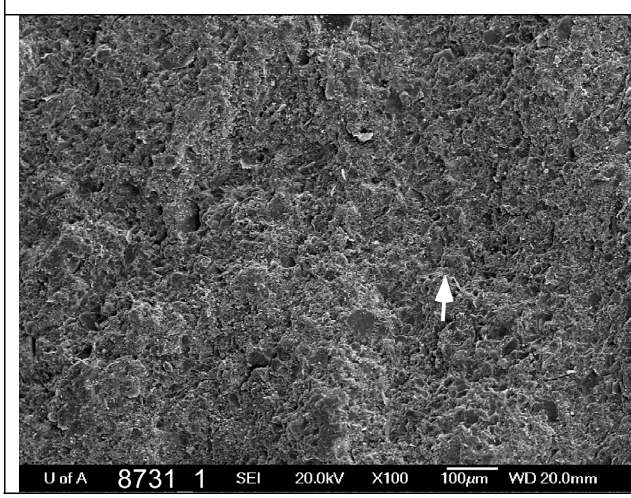


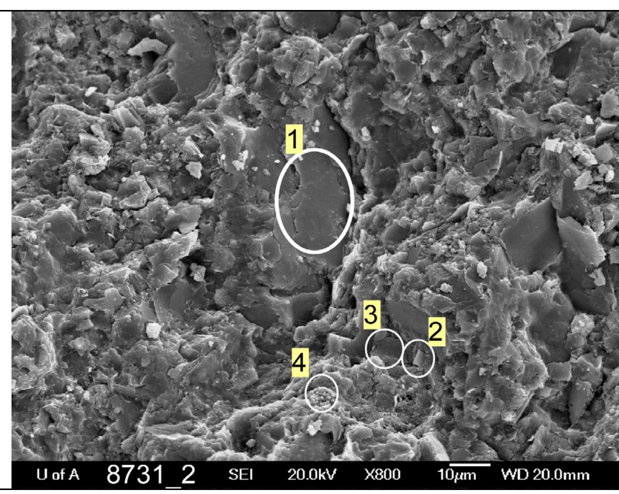

Image **8731_3**, taken at high magnification (11 000×), shows the suturing of the grains around a pyrite framboid. A small amount of porosity (<1 µm diameter) is evident within the framboid and off its northwest edge. Otherwise, the grains are very well sutured and coated, so individual grains are often difficult to discern.

Image **8731_4** (1500× magnification) was taken near the extreme southeast corner of image 8731_2. A field of pyrite crystals is apparent within the dashed yellow line. The crystals appear to be coating grains rather than having a framboid appearance. Mica plates are present at the tip of the yellow arrows.

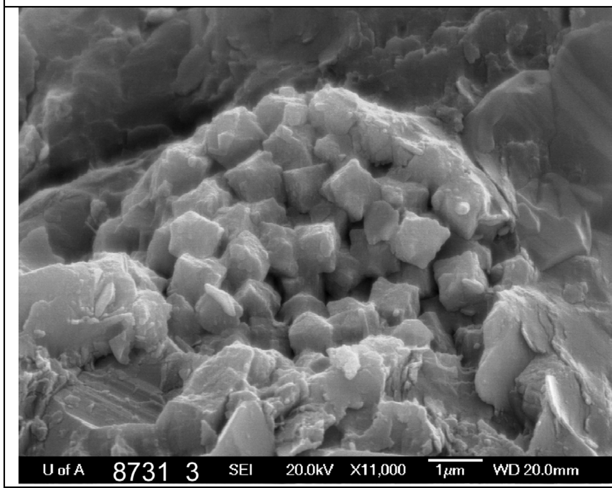


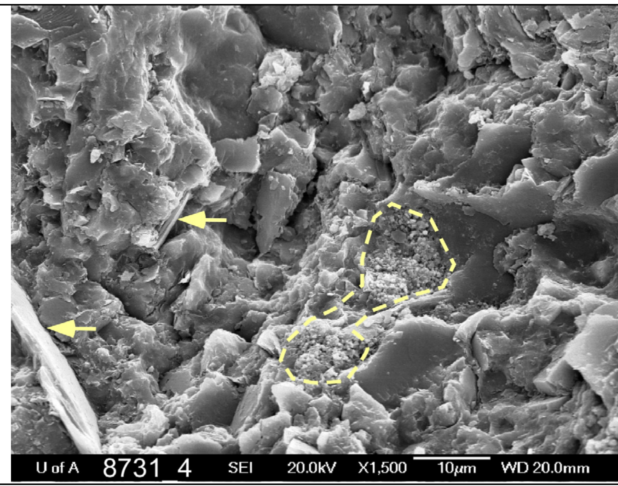


Image **8731_5** (8500× magnification) appears to be oil-stained. Grains of unknown mineralogy, approximately 0.5 to 1.0 µm in diameter, are either coated with the oil or, less frequently, lie atop the coating.

An EDX analysis (EDX not saved) on image **8731_6** (600× magnification) identified mica at site 1, dolomite at site 2 and possibly sodium feldspar and clay at site 3. Dolomite crystals are indicated by the white arrows. There is also a reasonable degree of porosity surrounding the large particles in the centre of the image. The pores are less than 5 µm in diameter.

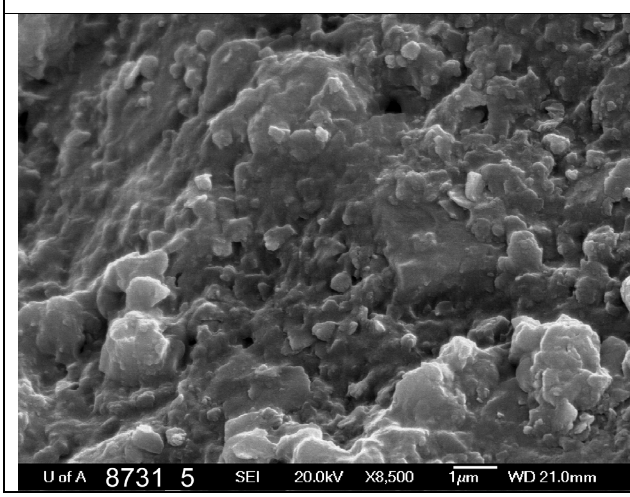


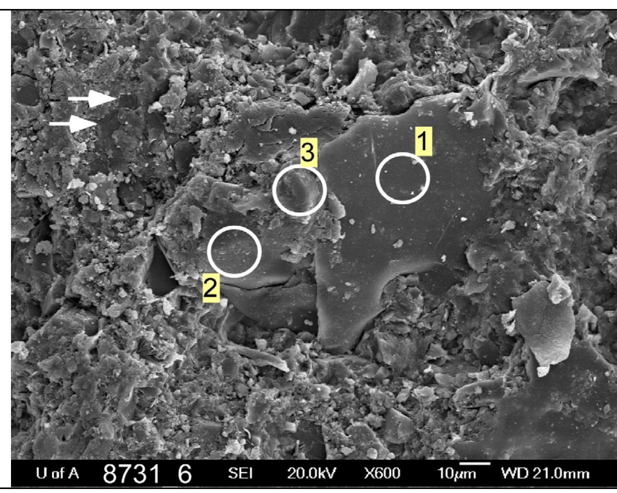

Image 8731_7 (1900× magnification) is perhaps a silicified organic particle, based on the particle’s morphology.  An EDX analysis of the particle (not saved) showed the presence of mainly silicon and aluminum. The particle in the middle of the view is likely organic.

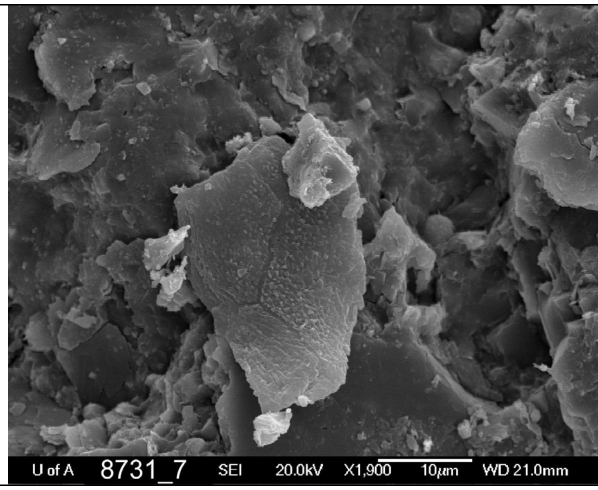


EDX results for sample 8731:

| Composition | Image | ID on Image |
|---|---|---|
| Muscovite (EDX_8731_002) | 8731_2 | 1 |
| Dolomite (EDX_8731_003) | 8731_2 | 2 |
| Calcite (EDX_8731_004) | 8731_2 | 3 |
| Pyrite (EDX_8731_005) | 8731_2 | 4 |
| Mica (EDX not saved) | 8731_6 | 1 |
| Dolomite (EDX not saved) | 8731_6 | 2 |
| Sodium feldspar and clay (EDX not saved) | 8731_6 | 3 |

Note: The depth of the EDX analysis is ~1–2 µm, so the chemistry below the surface may dominate the surface mineral.

### *Montney Formation, Sample 8739, UWI 103/10-34-064-19W5/00, 1776.2 m Core Depth*

The sample was taken in sandstone in the upper portion of the Montney Formation.

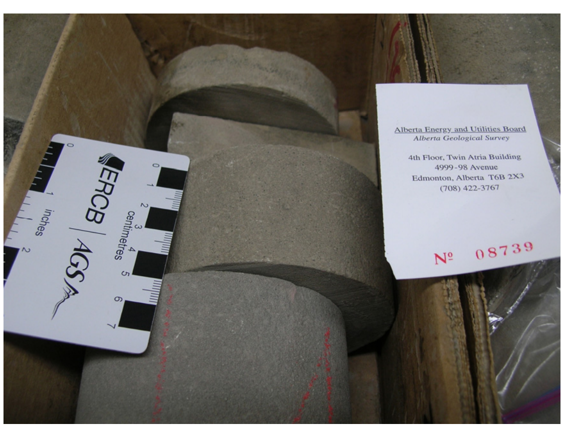

| Image | Magnification |
|---|---|
| 8739_1 | 100x |
| 8739_2 | 400x |
| 8739_3 | 1800x |
| 8739_4 | 2500x |
| 8739_5 | 300x |
| 8739_6 | 1000x |
| 8739_7 | 1800x |

Image **8739_1** is a low-magnification (100×) view of sandstone with a substantial number of pores, relatively speaking, greater than about 20 µm in diameter. An EDX overview suggests the sample is dominated by quartz and feldspar. A substantial amount of dolomite is also visible; a few crystals are identified by the white arrows. The yellow and red arrows indicate the locations of image 8739_2 and 8739_5, respectively.

In the middle of image **8739_2** (400× magnification), a columnar quartz crystal at site 1 has undergone a considerable amount of dissolution. An EDX analysis at site 2 suggests that the mineral is dolomite with low magnesium content. A similar crystal is shown at the tip of the white arrow. The yellow arrows indicate dolomite crystals that are euhedral.

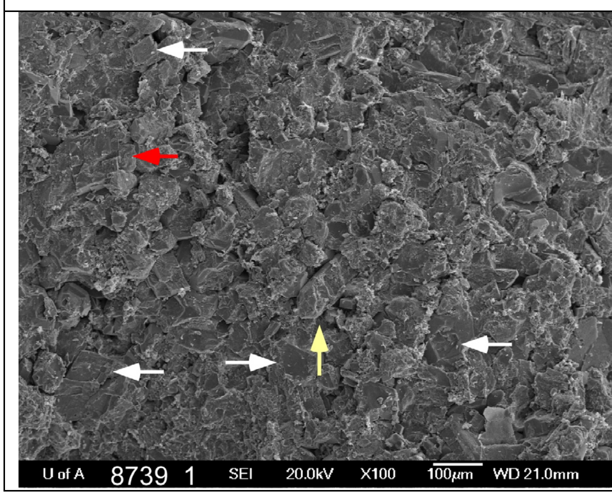


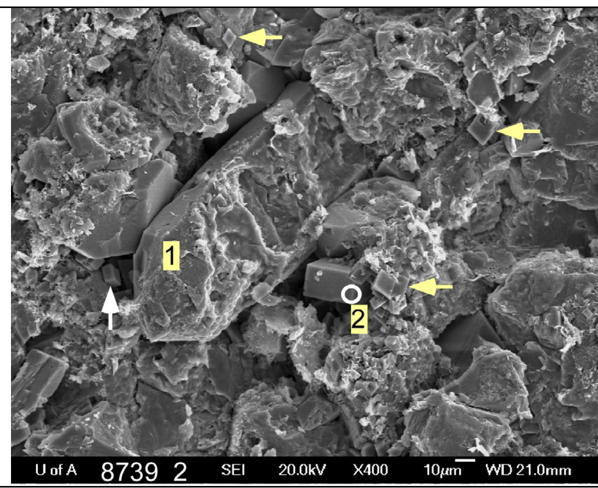

An EDX analysis of the clay seen in image **8739_3** (1800× magnification) suggests that the mineral is illite. Notice that the illite is partially blocking the relatively large pore in the background. As mentioned earlier, at least some of the illite is a late-stage authigenic mineral.

Image **8731_4** (2500× magnification) was taken near the left edge of the previous image. The grain in the middle is anchored at the base of the pore and seems to bisect the pore. Although there are hints of illite morphology in some areas of the image, we could not obtain a reasonable mineralogical analysis of the crystals.

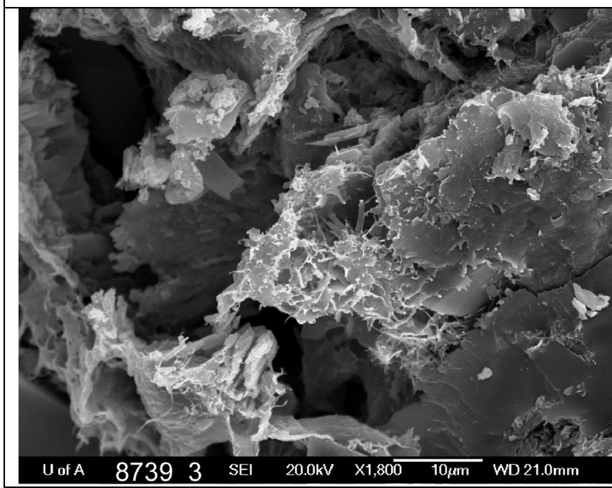


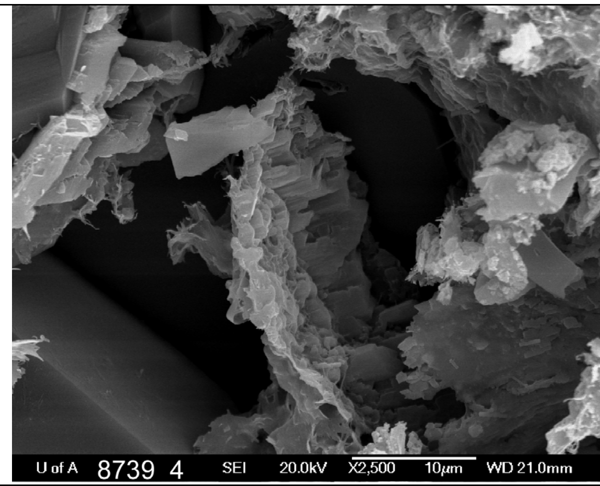


Image **8739_5** (300× magnification) shows dolomite crystals at site 1 (EDX not saved) and smaller rhombic crystals (indicated by the white arrows) that are presumably dolomite. Quartz grains were identified at sites 2 and 3 (EDX not saved). As in many of the images, a large amount of overgrowth at site 4 (presumably quartz) covers the grains and obscures the mineralogy and size of the grains. The largest pores in this image are much greater than 10 µm, unlike the silt-dominated images where pores of this size are relatively rare.

In image **8739_6** (1000× magnification), the rather large, odd-shaped crystal that spans much of the image (site 1), is dolomite (EDX not saved). Relative to the previous image and the smaller, more pristine dolomite crystal at site 2, we may be seeing ‘old’ and ‘new’ dolomite crystals representing separate stages in the dolomitization of the Montney Formation.

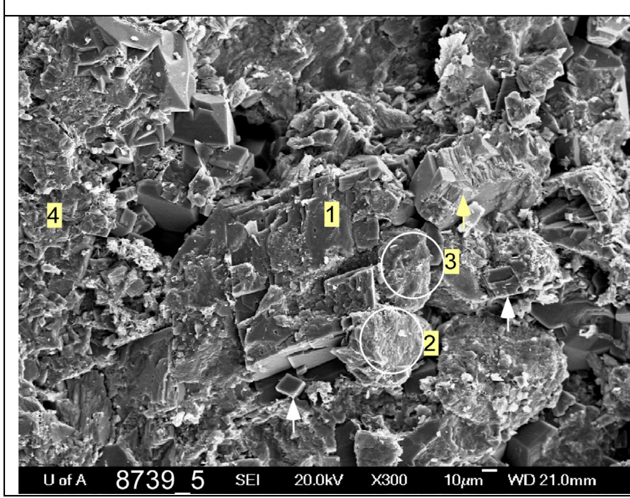


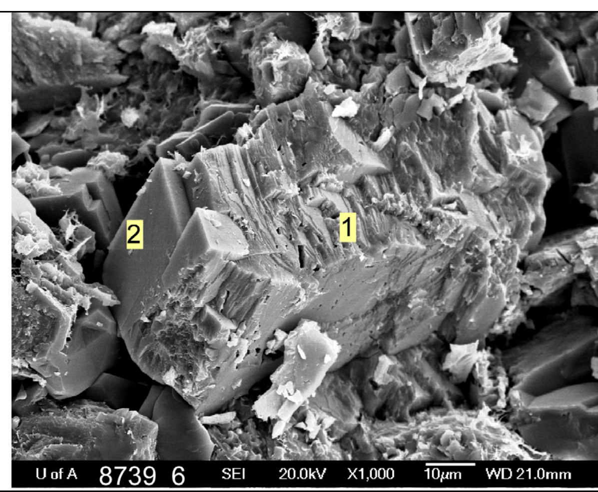

| Image **8739_7** (1800× magnification) identifies floating illite crystals exhibiting a cardhouse structure in the centre of the image. As in the other images, illite is often present in the pore throats. The crystal on the right of the image (quartz?; indicated by white arrow,) has undergone dissolution. The yellow arrow points to columnar quartz and the red arrow identifies a rhombic crystal of dolomite. |
|---|
| 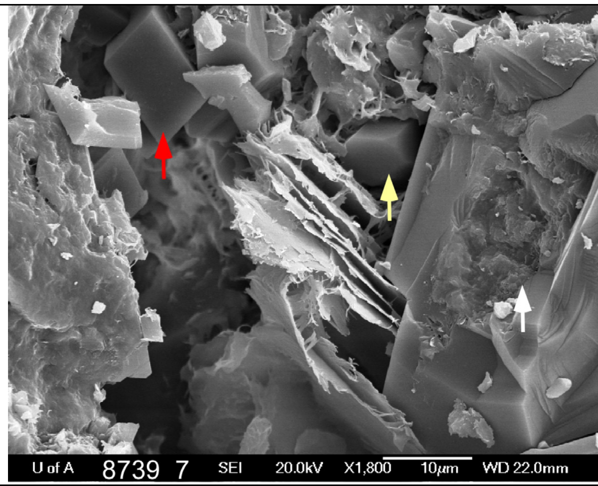 |

EDX results for sample 8739:

| Composition | Image | ID on Image |
|---|---|---|
| Quartz (EDX_8739_002) | 8739_2 | 1 |
| Dolomite (EDX_8739_002) | 8739_2 | 2 |
| Illite (EDX_8739_003) | 8739_3 | n/a |
| Dolomite (EDX not saved) | 8739_5 | 1 |
| Quartz (EDX not saved) | 8739_5 | 2 |
| Quartz (EDX not saved) | 8739_5 | 3 |
| Quartz overgrowth (EDX not saved) | 8739_5 | 4 |
| Dolomite (EDX not saved) | 8739_6 | 1 |
| Dolomite (EDX not saved) | 8739_6 | 2 |
| Quartz? (EDX not saved) | 8739_7 | White arrow |
| Columnar quartz (EDX not saved) | 8739_7 | Yellow arrow |
| Dolomite (EDX not saved) | 8739_7 | Red arrow |

Note: The depth of the EDX analysis is ~1–2 µm, so the chemistry below the surface may dominate the surface mineral.

### *Montney Formation, Sample 8744, UWI 102/11-34-61-19W5/00, 2163.5 m Core Depth*

The sample is grey, slightly sandy siltstone with fine-grained, calcareous sandstone laminae.


| Image | Magnification |
| --- | --- |
| 8744_1 | 100x |
| 8744_2 | 370x |
| 8744_3 | 1700x |
| 8744_4 | 500x |
| 8744_5 | 2000x |
| 8744_6 | 750x |
| 8744_7 | 6500x |

Image **8744_1** is a low-magnification (100×) view with a larger degree of porosity than many of the images we have seen previously. No bedding trend is evident in this view. An EDX analysis overview suggests the sample is dominated by dolomite and quartz. The white arrow points to the location of the next image.

Image **8744_2** is a higher magnification (370×) view of the porosity in the sample. An EDX analysis of particle mineralogy identifies the presence of feldspar at site 1, dolomite at site 2 and quartz at site 3. Grain and crystal sizes vary from ~4 to ~50 µm in the sample, and pore throats are up to 10 µm in diameter. Porosity is not evenly distributed. The white arrow points to the location of the next image.

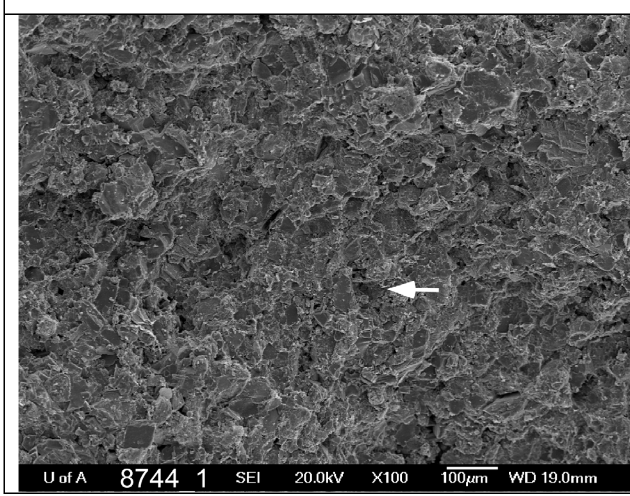


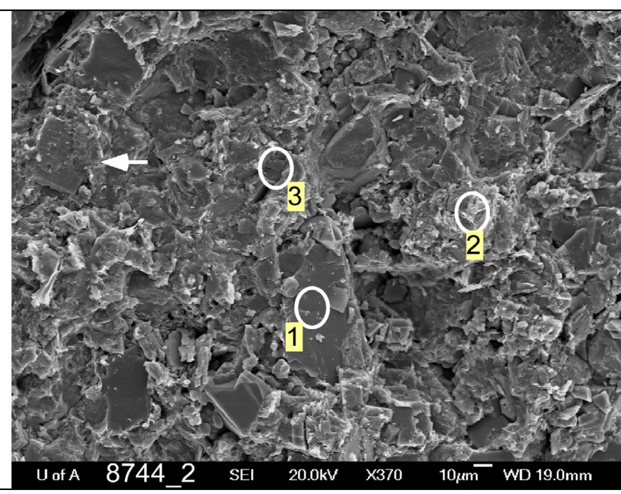

Image **8744_3** (1700× magnification) is an example of authigenic dolomite crystals (Dol; EDX not saved) that contains a few pores resting next to quartz (Qtz). The quartz surface is quite rough and may be overgrowth or perhaps represents a dissolution surface. We are not certain if the smooth surface identified at the tip of the red arrow is the surface of the quartz grain or represents a separate mineral. The opposite end of the red arrow may be resting on quartz overgrowth. Illite is present at the tip of the yellow arrow.

Image **8744_4** (500× magnification) was taken at a new site on the sample and highlights the large pore in the middle of the image. The area surrounding the pore is well cemented, with a few scattered pores less than ~10 µm in diameter.

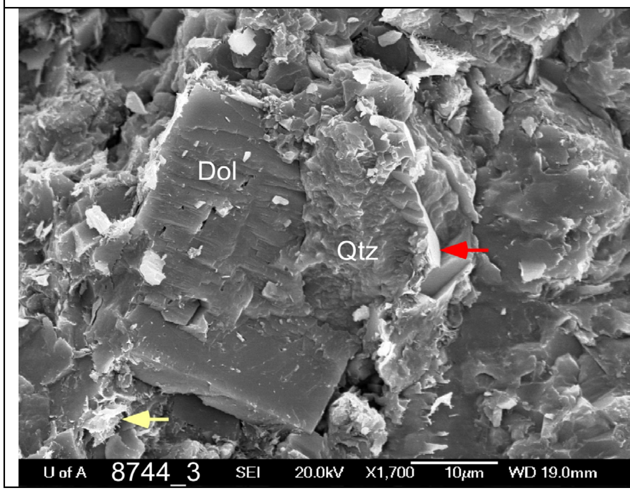


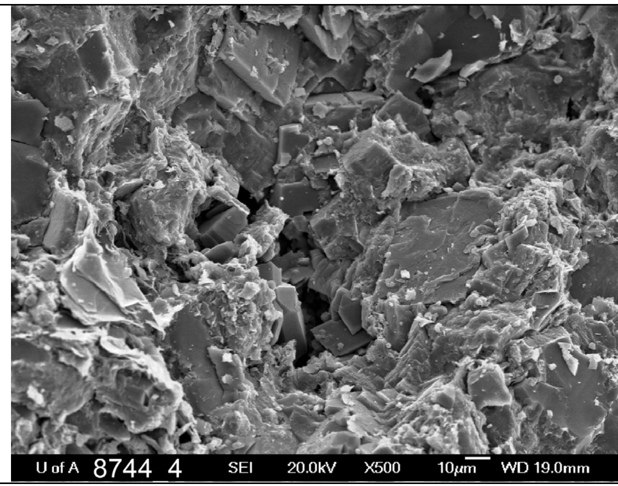


Image **8744_5** is a high-magnification (2000×) view of euhedral crystals lining the pore. On the left side of the pore are twinned dolomite crystals (Dol). The pristine nature of the crystals could indicate late diagenetic crystallization, given the degree of dissolution we have seen in other images. Dolomite crystals are also found on the right side of the pore, but these have a different morphology. We did not do an EDX analysis of the sediment on the right and left sides of the pore, but the material resembles quartz overgrowth (Qtz).

Image **8744_6** (750× magnification) is a view of a pore cavity. The columnar quartz crystal on the left is projecting into the pore. The large grain on the right is partially covered in clay and quartz overgrowth. The small crystals identified by the yellow arrows are likely carbonate. The white arrows point to clay sheets (illite?), although they are a little difficult to discern at this level of magnification. The red arrow points to the location of the next image.

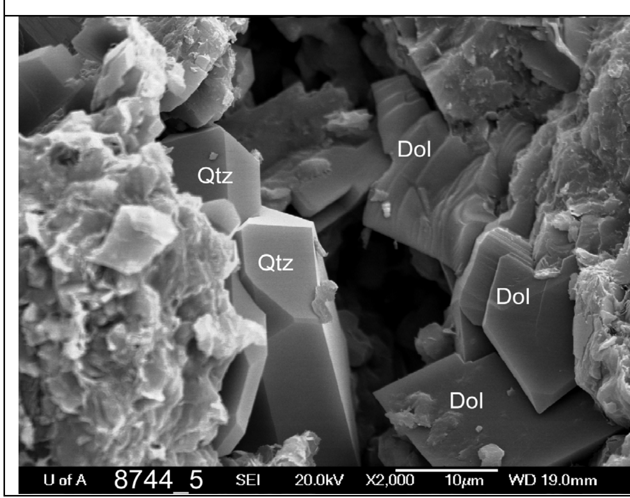


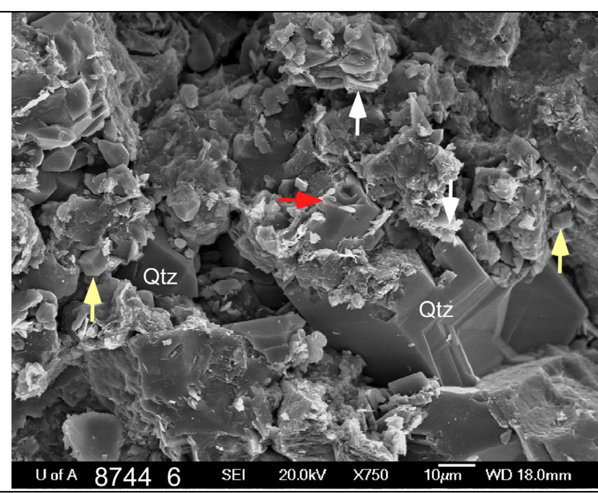

The large quartz crystal in the centre of image **8744_7** (6500× magnification) is surrounded by sheets of clay (illite?; white arrows). The quartz crystal has an interesting 'star' pattern that may be the site of a plucked quartz crystal.

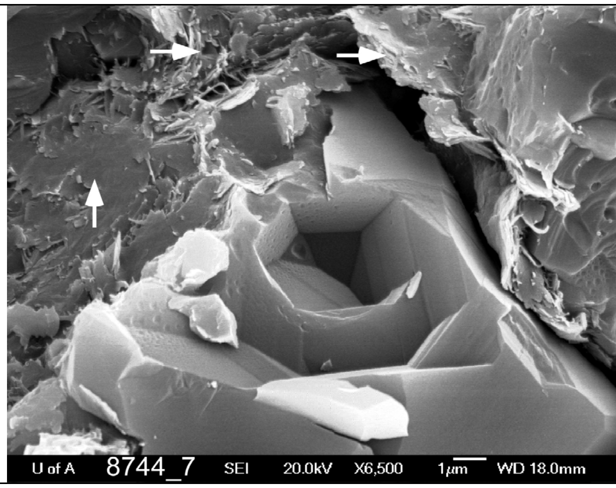


EDX results for sample 8744:

| Composition | Image | ID on Image |
|---|---|---|
| Feldspar (EDX not saved) | 8744_2 | 1 |
| Dolomite (EDX not saved) | 8744_2 | 2 |
| Quartz (EDX not saved) | 8739_2 | 3 |
| Dolomite (EDX not saved) | 8744_3 | Dol |
| Quartz (EDX not saved) | 8744_3 | Qtz |
| Dolomite (EDX not saved) | 8744_5 | Dol |
| Quartz overgrowth (EDX not saved) | 8744_5 | Qtz |

Note: The depth of EDX analysis is ~1–2 μm, so the chemistry below the surface may dominate the surface mineral.

### *Montney Formation, Sample 8858, 100/16-23-057-06W6/00, 2703.6 m (8870 ft.) Core Depth*

The sample is black to dark grey siltstone with rare sandstone laminae. The bedding trends north and the base of the sample is to the left.

| Image | Magnification |
|---|---|
| 8858_1 | 25x |
| 8858_2 | 100x |
| 8858_3 | 250x |
| 8858_4 | 500x |
| 8858_5 | 1000x |
| 8858_6 | 100x |
| 8858_7 | 250x |
| 8858_8 | 3500x |
| 8858_9 | 1000x |

Image **8858_1** is a low-magnification (25×) view that shows a weak north trend in bedding. Three distinct layers of bedding are present in the sample, but they are much less visible in the SEM image than in a hand sample. The next image is taken near the tip of the white arrow within the centre lamina. The red arrow points to the location of image 8858_6.

At 100× magnification in image **8858_2**, dark grains of partly silt-sized material begin to stand out against the lighter coloured background. Porosity is minimal at this scale. There is no apparent bedding trend. An EDX overview suggests the presence of quartz, feldspar and dolomite. The yellow and red arrows indicate the locations of image 8858_2 and 8858_6, respectively.

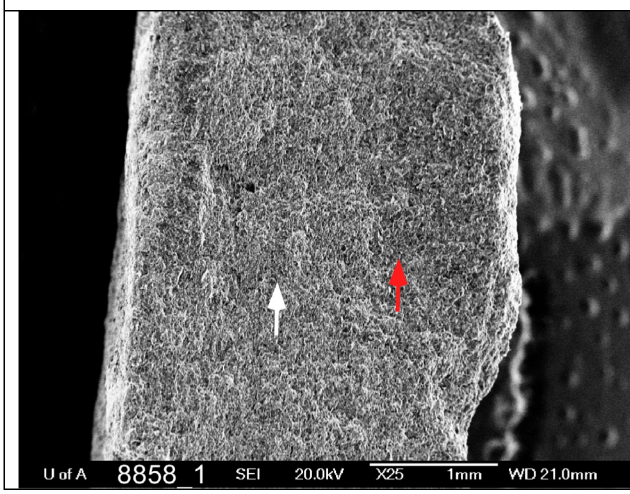


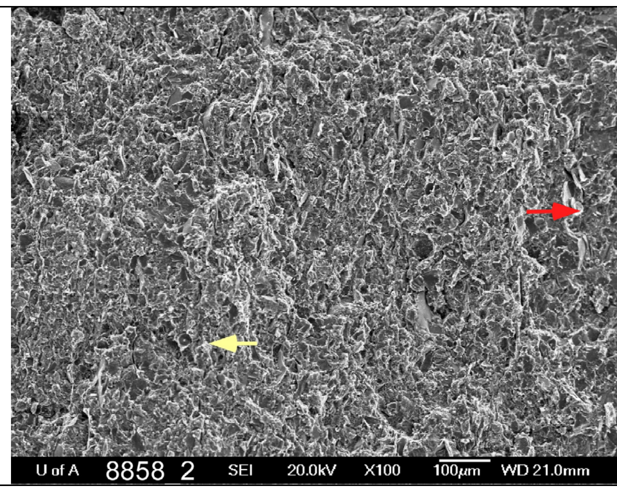

At 250× magnification, porosity is readily apparent in image **8858_3** and pores are generally less than 10 µm in diameter. Similar to other Montney images, mineral grains are often not easily visible due to the abundance of diagenetic mineralization (cement, quartz overgrowth, diagenetic minerals). The yellow arrow indicates the location of image 8858_4.

In image **8858_4** (500× magnification), the linear pore on the bottom left (white arrow) may be the site of a plucked mica, a piece of which appears at the bottom of the pore. Porosity seems to be evident at grain contacts, with secondary porosity perhaps more evident than primary porosity. An EDX analysis (EDX not saved) yielded quartz at site 1, potassium feldspar at site 2, a mixture of quartz and feldspar at site 3 and dolomite at site 4. The yellow arrow points to the location of image 8858_5.

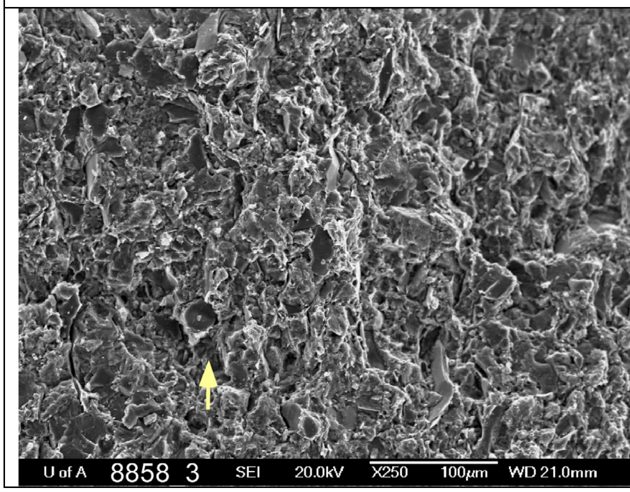


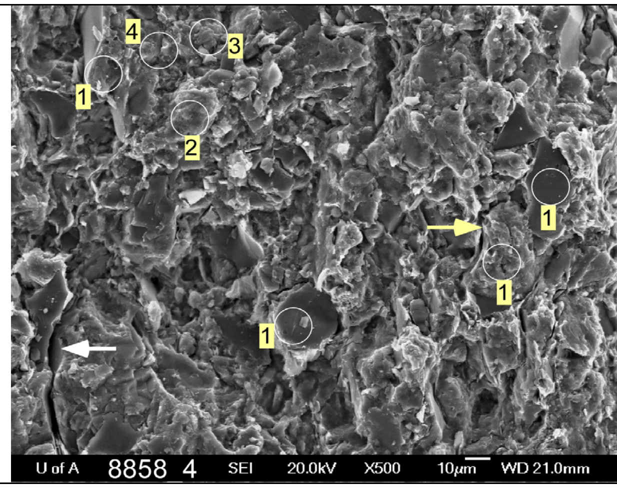


The purpose of image **8858_5** (1000× magnification) was to examine porosity development. Intraparticle pores are present (white arrow), as well as pores near grain contacts; however, the effectiveness or connectivity of the porosity is questionable. Again, it is difficult to discern grains due the large amount of cement. It is much easier to view crystals that are perhaps related to diagenesis than to discern actual primary silt-sized mineral grains. The red arrow indicates a small pyrite framboid is seen at.

An EDX overview of image **8858_6** (100× magnification) identified more calcite than in the central part of the sample. A comparison of images 8858_2 and 8858_6 indicates that image 8858_6 has a coarser texture than 8858_2. Image 8858_6 is an example of the coarse laminae seen in the core photograph, which are actually coarse siltstone in this case. The white and red arrows indicate the locations of images 8858_7 and 8858_9.

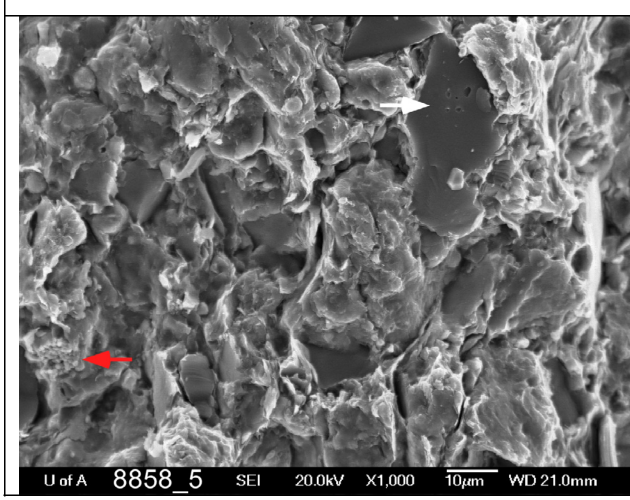


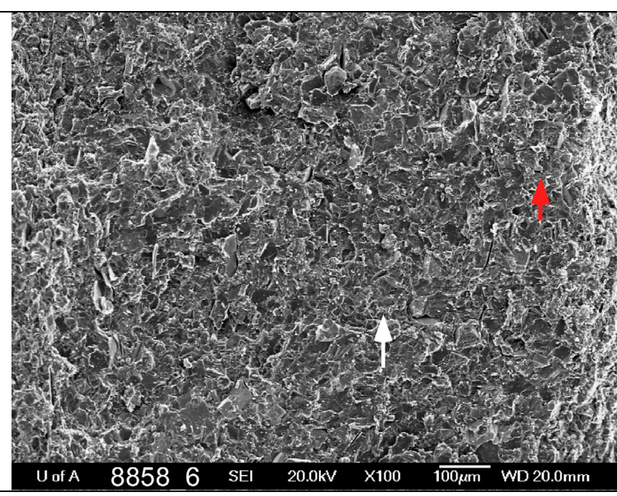

An EDX analysis (not saved) of image **8858_7** (250× magnification) indicates the presence of quartz at site 1, feldspar at site 2, sodium feldspar at site 3, zinc sulphide at site 4 (EDX 8858_004), pyrite within a small cavity of another mineral at site 5 and dolomite at site 6 (EDX_8858_003). Interestingly, calcium shows up on the EDX overview of the previous image but no calcite was found in our analysis of image 8858_7; perhaps the dolomite is low in magnesium.

Image **8858_8** shows the zinc sulphide mineral at 3500× magnification. The mineral 'layers' may actually be cleavage or mineral zones. We do not know the mineralogy of the white grains resting on the sulphide.

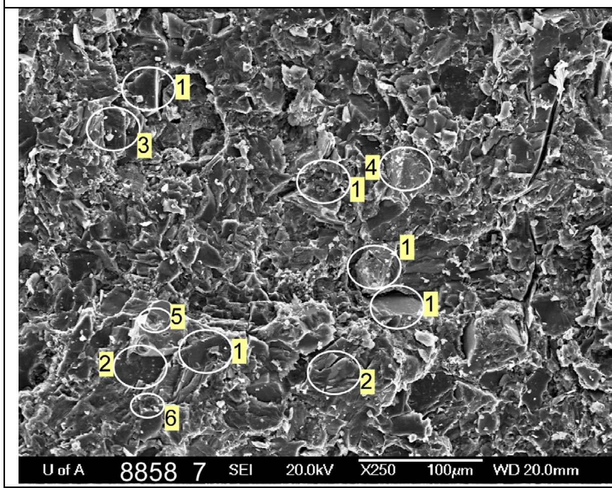


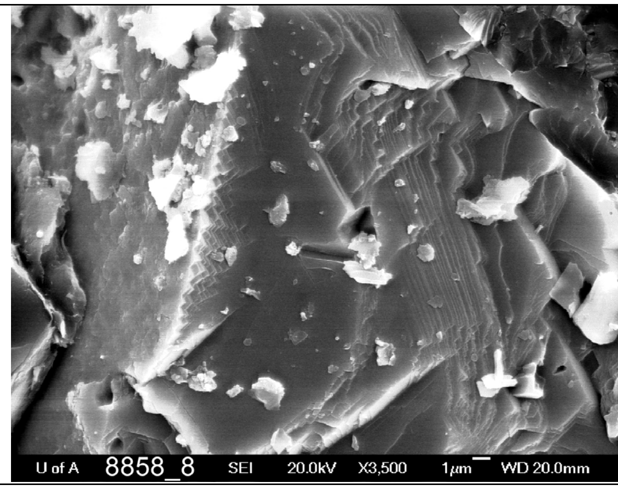


An EDX analysis (not saved) of image **8858_9** (1000× magnification) indicates the presence of quartz at site 1, pyrite at site 2, dolomite at site 3 and feldspar at site 4.

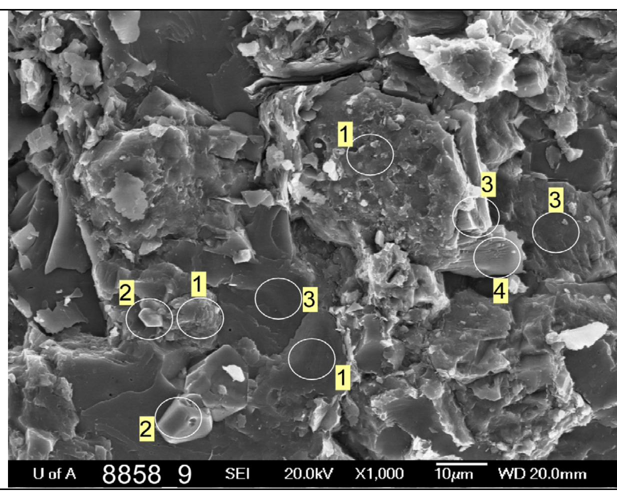

EDX results for sample 8858:

| Composition | Image | ID on Image |
|---|---|---|
| Dolomite (EDX_8858_003) | 8858_4 | 4 |
| Quartz (EDX not saved) | 8858_7 | 1 |
| Feldspar (EDX not saved) | 8858_7 | 2 |
| Sodium feldspar (EDX not saved) | 8858_7 | 3 |
| Zinc sulphide (EDX not saved) | 8858_7 | 4 |
| Pyrite (EDX not saved) | 8858_7 | 5 |
| Dolomite (EDX not saved) | 8858_7 | 6 |
| Zinc Sulphide (EDX 8858 004) | 8858_8 | n/a |
| Quartz (EDX not saved) | 8858_9 | 1 |
| Pyrite (EDX not saved) | 8858_9 | 2 |
| Dolomite (EDX not saved) | 8858_9 | 3 |
| Feldspar (EDX not saved) | 8858_9 | 4 |

Note: The depth of EDX analysis is ~1–2 µm, so the chemistry below the surface may dominate the surface mineral.

### *Montney Formation, Sample 8878, UWI 100/16-31-066-23W5/00, 1718.1 m Core Depth*

The sample is massive grey siltstone.


| Image | Magnification |
|---|---|
| 8878_1 | 25x |
| 8878_2 | 100x |
| 8878_3 | 500x |
| 8878_4 | 1500x |
| 8878_5 | 1800x |
| 8878_6 | 7500x |
| 8878_7 | 2700x |
| 8878_8 | 2000x |

Image **8878_1** is a low-magnification (25×) view with little indication of bedding, although the general trend is northeast. The texture appears relatively homogeneous.

At higher magnification in image **8878_2** (100× magnification), dark grey silt- and sand-sized grains are visible. The silt particles are scattered rather than in discrete laminae. Porosity is represented by the black areas and is distributed throughout the sample. An EDX overview suggests the presence of quartz, potassium feldspar, dolomite, and pyrite. Image 8878_3 was taken near the centre of this image.

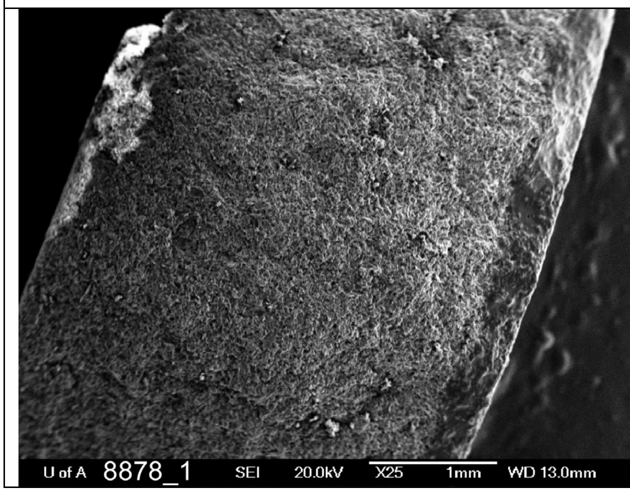


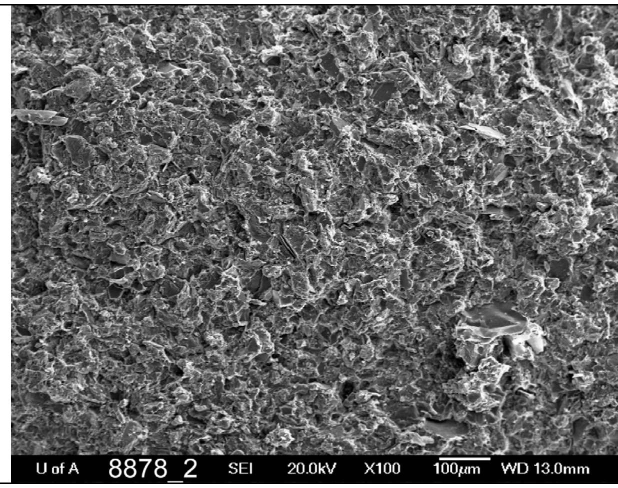


As with most Montney Formation SEM images, image **8878_3** (500× magnification) looks very busy; it is difficult to get a clear view of silt- or sand-sized grains. An EDX analyses (not saved) of image 8878_3 reveals potassium feldspar at site 1, potassium feldspar with some illite at site 2, pyrite at site 3, mostly illite at site 4, sodium feldspar at site 5 and quartz covered with illite at site 6. There is a reasonable amount of porosity in the sample, with a few of them being large (>10 µm) but more being less than 5 µm. The next images will focus on sites 1, 5 and 6 (image 8878_4), sites 2 and 3 (image 8878_5), site 6 again (image 8878_6) and site 5 (image 8878_7); finally, image 8878_8 was taken near the red arrow.

The quartz grain covered with illite from the previous image is in the centre of image **8878_4** (1500× magnification). The thickness of the illite must be less than 1–2 µm or the EDX would not have detected the quartz grain. Fibrous illite can be seen scattered in other areas of the image (e.g., red arrow). The potassium feldspar grain identified earlier (white arrow) and an unnamed grain (yellow arrow) both contain intraparticle porosity. The green arrows point to what may be dolomite crystals (for a comparison, see image 8739_2).

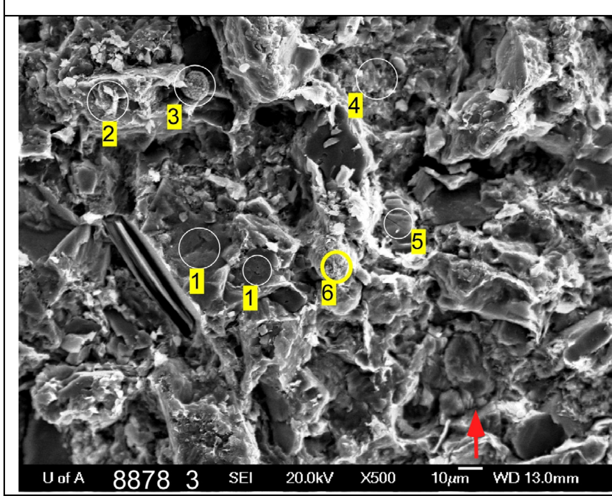


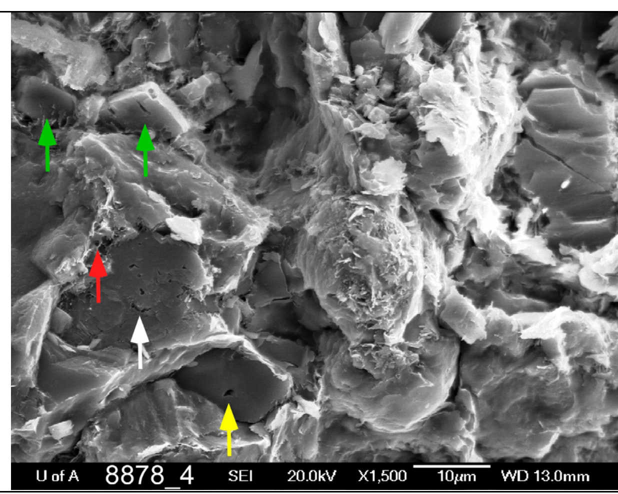

Image **8878_5** is a higher magnification (1800×) view of the potassium feldspar at site 2 of image 8878_3 and the pyrite at site 3. Many of the edges of the grain (white areas; red arrows) are altering to illite; you may have to zoom in on the image to get a better view. Additionally, the grain identified by the yellow arrow appears to be in the same state of alteration. This lends credence to the view that at least some of the illite is a late-stage diagenetic-alteration product.

Image **8878_6** (7500× magnification) shows fibrous illite from site 6 of image 8878_3. An EDX analysis indicates that the illite is covering a quartz grain. Microporosity is clearly evident in the dark areas near the red arrow.

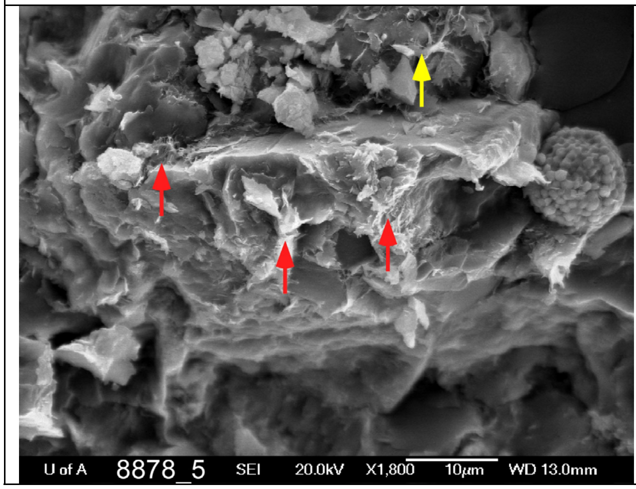


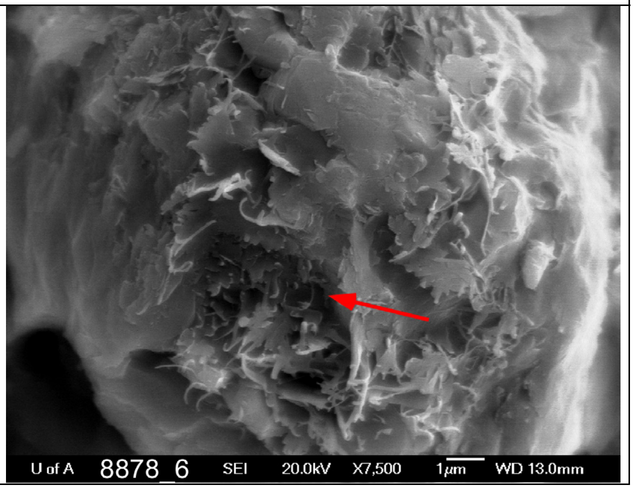


Image **8878_7** (2700× magnification) is a close-up view of the sodium feldspar grain (EDX_8878_003) seen in image 8878_3. Zooming in on the edges of the grain (red arrows) reveals what appears to be alteration to illite. The fracture in the grain appears to be fresh, suggesting that it was induced during core retrieval.

Image **8878_8** (2000× magnification) was used to identify mineralogy. Potassium feldspar is at site 1, quartz at site 2 and dolomite at site 3. Fibrous illite is identified by the red arrows.

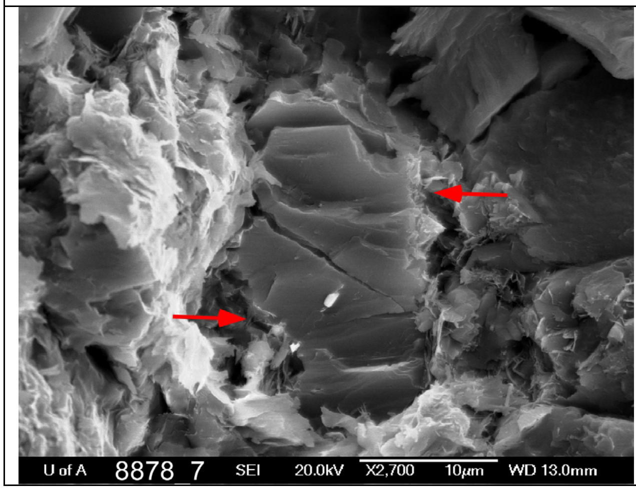


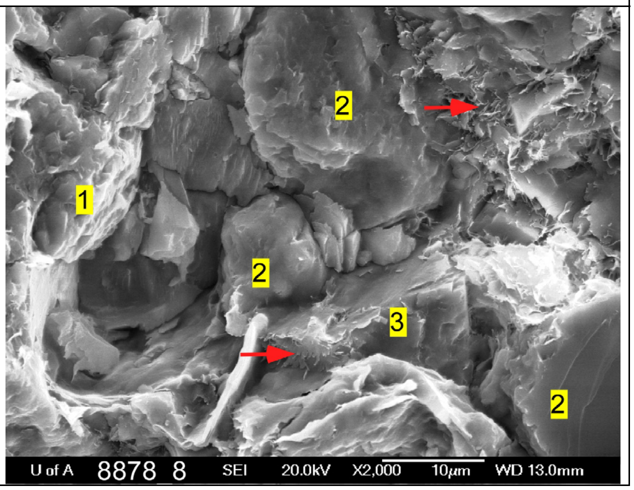

EDX results for sample 8878:

| Composition | Image | ID on Image |
|---|---|---|
| Potassium feldspar (EDX not saved) | 8878_3 | 1 |
| Potassium feldspar with illite (EDX_8878_002) | 8878_3 | 2 |
| Pyrite | 8878_3 | 3 |
| Illite | 8878_3 | 4 |
| Sodium feldspar | 8878_3 | 5 |
| Quartz and illite | 8878_3 | 6 |
| Illite alteration from feldspar | 8878_5 | Red and yellow arrows |
| Sodium feldspar (EDX_8878_003) | 8878_7 | |
| Potassium feldspar | 8878_8 | 1 |
| Quartz | 8878_8 | 2 |
| Dolomite | 8878_8 | 3 |
| Fibrous illite | 8878_8 | Red arrows |

Note: The depth of EDX analysis is ~1–2 µm, so the chemistry below the surface may dominate the surface mineral.

### *Montney Formation, Sample 8901, UWI 100/06-14-066-06W6/00, 3034.3 m Core Depth*

The sample is dark grey, noncalcareous siltstone.


| Image | Magnification |
|---|---|
| 8901_1 | 25x |
| 8901_2 | 100x |
| 8901_3 | 250x |
| 8901_4 Backscatter | 500x |
| 8901_5 | 2700x |
| 8901_6 Backscatter | 2700x |

Image **8901_1** is a low-magnification (25×) view that shows the development of fractures (white arrows) that are open and fresh. An EDX overview of the sample suggests a dominance of quartz, feldspar and dolomite. There is a scattering of dark, lower-sand–sized grains in the image. Image 8901_2 was taken near the centre of 8901_1.

The white arrow in image **8901_2** (100× magnification) identifies an open fracture (white arrow) that is difficult to follow east of the arrow. Note that the fracture changes trend near the left side of the image. There are hints of additional fractures in other parts of the image. Very little non-fracture porosity is visible at this scale of observation. Image 8901_3 was taken to the left of the arrow.

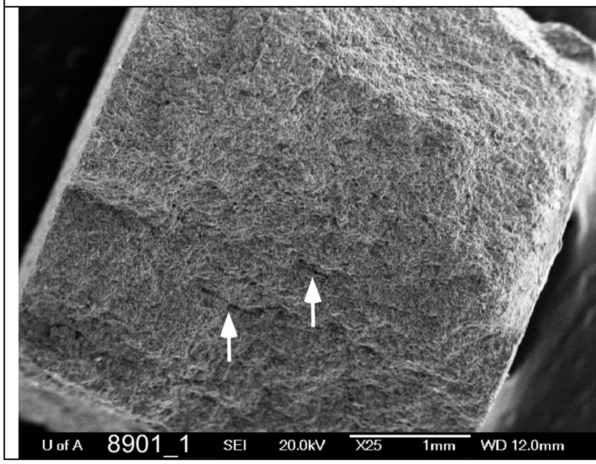


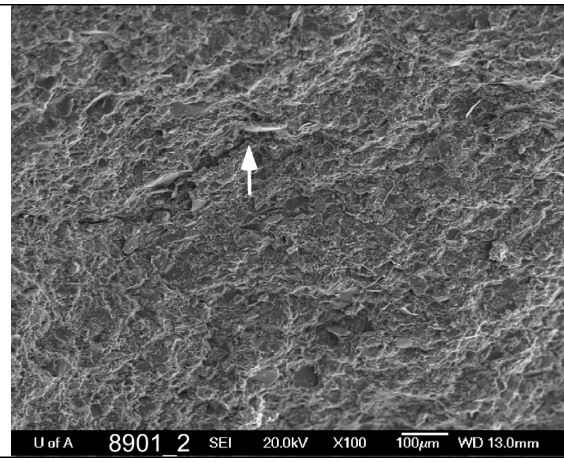


Image **8901_3** is a higher magnification (250×) view showing the trend and nature of the fracture. An EDX analysis of particles (not saved) yielded the following results: quartz at site 1, mica at site 2 and feldspar at sites 3 and 4. The EDX analysis showed the chemistry at site 4 to have strong peaks indicating potassium aluminum silicate, more so than at site 3. This may be related to a coating on the mineral at site 3, or perhaps the beam was slightly misdirected at site 3. The next image was taken near the white arrow.

Image **8901_4** (500× magnification) is a backscattering image that indicates an abundance of heavy minerals in the sample (heavy minerals show up as 'white' particles). This is one of the better quality backscattering images taken during this project. The white arrow points to the location of the feldspar seen at site 3 in the previous image. Pyrite framboids are identified by the small white circles. We cannot be certain of how much pyrite, whether framboidal or other morphologies, is present relative to other heavy minerals. Image 8901_5 was taken near the large circle to investigate the mineralogy of the large white particle.

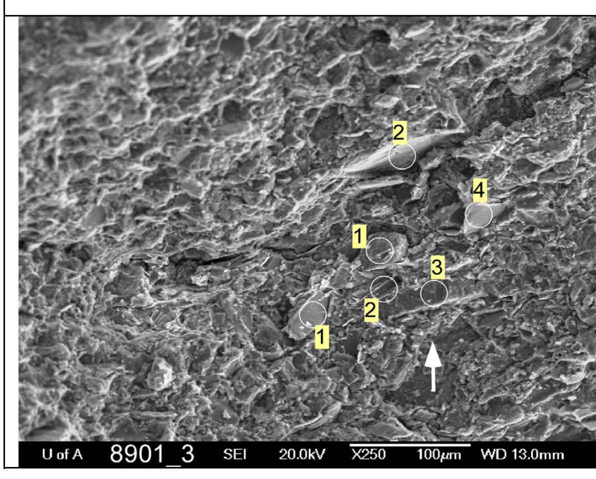


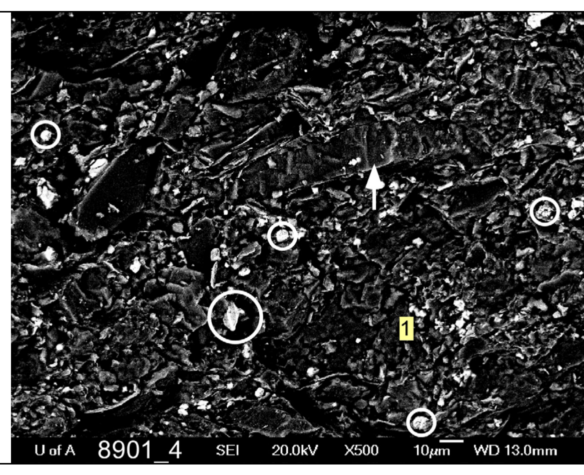

An EDX analysis (not saved) of image **8901_5** (2700× magnification) clearly shows the particle at site 1 to be pyrite, although this is an odd morphology for pyrite. Note that the depth of EDX analysis is about 1–2 µm, so the chemistry below the surface may dominate the surface mineral. Other minerals identified in this view are potassium feldspar at site 2, quartz at site 3 and dolomite at site 4. The area in the square shows the presence of small crystals of pyrite that will be investigated in image 8901_6, along with the minerals identified by the white arrows.

Image **8901_6** (2700× magnification) is a backscattering view of the previous image that perhaps leads to more questions than answers regarding the presence of heavy minerals in the sample. The large pyrite particle in the centre is properly identified, as is the area within the white circle. The red arrow identifies a 'heavy' mineral on the quartz particle that is not identified. Furthermore, the upper yellow arrow presumably identifies a heavy mineral, except that the particle appears to be very finely laminated (i.e., clay-like). This is not a habit of pyrite with which we are familiar. The abundance of pyrite or other conductive minerals in Alberta shale may be an area of investigation for the future, as this is a critical part of the well-log evaluation of shale.

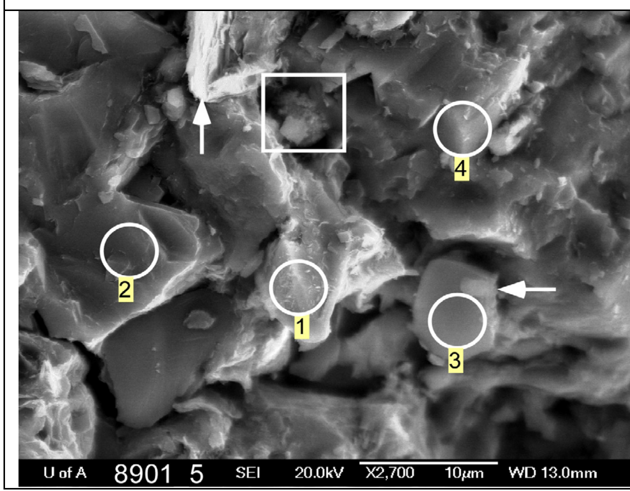


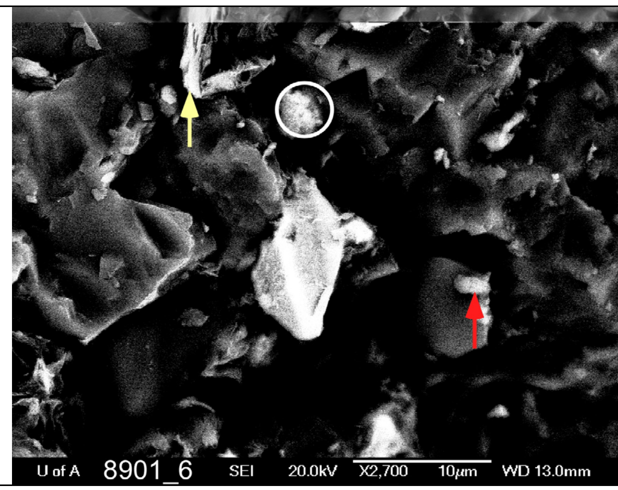


EDX results for sample 8901:

| Composition | Image | ID on Image |
|---|---|---|
| Quartz (EDX not saved) | 8901_3 | 1 |
| Mica (EDX not saved) | 8901_3 | 2 |
| Feldspar (EDX not saved) | 8901_3 | 3 |
| Feldspar (EDX_8901_002) | 8901_3 | 4 |
| Pyrite | 8901_5 | 1 |
| Potassium feldspar (EDX not saved) | 8901_5 | 2 |
| Quartz (EDX not saved) | 8901_5 | 3 |
| Dolomite (EDX not saved) | 8901_5 | 4 |

Note: The depth of EDX analysis is about 1–2 µm, so the chemistry below the surface may dominate the surface mineral.

### *Montney Formation, Sample 8926, UWI 100/15-08-081-12W6/00, 1827.7 m Core Depth*

The sample is dark grey siltstone with thin (<1mm), light-coloured calcareous laminae and lenses (1–6 mm thick).


| Image | Magnification |
|---|---|
| 8926_1 | 23x |
| 8926_2 | 100x |
| 8926_3 | 250x |
| 8926_4 | 1000x |

Image **8926_1** is a low-magnification (23×) view with no indication of bedding. An EDX overview indicates a dominance of quartz, potassium feldspar, dolomite and pyrite. Titanium also shows up on the chemical spectrum.

At 100× magnification, there is still no indication of bedding in image **8926_2**. There appears to be more matrix (non-dark grains) than dark grains. Some of the dark grains are sand sized or near the sand-silt boundary. Grain roundness and sphericity cover the entire spectrum, although more angular particles with poor sphericity appear to dominate. There are quite a number of sites where it appears that mica has been plucked from the sample. Porosity appears to be fairly well distributed at this level of magnification. Image 8926_3 was taken in the centre of this image.

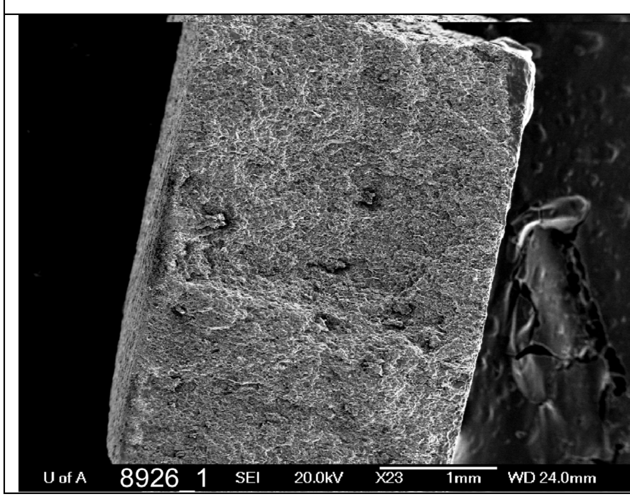


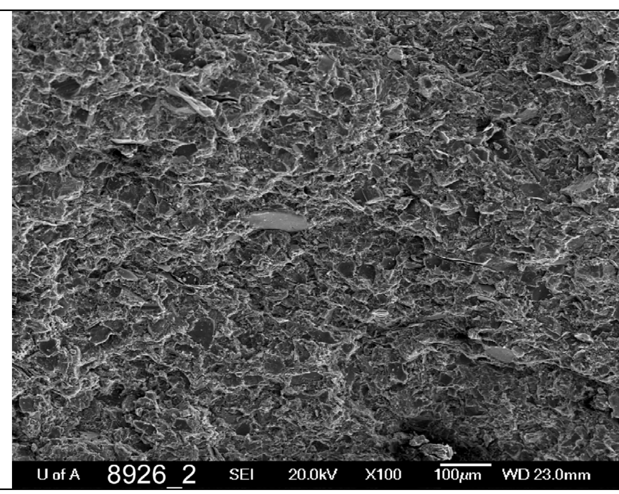

An EDX analysis of minerals in image **8926_3** (250× magnification) yielded mica, likely muscovite, at site 1, mica at site 2, sodium feldspar at site 3, quartz at site 4 and an indeterminate mixture of non-clay minerals at site 5. Note that site 5 resembles the greyish matrix throughout much of the image; hence, the matrix may be composed of a variety of small grains of non-clay minerals and cements. Most of the mica plates in the image are east- trending, although a few show some curvature (white arrow) or an alternate trend (yellow arrow), so there has been some local disturbance (compaction effects?) of the sample. The red arrow points to the location of image 8926_4.

Image **8926_4** (1000× magnification) was taken to examine porosity. Pore sizes below 10 µm are most abundant, with one large pore located in the upper centre of the image (red arrow). Porosity is fairly well distributed, although small pores (< 5 µm) appear better distributed than large ones. Intragranular and intergranular porosity are both present. Note the curvature of the mica in the lower left of the image.

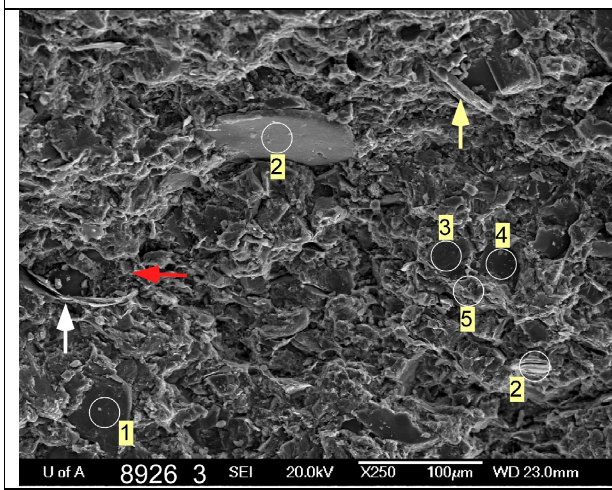


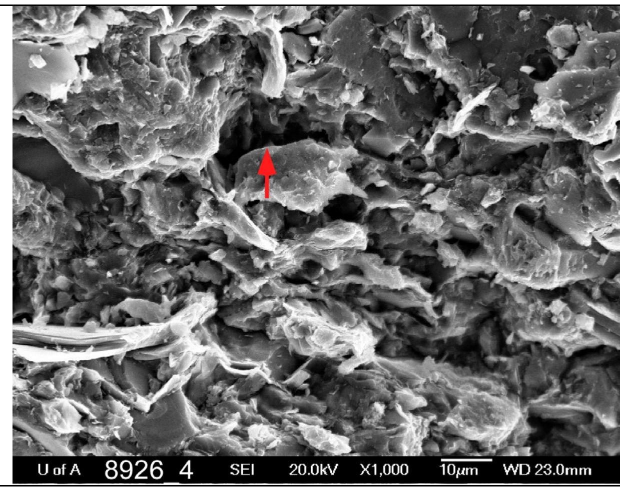


EDX results for sample 8926:

| Composition | Image | ID on Image |
|---|---|---|
| Mica, likely muscovite (EDX_8926_002) | 8826_3 | 1 |
| Mica (EDX not saved) | 8826_3 | 2 |
| Sodium feldspar (EDX not saved) | 8826_3 | 3 |
| Quartz (EDX not saved) | 8826_3 | 4 |
| Mixture (EDX not saved) | 8826_3 | 5 |

Note: The depth of EDX analysis is about 1–2 µm, so the chemistry below the surface may dominate the surface mineral.

## Appendix 6 – Montney Formation Mercury Porosimetry Graphs

## Incremental Intrusion - Montney sample 8702

"Provides a convenient means to observe the diameter at which pore volume is concentrated" (Webb and Orr, 1997).

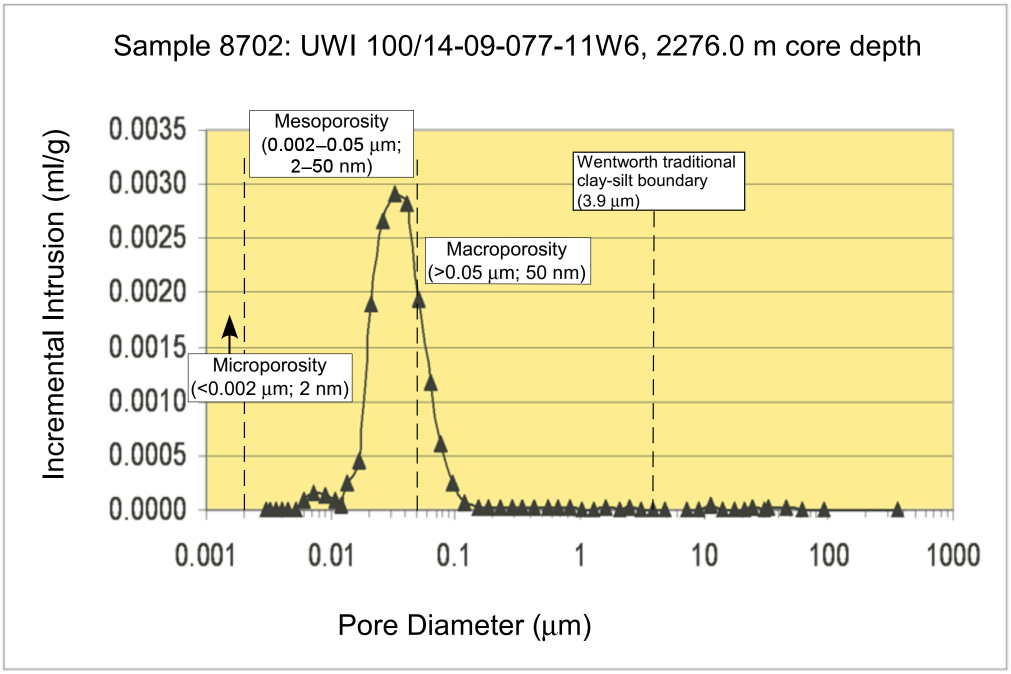


## Log Differential Intrusion - Montney sample 8702

"The compression effect resulting from the use of a log scale is compensated for by dividing the specific incremental intrusion volume by the difference in logarithms of the pore diameters. This results in a curve in which equal peak areas represent equal pore volumes. This plot works best when the data points are equally spaced." (Webb and Orr, 1997).

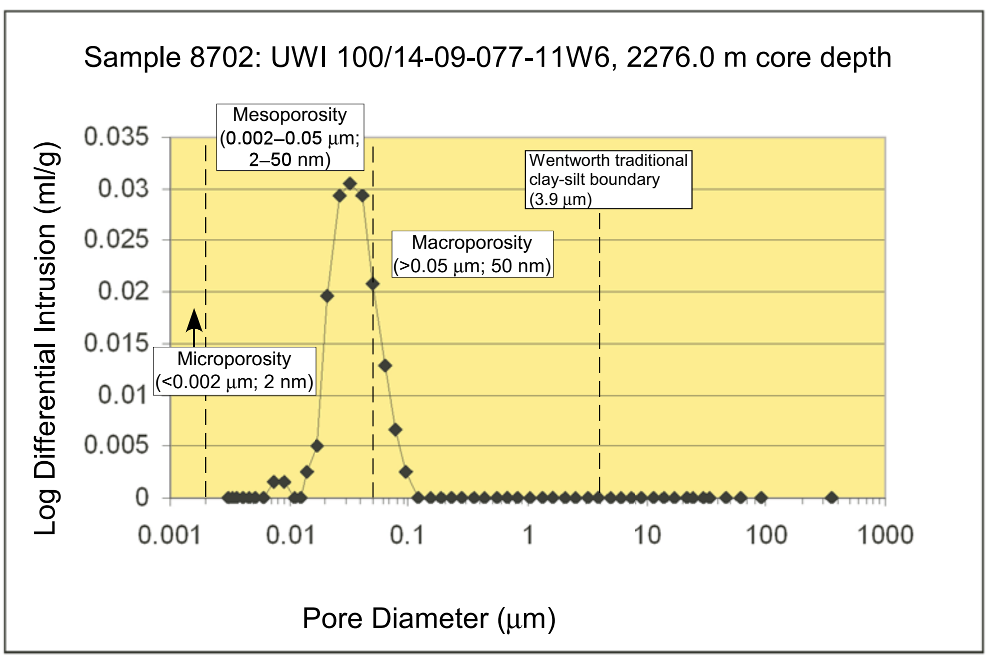

## Appendix 7 – Montney Formation Permeametry

| Sample No. | Depth (ft.) | Depth (m) | Ka | Kl | Comment | Approximate Angle to Bedding | Date | Probe Tip |
|---|---|---|---|---|---|---|---|---|
| 8115 | | 2618.75 | 0.03100 | 0.01030 | surface properly horizontal | 5° to bedding plane | 25-03-09 | Small |
| 8115 | | 2618.75 | 0.02920 | 0.00948 | surface properly horizontal | 5° to bedding plane | 25-03-09 | Small |
| 8115 | | 2618.75 | 0.02880 | 0.00931 | surface properly horizontal | 5° to bedding plane | 25-03-09 | Small |
| 8115 | | 2618.75 | 0.02680 | 0.00845 | surface properly horizontal | 5° to bedding plane | 25-03-09 | Small |
| 8115 | | 2618.75 | 0.03240 | 0.01090 | surface properly horizontal | 5° to bedding plane | 25-03-09 | Small |
| 8115 | | 2618.75 | 0.03020 | 0.00989 | surface properly horizontal | 5° to bedding plane | 25-03-09 | Small |
| 8115 | | 2618.75 | 0.03760 | 0.01330 | surface properly horizontal | 5° to bedding plane | 25-03-09 | Small |
| 8115 | | 2618.75 | 0.03560 | 0.01230 | surface properly horizontal | 5° to bedding plane | 25-03-09 | Small |
| 8115 | | 2618.75 | 3.06000 | 2.39000 | surface properly horizontal (natural fracture visible in the rock here) | 5° to bedding p. (~30° to fracture p.) | 25-03-09 | Small |
| 8115 | | 2618.75 | 3.07000 | 2.40000 | surface properly horizontal (natural fracture visible in the rock here) | 5° to bedding p. (~30° to fracture p.) | 25-03-09 | Small |
| 8115 | | 2618.75 | 0.04480 | 0.01670 | surface properly horizontal | 5° to bedding plane | 25-03-09 | Small |
| 8115 | | 2618.75 | 0.04240 | 0.01550 | surface properly horizontal | 5° to bedding plane | 25-03-09 | Small |
| 8115 | | 2618.75 | 23.60000 | 20.60000 | sample properly horizontal (natural fracture visible in the rock here) | 5° to bedding p. (~30° to fracture p.) | 25-03-09 | Small |
| 8115 | | 2618.75 | 23.60000 | 20.50000 | sample properly horizontal (natural fracture visible in the rock here) | 5° to bedding p. (~30° to fracture p.) | 25-03-09 | Small |
| 8119 | | 2358.2 | 0.09170 | 0.04160 | slight misalignment of sample surface (5-10°) | along bedding plane | 25-03-09 | Small |
| 8119 | | 2358.2 | 0.08910 | 0.04020 | slight misalignment of sample surface (5-10°) | along bedding plane | 25-03-09 | Small |
| 8119 | | 2358.2 | 0.03870 | 0.01370 | repeat measurement, surface properly horizontal | along bedding plane | 25-03-09 | Small |
| 8119 | | 2358.2 | 0.03700 | 0.01290 | repeat measurement, surface properly horizontal | along bedding plane | 25-03-09 | Small |
| 8119 | | 2358.2 | 0.07390 | 0.03170 | slight misalignment of sample surface (5-10°) | along bedding plane | 25-03-09 | Small |
| 8119 | | 2358.2 | 0.07100 | 0.03010 | slight misalignment of sample surface (5-10°) | along bedding plane | 25-03-09 | Small |
| 8119 | | 2358.2 | 0.03770 | 0.01320 | repeat measurement, surface properly horizontal | along bedding plane | 25-03-09 | Small |
| 8119 | | 2358.2 | 0.03640 | 0.01270 | repeat measurement, surface properly horizontal | along bedding plane | 25-03-09 | Small |
| 8707 | 1750.2 | | 0.92400 | 0.63900 | surface properly horizontal | along bedding plane | 25-03-09 | Small |
| 8707 | 1750.2 | | 0.86000 | 0.58800 | surface properly horizontal | along bedding plane | 25-03-09 | Small |
| 8707 | 1750.2 | | 0.02620 | 0.00818 | surface properly horizontal | perpendicular to bedding | 25-03-09 | Small |
| 8707 | 1750.2 | | 0.02480 | 0.00757 | surface properly horizontal | perpendicular to bedding | 25-03-09 | Small |
| 8707 | 1750.2 | | 0.03490 | 0.01200 | surface properly horizontal | perpendicular to bedding | 25-03-09 | Small |
| 8707 | 1750.2 | | 0.03300 | 0.01110 | surface properly horizontal | perpendicular to bedding | 25-03-09 | Small |
| 8718 | 1899.4 | | 0.03620 | 0.01260 | slight misalignment of sample surface (5-10°) | along bedding plane | 25-03-09 | Small |
| 8718 | 1899.4 | | 0.03450 | 0.01180 | slight misalignment of sample surface (5-10°) | along bedding plane | 25-03-09 | Small |
| 8718 | 1899.4 | | 0.02390 | 0.00714 | slight misalignment of sample surface (5-10°) | along bedding plane | 25-03-09 | Small |
| 8718 | 1899.4 | | 0.02250 | 0.00661 | slight misalignment of sample surface (5-10°) | along bedding plane | 25-03-09 | Small |
| 8718 | 1899.4 | | 0.03120 | 0.01030 | slight misalignment of sample surface (5-10°) | along bedding plane | 25-03-09 | Small |
| 8718 | 1899.4 | | 0.02980 | 0.00965 | slight misalignment of sample surface (5-10°) | along bedding plane | 25-03-09 | Small |
| 8718 | 1899.4 | | 0.01930 | 0.00535 | repeat measurement, surface properly horizontal | along bedding plane | 25-03-09 | Small |
| 8718 | 1899.4 | | 0.01780 | 0.00478 | repeat measurement, surface properly horizontal | along bedding plane | 25-03-09 | Small |
| 8786 | 2235.25 | | 1.78000 | 1.32000 | slight misalignment of sample surface (5-10°) | along bedding plane | 25-03-09 | Small |
| 8786 | 2235.25 | | 1.80000 | 1.34000 | slight misalignment of sample surface (5-10°) | along bedding plane | 25-03-09 | Small |
| 8786 | 2235.25 | | 0.03100 | 0.01020 | repeat measurement, surface properly horizontal | along bedding plane | 25-03-09 | Small |
| 8786 | 2235.25 | | 0.02920 | 0.00940 | repeat measurement, surface properly horizontal | along bedding plane | 25-03-09 | Small |
| 8840 | | 8167 | 0.06700 | 0.02810 | slight misalignment of sample surface (5-10°) | 30° to bedding plane | 25-03-09 | Small |
| 8840 | | 8167 | 0.02300 | 0.00681 | repeat measurement, surface properly horizontal | 30° to bedding plane | 25-03-09 | Small |
| 8840 | | 8167 | 0.33000 | 0.19700 | slight misalignment of sample surface (5-10°) | 30° to bedding p. (~parallel to v.) | 25-03-09 | Small |
| 8840 | | 8167 | 0.31300 | 0.18500 | slight misalignment of sample surface (5-10°) | 30° to bedding p. (~parallel to v.) | 25-03-09 | Small |
| 8840 | | 8167 | 0.02630 | 0.00816 | repeat measurement, surface properly horizontal | 30° to bedding p. (~parallel to v.) | 25-03-09 | Small |
| 8840 | | 8167 | 0.02490 | 0.00760 | repeat measurement, surface properly horizontal | 30° to bedding p. (~parallel to v.) | 25-03-09 | Small |
| 8840 | | 8167 | 0.04090 | 0.01480 | slight misalignment of sample surface (5-10°) | 30° to bedding plane | 25-03-09 | Small |
| 8840 | | 8167 | 0.03900 | 0.01390 | slight misalignment of sample surface (5-10°) | 30° to bedding plane | 25-03-09 | Small |
| 8840 | | 8167 | 0.02840 | 0.00908 | repeat measurement, surface properly horizontal | 30° to bedding plane | 25-03-09 | Small |
| 8840 | | 8167 | 0.02650 | 0.00828 | repeat measurement, surface properly horizontal | 30° to bedding plane | 25-03-09 | Small |
| 8856 | | 8846 | 0.19600 | 0.10600 | slight misalignment of sample surface (5-10°) | along bedding plane | 25-03-09 | Small |
| 8856 | | 8846 | 0.19100 | 0.10300 | slight misalignment of sample surface (5-10°) | along bedding plane | 25-03-09 | Small |
| 8856 | | 8846 | 0.15200 | 0.07790 | slight misalignment of sample surface (5-10°) | along bedding plane | 25-03-09 | Small |
| 8856 | | 8846 | 0.14900 | 0.07600 | slight misalignment of sample surface (5-10°) | along bedding plane | 25-03-09 | Small |
| 8856 | | 8846 | 0.04650 | 0.01740 | slight misalignment of sample surface (5-10°) | along bedding plane | 25-03-09 | Small |
| 8856 | | 8846 | 0.04400 | 0.01630 | slight misalignment of sample surface (5-10°) | along bedding plane | 25-03-09 | Small |
| 8856 | | 8846 | 0.03540 | 0.01220 | slight misalignment of sample surface (5-10°) | along bedding plane | 25-03-09 | Small |
| 8856 | | 8846 | 0.03350 | 0.01130 | slight misalignment of sample surface (5-10°) | along bedding plane | 25-03-09 | Small |
| 8856 | | 8846 | 0.04370 | 0.01610 | slight misalignment of sample surface (5-10°) | along bedding plane | 25-03-09 | Small |
| 8856 | | 8846 | 0.04160 | 0.01510 | slight misalignment of sample surface (5-10°) | along bedding plane | 25-03-09 | Small |
| 8856 | | 8846 | 0.05710 | 0.02280 | slight misalignment of sample surface (5-10°) | along bedding plane | 25-03-09 | Small |
| 8856 | | 8846 | 0.03310 | 0.01120 | repeat measurement, surface properly horizontal | along bedding plane | 25-03-09 | Small |
| 8856 | | 8846 | 0.03130 | 0.01030 | repeat measurement, surface properly horizontal | along bedding plane | 25-03-09 | Small |
| 8856 | | 8846 | 1.56000 | 1.13000 | slight misalignment of sample surface (5-10°) | along bedding plane | 25-03-09 | Small |
| 8856 | | 8846 | 1.30000 | 0.92700 | slight misalignment of sample surface (5-10°) | along bedding plane | 25-03-09 | Small |
| 8856 | | 8846 | 0.27800 | 0.16100 | slight misalignment of sample surface (5-10°) | along bedding plane | 25-03-09 | Small |
| 8856 | | 8846 | 0.04300 | 0.01580 | repeat measurement, surface properly horizontal | along bedding plane | 25-03-09 | Small |
| 8856 | | 8846 | 0.04110 | 0.01490 | repeat measurement, surface properly horizontal | along bedding plane | 25-03-09 | Small |
| 8878 | 1718.1 | | 0.06060 | 0.02460 | slight misalignment of sample surface (5-10°) | along bedding plane | 25-03-09 | Small |
| 8878 | 1718.1 | | 0.05810 | 0.02340 | slight misalignment of sample surface (5-10°) | along bedding plane | 25-03-09 | Small |
| 8878 | 1718.1 | | 0.04830 | 0.01830 | slight misalignment of sample surface (5-10°) | along bedding plane | 25-03-09 | Small |
| 8878 | 1718.1 | | 0.04600 | 0.01720 | slight misalignment of sample surface (5-10°) | along bedding plane | 25-03-09 | Small |
| 8878 | 1718.1 | | 0.03860 | 0.01370 | slight misalignment of sample surface (5-10°) | along bedding plane | 25-03-09 | Small |
| 8878 | 1718.1 | | 0.05590 | 0.02220 | repeat measurement, surface properly horizontal | along bedding plane | 25-03-09 | Small |
| 8878 | 1718.1 | | 0.05270 | 0.02060 | repeat measurement, surface properly horizontal | along bedding plane | 25-03-09 | Small |
| 8878 | 1718.1 | | 0.04430 | 0.01640 | repeat measurement, surface properly horizontal | along bedding plane | 25-03-09 | Small |
| 8878 | 1718.1 | | 0.04240 | 0.01550 | repeat measurement, surface properly horizontal | along bedding plane | 25-03-09 | Small |
| 8878 | 1718.1 | | 0.05250 | 0.02050 | slight misalignment of sample surface (5-10°) | along bedding plane | 25-03-09 | Small |
| 8878 | 1718.1 | | 0.05070 | 0.01960 | slight misalignment of sample surface (5-10°) | along bedding plane | 25-03-09 | Small |
| 8878 | 1718.1 | | 0.05120 | 0.01980 | repeat measurement, surface properly horizontal | along bedding plane | 25-03-09 | Small |
| 8878 | 1718.1 | | 0.04860 | 0.01850 | repeat measurement, surface properly horizontal | along bedding plane | 25-03-09 | Small |
| 8902 | 3037.8 | | 0.02410 | 0.00727 | surface properly horizontal | along bedding plane | 25-03-09 | Small |
| 8908 | 1116.85 | | 0.56700 | 0.36700 | surface properly horizontal | along bedding plane | 25-03-09 | Small |
| 8908 | 1116.85 | | 0.56800 | 0.36800 | surface properly horizontal | along bedding plane | 25-03-09 | Small |
| 8908 | 1116.85 | | 0.56100 | 0.36300 | surface properly horizontal | along bedding plane | 25-03-09 | Small |
| 8908 | 1116.85 | | 0.56200 | 0.36400 | surface properly horizontal | along bedding plane | 25-03-09 | Small |
| 8918 | 1235.6 | | 0.13100 | 0.06500 | slight misalignment of sample surface (5-10°) | along bedding plane | 25-03-09 | Small |
| 8918 | 1235.6 | | 0.12200 | 0.05660 | slight misalignment of sample surface (5-10°) | along bedding plane | 25-03-09 | Small |
| 8918 | 1235.6 | | 0.10800 | 0.05110 | repeat measurement, surface properly horizontal | along bedding plane | 25-03-09 | Small |
| 8918 | 1235.6 | | 0.10600 | 0.05020 | repeat measurement, surface properly horizontal | along bedding plane | 25-03-09 | Small |
| 8918 | 1235.6 | | 0.12900 | 0.06360 | slight misalignment of sample surface (5-10°) | along bedding plane | 25-03-09 | Small |
| 8918 | 1235.6 | | 0.18500 | 0.09890 | slight misalignment of sample surface (5-10°) | along bedding plane | 25-03-09 | Small |
| 8918 | 1235.6 | | 0.10400 | 0.04880 | repeat measurement, surface properly horizontal | along bedding plane | 25-03-09 | Small |
| 8918 | 1235.6 | | 0.10100 | 0.04750 | repeat measurement, surface properly horizontal | along bedding plane | 25-03-09 | Small |

**Legend:**

| Column Label | Label Description |
|---|---|
| Sample No. | AGS sample number |
| Depth (ft., m) | Sample depth in original units |
| Ka | Permeability to air in mD |
| Kl | Permeability to liquid (nitrogen) in mD |
| Comment | Comment on the horizontality of the sample surface during measurement |
| Approximate Angle to Bedding | Measured angle of the measurement spot to bedding or observable fractures |
| Date | Date of analysis |
| Probe Tip | Probe tip size (small or large) |

Note: Leak permeability tests (Kg) of probe seals (before sample analysis) yielded values of ~0.0034–0.0043 mD

## Appendix 8 – Montney Formation Helium Pycnometry

| Sample No. | Site No. | Run No. | Vr ($cm^3$) | Vc ($cm^3$) | P1 (psi) | P2 (psi) | P1/P2 | (P1/P2)–1 | Vs ($cm^3$) | Avg. Vs ($cm^3$) | Wt. (g) | Gdensity ($g/cm^3$) |
|---|---|---|---|---|---|---|---|---|---|---|---|---|
| 8702 | M27 | 1 | 88.512 | 147.903 | 17.296 | 6.507 | 2.658 | 1.658 | 1.145 | | | |
| 8702 | M27 | 2 | 88.512 | 147.903 | 17.245 | 6.489 | 2.658 | 1.658 | 1.188 | | | |
| 8702 | M27 | 3 | 88.512 | 147.903 | 17.257 | 6.493 | 2.658 | 1.658 | 1.169 | 1.167 | 3.060 | 2.622 |
| 8764 | M19 | 1 | 88.512 | 147.903 | 17.308 | 6.524 | 2.653 | 1.653 | 1.595 | | | |
| 8764 | M19 | 2 | 88.512 | 147.903 | 17.320 | 6.531 | 2.652 | 1.652 | 1.684 | | | |
| 8764 | M19 | 3 | 88.512 | 147.903 | 17.313 | 6.527 | 2.653 | 1.653 | 1.635 | 1.638 | 4.290 | 2.619 |
| 8858 | M2 | 1 | 88.512 | 147.903 | 17.210 | 6.485 | 2.654 | 1.654 | 1.520 | | | |
| 8858 | M2 | 2 | 88.512 | 147.903 | 17.229 | 6.493 | 2.653 | 1.653 | 1.551 | | | |
| 8858 | M2 | 3 | 88.512 | 147.903 | 17.360 | 6.543 | 2.653 | 1.653 | 1.573 | 1.548 | 4.000 | 2.584 |
| 8878 | M9 | 1 | 88.512 | 147.903 | 17.319 | 6.530 | 2.652 | 1.652 | 1.662 | | | |
| 8878 | M9 | 2 | 88.512 | 147.903 | 17.260 | 6.508 | 2.652 | 1.652 | 1.671 | | | |
| 8878 | M9 | 3 | 88.512 | 147.903 | 17.308 | 6.526 | 2.652 | 1.652 | 1.667 | 1.666 | 4.400 | 2.640 |
| 8904 | M8 | 1 | 88.512 | 147.903 | 17.384 | 6.533 | 2.661 | 1.661 | 0.889 | | | |
| 8904 | M8 | 2 | 88.512 | 147.903 | 17.254 | 6.485 | 2.661 | 1.661 | 0.920 | | | |
| 8904 | M8 | 3 | 88.512 | 147.903 | 17.251 | 6.484 | 2.661 | 1.661 | 0.924 | 0.911 | 2.420 | 2.656 |
| 8908 | M39 | 1 | 88.512 | 147.903 | 17.220 | 6.492 | 2.652 | 1.652 | 1.637 | | | |
| 8908 | M39 | 2 | 88.512 | 147.903 | 17.262 | 6.508 | 2.652 | 1.652 | 1.643 | | | |
| 8908 | M39 | 3 | 88.512 | 147.903 | 17.297 | 6.522 | 2.652 | 1.652 | 1.672 | 1.651 | 4.300 | 2.605 |

**Legend**

| Column Label | Label Description |
|---|---|
| Sample No. | AGS sample number |
| Site No. | Site location number |
| Run No. | Number of times each sample was tested |
| Vr | Reference volume = 88.512 $cm^3$ |
| Vc | Volume of sample cell = 147.903 $cm^3$ |
| P1 | Pressure reading after pressurizing the reference volume |
| P2 | Pressure reading after including Vc |
| Vs | Volume of the solid |
| Avg. Vs | Average volume of the solid |
| Wt. | Weight of the sample |
| Gdensity | Grain density |